

11281

UNIVERSIDAD NACIONAL AUTONOMA
DE MEXICO

5
Ley

FACULTAD DE MEDICINA



• USO DE TOXINAS COMO SENSORES
ESTRUCTURALES DE CANALES DE
POTASIO

TESIS

QUE PARA OBTENER EL GRADO DE:
DOCTOR EN CIENCIAS BIOMEDICAS

PRESENTA
LUIS ALFONSO VACA DOMINGUEZ

MEXICO, D.F.

1994

TESIS CON
FALLA DE ORIGEN
TESIS CON
FALLA DE ORIGEN



UNAM – Dirección General de Bibliotecas Tesis Digitales Restricciones de uso

DERECHOS RESERVADOS © PROHIBIDA SU REPRODUCCIÓN TOTAL O PARCIAL

Todo el material contenido en esta tesis está protegido por la Ley Federal del Derecho de Autor (LFDA) de los Estados Unidos Mexicanos (México).

El uso de imágenes, fragmentos de videos, y demás material que sea objeto de protección de los derechos de autor, será exclusivamente para fines educativos e informativos y deberá citar la fuente donde la obtuvo mencionando el autor o autores. Cualquier uso distinto como el lucro, reproducción, edición o modificación, será perseguido y sancionado por el respectivo titular de los Derechos de Autor.

El trabajo experimental de esta tesis Doctoral fue realizado en el laboratorio* del Dr. Lourival Domingos Possani Postay, ubicado en el Instituto de Biotecnología de la Universidad Nacional Autónoma de México, Cuernavaca Morelos, México y en el laboratorio de la Dra. Diana Lee Kunze del Colegio de Medicina de Baylor en Houston, Texas, USA.

* Financiado en parte por Howard Hughes Medical Institute grant No. 75191-527104 y CONACYT-Mexico No. 0018-N9105 y DGAPA-UNAM No. IN-205893 al Dr. Possani.

Comite de Tesis:

Presidente: Dr. Jesús Adolfo García-Sainz
Secretario: Dr. Alfonso Carabez Trejo
Primer Vocal: Dr. Lourival Domingos Possani Postay
Segundo Vocal: Dra. Marcia Hiriart
Tercer Vocal: Dra. Diana Lee Kunze
Suplente: Dr. Guillermo Mendoza Hernández
Suplente: Dr. Alberto Darszon Israel

Sustentante:

M. en C. Luis Alfonso Vaca Domínguez

Asesor del tema:

Dr. Lourival Domingos Possani Postay

Agradecimientos.

Quisiera dedicar la presente tesis a mi esposa por su continuo apoyo y entusiasmo hacia mi trabajo.

Quiero agradecer el tiempo y esfuerzo dedicado a mi persona por parte de mis tutores Dr. Lourival Possani y Dra. Diana Lee Kunze.

INDICE

Lista de abreviaturas	6
Summary	7
Resumen	8
Introducción	9
Antecedentes :	
1. Que es un canal iónico ?.	10
2. Diversidad en canales de potasio activados por calcio.	12
3. Como se estudia un canal iónico ?.	13
4. Que es una toxina ?.	13
5. La familia de toxinas bloqueadoras de canales de potasio.	14
6. Especificidad de toxinas contra canales de potasio activados por calcio.	14
7. Estudios sobre la estructura y función de canales iónicos.	15
8. Por que las toxinas bloquean canales iónicos ?.	17
9. Noxiustoxina (NTX).	19
10. La Noxiustoxina bloquea varios canales de potasio.	19
11. El sitio tóxico de la NTX se encuentra en la región amino terminal.	19
Articulo como primer autor	20
Articulo como co-autor	28
Discusión y conclusiones	47
Planes futuros	49
Anexos	50
Referencias	60

ABREVIATURAS

NTX	=	Noxiustoxina.
CTX	=	Caribdotoxina.
IBX	=	Iberotoxina.
K _{Ca}	=	Canales de potasio activados por calcio.
V	=	Voltaje.
I	=	Corriente.
mM	=	Mili Molar.
µM	=	Micro Molar.
pS	=	Pico Siemen.
pA	=	Pico Amperio.
mV	=	Mili Voltio.
ms	=	Milisegundos.
pH	=	Potencial de hidrógeno.
IC ₅₀	=	Constante de inhibición media.
Ca ²⁺	=	Calcio.
K ⁺	=	Potasio.
PM	=	Peso molecular.
Po	=	Probabilidad de apertura.
To	=	Tiempo de apertura.
Tc	=	Tiempo de cerrado.

SUMMARY

Using the outside-out configuration of the patch clamp method we have studied the effect of several synthetic peptides corresponding to various segments from the N-terminal region of Noxiustoxin (NTX) on single Ca^{2+} -activated K^+ (KC_{a}) channels of small conductance obtained from cultured bovine aortic endothelial cells. These peptides induced diverse degrees of fast blockade in the endothelial KC_{a} channel. The most effective blockers were the peptides NTX_{1-39} ($\text{IC}_{50} = 0.5 \mu\text{M}$) and NTX_{1-20} comprising the first 20 amino acids from the native toxin ($\text{IC}_{50} \approx 5 \mu\text{M}$), while the less effective was the hexapeptide NTX_{1-6} , from the first 6 amino acid residues of NTX ($\text{IC}_{50} = 500 \mu\text{M}$). This was the minimum sequence required to block the channel.

By testing overlapping sequences from the entire molecule, specially those corresponding to the N-terminal region of NTX, we have been able to determine their different apparent affinities for the KC_{a} channel. Synthetic peptides from the C-terminal region produced no effect on the KC_{a} channel at the concentrations tested (up to 1 mM). These results confirm that in the N-terminal region of the NTX is located part of the sequence that may recognize K^+ channels, as we have suggested previously, from *in vivo* experiments. The blockade induced by native NTX was poorly affected by changes in membrane potential, however the blockage induced by synthetic peptides lacking the C-terminal region was partially released by depolarization.

RESUMEN

Por medio de la configuración de afuera hacia afuera del método de fijación de voltaje, hemos estudiado el efecto de varios péptidos sintéticos correspondientes a la secuencia amino terminal de la Noxiustoxina (NTX) en el canal de potasio activado por calcio de endotelio de aorta de vaca. Estos péptidos produjeron diversos grados de bloqueo rápido en dicho canal. Los péptidos más efectivos fueron el péptido 1-39 (IC_{50} 0.5 μM) y el péptido 1-20 (IC_{50} 5 μM). El péptido menos potente fué el hexapéptido 1-6 (IC_{50} 500 μM). Esta fué la secuencia mínima capaz de bloquear al canal de potasio.

Probando secuencias sobrelapadas de la molécula entera hemos encontrado que solamente secuencias correspondientes al amino terminal son capaces de bloquear al canal con distintas afinidades. Péptidos sintéticos de la región carboxilo terminal no produjeron ningún efecto sobre el canal a concentraciones tan altas como 1 mM.

Estos resultados confirman nuestras observaciones iniciales con estudios *en vivo*, los cuales indican que en la región amino terminal se encuentra el sitio de pegado al canal de potasio. El bloqueo producido por NTX nativa es insensible a cambios en el voltaje, sin embargo, el bloqueo producido por péptidos en los cuales se ha eliminado la región 10-20 es atenuado por medio de voltajes depolarizantes.

INTRODUCCION

El endotelio es una monocapa de células la cual se localiza recubriendo la parte más íntima de los vasos sanguíneos en el sistema cardiovascular. Los elegantes estudios realizados por Moncada y colaboradores dejaron al descubierto el papel del endotelio en la regulación del tono vascular [25]. Actualmente se sabe que el endotelio juega un papel dinámico en la regulación de varias funciones cardiovasculares incluyendo coagulación, arterogénesis e inflamación.

El endotelio realiza estas funciones secretando varias substancias vasoactivas tales como óxido nitroso, un poderoso vasodilatador, endotelina, un péptido vasoconstrictor y una serie de prostaglandinas [11,25]. El estímulo que regula la síntesis y secreción de estas substancias proviene de varios agonistas, entre los que se cuentan a la bradicinina, el ATP, la histamina y otros [11].

Uno de los primeros eventos ocurridos en respuesta a la estimulación por agonista consiste en la activación de un canal de potasio activado por calcio (K_{Ca}).

El papel que juega dicho canal en la respuesta del endotelio a agonistas no está definido hasta el momento, sin embargo, el uso de bloqueadores específicos puede ayudar a determinarlo.

Toxinas extraídas del veneno de varios animales ponzoñosos han sido utilizadas como herramientas en la separación, aislamiento y caracterización de canales iónicos [17,30]. Se han descubierto toxinas que bloquean específicamente a canales de sodio, calcio y potasio [9,17,24,30].

Dentro de la familia de toxinas bloqueadoras de canales de potasio, existe un grupo de toxinas las cuales bloquean canales K_{Ca} . Dichas toxinas son la iberotoxina (IBX) obtenida del veneno del alacrán *Buthus tamulus* [4], la caribdotoxina (CTX) obtenida del veneno del alacrán *Leiurus quinquestriatus quinquestriatus* [23] y la noxiustoxina (NTX) obtenida del alacrán mexicano *Centruroides noxius* Hoffmann [31]. Esta última fue la primera toxina reportada en la literatura como un potente bloqueador de canales de potasio [6]. Estas toxinas comparten aproximadamente entre 50 y 70 % de similitud en su secuencia de aminoácidos.

El uso de estas toxinas ha permitido además la obtención de importante información acerca de la estructura y funcionamiento de canales de potasio. Estudios realizados durante los últimos años han demostrado la presencia de receptores específicos para diversas toxinas [17].

El presente trabajo tiene por objetivo el estudio de la interacción entre varios péptidos sintéticos correspondientes a la estructura primaria de la NTX y el canal K_{Ca} de endotelio. La finalidad de dicho objetivo consiste en la identificación de la secuencia de aminoácidos en la NTX responsable por el pegado al sitio receptor del canal.

El fin del presente trabajo es el de utilizar regiones sintéticas de la NTX como sensores estructurales para obtener información de como dicha toxina interactúa con el canal K_{Ca} para bloquearlo. Dicha información puede ser utilizada para tratar de entender los mecanismos moleculares de apertura, cierre y bloqueo de canales iónicos, así como para determinar si todas las toxinas interactúan de la misma forma con canales iónicos al inducir el bloqueo de los mismos.

Esta información se puede utilizar, además, en el diseño de nuevos fármacos los cuales pueden bloquear selectivamente a tipos específicos de canales de potasio. Al entender con más claridad como las diversas toxinas interactúan con canales iónicos, podremos identificar mecanismos de bloqueo y determinar que secuencias de aminoácidos son importantes en la modulación de la afinidad de dichas toxinas por sus respectivos receptores.

ANTECEDENTES

1. Que es un canal iónico ?.

Un canal iónico es una proteína la cual se encuentra formando un poro en la membrana celular. Dicho poro posee en su interior un filtro de selectividad, lo que le permite discriminar entre diversos iones en solución y permitir el paso solo a cierto tipo de iones. En base a su selectividad los canales iónicos se dividen en varias familias: canales de potasio, calcio, sodio y cloro [17]. La figura 1 ilustra la topografía de canales iónicos basada en predicciones de indices de hidrofobicidad. Dicha figura muestra la posible estructura que varios canales iónicos pueden adoptar al insertarse en la membrana plasmática [17].

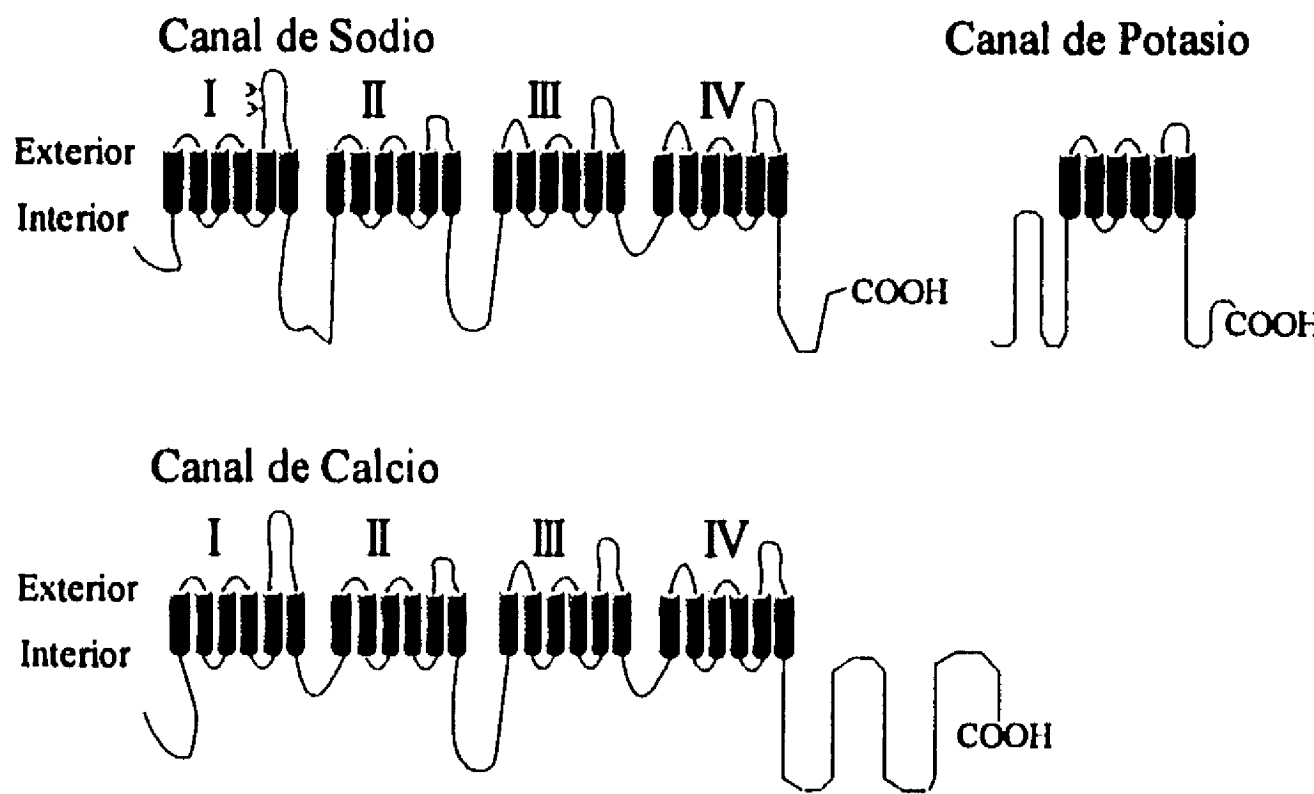


Fig. 1. Topografía de canales iónicos. Esta figura muestra la estructura de canales iónicos de acuerdo a predicciones en base a índices hidróficos. Los cilindros sombreados representan las regiones transmembranales. Nótese las indicaciones exterior e interior, mostrando la parte intracelular y extracelular de los canales. El canal de potasio se forma de cuatro motivos repetidos, mientras que en los canales de sodio y calcio dichos motivos se encuentran unidos covalentemente (I, II, III, IV). Cada motivo se forma de seis segmentos los cuales atraviesan la membrana celular de lado a lado. Este diagrama fue obtenido de [17].

Desde el descubrimiento de los canales iónicos, muchos investigadores han pasado años de su vida tratando de entender preguntas muy simples tales como las siguientes: ¿cómo funcionan los canales iónicos ?, ¿qué mecanismos permiten que un canal se abra y se cierre ? [17]. Dichas preguntas aunque simples de formular, requieren de una explicación extraordinariamente compleja la cual no ha podido obtenerse enteramente por los medios experimentales utilizados hasta la fecha.

El descubrimiento de bloqueadores selectivos contra canales iónicos abrió una nueva era de posibilidades experimentales. Utilizando dichos bloqueadores no solo nos permite echar un vistazo de cerca a los mecanismos de apertura, cierre y bloqueo de canales, sino que además nos brinda la oportunidad de modificar dichos agentes bloqueadores y utilizarlos con fines terapéuticos [7,9,24].

Existen un numero enorme de bloqueadores de canales iónicos los cuales se utilizan en la actualidad con fines curativos. Las sulfonilureas, como la tolbutamida, se usan como hipoglucemiantes en el tratamiento de pacientes diabéticos. Estas substancias bloquean selectivamente al canal dependiente de adenosina trifosfato (ATP) en células beta del páncreas [36]. Nicorandil es un fuerte vasodilatador utilizado en pacientes con angina de pecho para relajar arterias coronarias y restablecer la circulación cardiaca. Esta substancia bloquea canales de gran conductancia dependientes de calcio en músculo liso. Por años se han utilizado bloqueadores de canales de sodio, como la lidocaina, como anestésicos y antiarrítmicos. Verapamil, un bloqueador de canales de calcio, se utiliza exitosamente en el tratamiento de hipertensión [24].

La familia de canales de potasio a su vez se divide en 6 clases de acuerdo al criterio de varios grupos trabajando con estos canales [7,9,24]. Debido a que la presente tesis se dirige hacia el estudio de toxinas bloqueadoras de canales de potasio, a continuación se presenta una breve descripción de estas clases de canales de potasio:

Canales de potasio rectificadores externos: Dentro de este grupo de canales se encuentra el rectificador tardío. Este canal fue originalmente descrito en los estudios, ya clásicos, de Hodgkin & Huxley en 1952 [18]. Este canal juega un papel importante en la fase de repolarización durante los potenciales rápidos de acción en neuronas y músculo esquelético. Se han descrito conductancias unitarias que varian de 2-200 pS en varias preparaciones [5,8,32]. El canal es bloqueado por tetraetilamonio (TEA), aunque este agente no es muy específico para esta clase de canal.

Canales de potasio rectificadores internos: Este tipo de canal se activa durante pulsos hiperpolarizantes mayores de -70 mV. Este canal se encuentra en prácticamente todos los tejidos estudiados hasta la fecha. En el endotelio este tipo de canal es la única corriente que se observa en células no estimuladas por agonistas [41]. Se ha postulado que dicho canal sirve para mantener el potencial de membrana a -70 mV [41]. Se han reportado conductancias unitarias de alrededor de 5-27 pS, dependiendo del tipo de preparación [10,21,27,34]. Este canal es bloqueado por concentraciones micromolares de bario [24]. Recientemente se ha descubierto que dicho canal es bloqueado por 2,5-di(tert-butil)-1,4-benzohidroxiquinona (BHQ), un agente que bloquea a la ATPasa de calcio de retículo endoplásmico [16]. El canal inhibido por ATP es otro ejemplo de canales rectificadores internos [36]. Este canal es sensible a sulfonilureas.

Canales de potasio de corriente transitoria: Estos canales se describieron originalmente en neuronas de molusco [15]. Actualmente se sabe que dichos canales se encuentran en diferentes tipos de tejidos. Esta clase de canales se caracteriza porque se inactiva a potenciales de reposo. Este canal se activa rápidamente con potenciales hiperpolarizantes, sin embargo, su activación es transitoria. El agente bloqueador más utilizado con este canal es 4-aminopiridina, aunque este canal es también sensible a TEA. Se cree que el papel de este canal es el de ayudar a una despolarización gradual en neuronas, lo cual permite descargas graduales de potenciales de acción [24]. Este canal ganó gran popularidad en los últimos años al descubrirse que el gen que codifica dicho canal estaba afectado en la mosca de la fruta (*Drosophila*), lo cual confería un fenotipo muy peculiar a la mosca. Dicho fenotipo se caracteriza por movimientos rápidos e involuntarios en las

extremidades del insecto. Lo anterior contribuyó a que dicho gene se denominara *Shaker*, que traducido del inglés significa "temblar" o "agitar".

Canal de potasio S: Este tipo de canal se describió en neuronas de *Aplysia* y se caracteriza por ser regulado por serotonina (de ahí el nombre de canal S) [38]. Se han reportado conductancias unitarias de alrededor de 55 pS. Este canal es bloqueado por bario y TEA [26,33].

Canales de potasio M: Estos canales se describieron originalmente en neuronas de vertebrados [20]. Su nombre proviene de receptores muscarínicos los cuales activan al canal. El canal es bloqueado por bario y TEA.

Canales de potasio activados por calcio: Esta clase de canales tienen una distribución generalizada (al igual que el rectificador interno) [3,29,27]. Su característica principal es que se activan con concentraciones micromolares de calcio intracelular. Por el contrario, concentraciones bajas de calcio intracelular inactivan al canal. Esta clase de canales a su vez, se subdividen en tres categorías: canales de gran conductancia (denominados tambien **Maxi canales**), de mediana y de pequeña conductancia.

Además se distinguen por su conductancia unitaria, estos tres grupos se diferencian además en su dependencia a voltaje, su sensibilidad a calcio intracelular y su sensibilidad a bloqueadores de canales de potasio.

2. Diversidad en canales de potasio activados por calcio (K_{Ca}).

Como se mencionó con anterioridad, los canales K_{Ca} se subdividen a su vez en tres grupos: los de pequeña conductancia, mediana y gran conductancia (**Maxi canales**). Estos tres tipos de canales K_{Ca} se encuentran distribuidos en diferentes tejidos de mamíferos. En algunas ocasiones es posible encontrar más de un tipo en el mismo tejido, pero generalmente sólo se encuentra un tipo de canal por tejido. La función de este tipo de canales apenas empieza a explorarse. Por ejemplo, en neuronas canales K_{Ca} parecen jugar un papel importante en la fase de repolarización después de un potencial de acción [7,24]. En células secretoras (como glándulas salivales y sudoríparas) estos canales sirven como conductos para la secreción de potasio [24]. Gracias a que toxinas de diversos animales bloquean selectivamente a canales de pequeña, mediana y gran conductancia, ha sido posible estudiar algunas de las funciones de estos canales.

El canal de pequeña conductancia es bloqueado por apamina, una toxina obtenida del veneno de abeja *Apis mellifera* [3]. Este canal en general no es dependiente de voltaje y posee una sensibilidad a calcio mayor que el **Maxi** canal. Este canal no es sensible a NTX, IBX o CTX. El canal de mediana conductancia es insensible a apamina, sensible a NTX y CTX y voltaje independiente. Este canal es muy poco sensible a TEA, pero es bloqueado por concentraciones micromolares de tetrabutilamonio (TBA). Recientemente se ha reportado que la sensibilidad a calcio en este canal puede ser regulada por proteínas G [41]. Finalmente el canal de gran conductancia es sensible a NTX, CTX e IBX y a concentraciones micromolares de TEA. El estudio de este canal ha cobrado gran ímpetu desde que se descubrió que el gen de *Drosophila* denominado *Slo* codifica varios tipos de canales **Maxi** [1].

3. Como se estudia un canal iónico ?.

Existen varias técnicas las cuales han sido utilizadas a lo largo de los últimos años para el estudio de canales iónicos. Dentro de estas técnicas una de las más poderosas es sin duda la de fijación de voltaje (Patch Clamp) [14]. Dicha técnica en su configuración de canal único permite la medición de corrientes microscópicas generadas por el paso de iones a través del poro de un canal único.

Esta técnica y la de incorporación de canales en bicapas lipídicas son las únicas que permiten medir la actividad de una sola proteína. La actividad eléctrica obtenida de esta forma representa la actividad de una sola molécula de canal (un canal único), a diferencia de otras técnicas las cuales miden la actividad de una población de canales [17].

Ya que la técnica de fijación de voltaje se va a utilizar intensamente a lo largo del desarrollo de la presente tesis, a continuación se incluye una breve descripción de la misma con el fin de permitir una mejor comprensión de los resultados presentados más adelante.

La técnica de fijación de voltaje. Por medio de capilares de vidrio los cuales se afilan y pulen en uno de sus extremos es posible obtener sellos de altísima resistencia en membranas biológicas. En el interior de este capilar de vidrio se coloca un electrodo el cual va conectado a un amplificador de corriente. Dicho electrodo se utiliza, a su vez, para inyectar voltaje a la célula en estudio. El electrodo mide el paso de corriente a través de la membrana biológica (membrana celular). Dicha corriente es generada por el paso de iones a través del poro de un canal iónico (el cual se encuentra en el pedazo de membrana celular aislado por el capilar de vidrio). De este modo, las transiciones de un canal entre los estados de cerrado y abierto se miden como saltos de corriente. La Figura 2 muestra como se realiza una de estas mediciones.

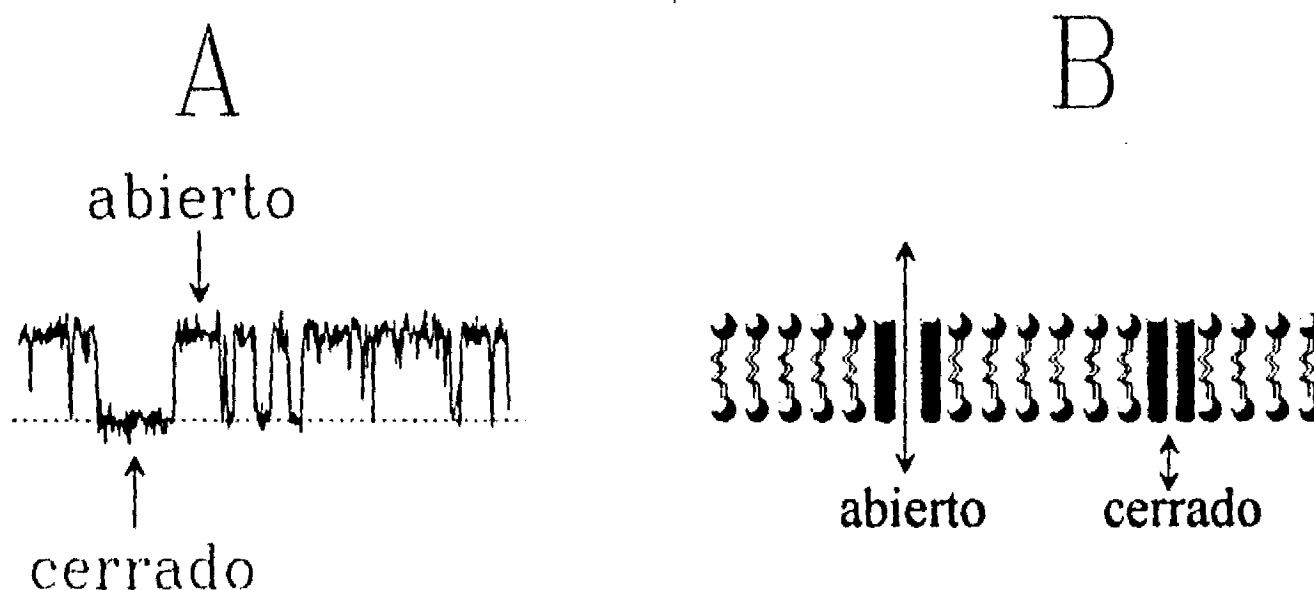


Fig 2. La técnica de fijación de voltaje: Panel A, ejemplo del paso de corriente a través de un canal iónico. El registro indica los saltos de corriente producidos por el paso de iones tal y como lo registra el amplificador. Panel B, representación esquemática del canal en la membrana. Nótese como el paso de iones (señalado por las flechas verticales) se interrumpe cuando el canal se cierra.

4. Que es una toxina ?.

El veneno de varios animales ponzoñosos contiene péptidos de diversos tamaños los cuales bloquean selectivamente canales iónicos. Los péptidos de bajo peso molecular (alrededor

de 40 aminoácidos) bloquean canales de potasio mientras que los péptidos de mayor peso molecular (alrededor de 70 aminoácidos) bloquean canales de sodio [30].

Las toxinas además poseen especificidad en especie animal, es decir, algunas toxinas bloquean canales en mamíferos mientras que otras sólo bloquean canales de crustáceos o insectos [24,30].

Las toxinas se purifican por medio de varios pasos cromatográficos entre los que se cuentan filtración en gel (separación por peso molecular) y cromatografía de intercambio iónico (separación por carga) culminando con cromatografía líquida de alta resolución (HPLC) la cual separa por características hidrofóbicas. Al final se obtiene una proteína pura la cual se verifica por medio de análisis de aminoácidos [30].

5. La familia de toxinas bloqueadoras de canales de potasio.

Dentro de las toxinas obtenidas de venenos de alacranes, las toxinas bloqueadoras de canales de potasio comparten diversos grados de similitud en su secuencia de aminoácidos. Por ejemplo, la secuencia de la NTX es alrededor de 50% similar a la secuencia de la CTX. A su vez, la CTX comparte alrededor de 70% de similitud con la recientemente aislada iberotoxina (IBX). La figura 3 muestra el alineamiento de las tres toxinas mencionadas con anterioridad (NTX, CTX e IBX). En esta figura se puede apreciar las regiones de similitud entre las tres toxinas. Nótese además que todas las toxinas conservan sus tres puentes disulfuro. Siendo estructuras relativamente pequeñas ($PM < 4000$) es notable la presencia de tres puentes disulfuro, lo cual sugiere una estructura compacta.

COMPARACION DE SECUENCIAS ENTRE TRES TOXINAS DE ALACRANES

NTX	T	I	I	N	V	K	C	T	S	P	K	Q	C	S	K	P	C	K	E	L	Y	G	S	S	A	G	A	K	C	M	N	G	K	C	K	C	Y	N	N	-COOH
CTX	Z	F	T	N	V	S	C	T	T	S	K	E	W	S	V	C	Q	R	L	H	N	T	S	R	G	-	K	C	M	N	K	K	C	R	C	Y	S	-COOH		
IBX	Z	F	T	D	V	D	C	S	V	S	K	E	W	S	V	C	K	D	L	F	G	V	D	R	G	-	K	C	M	G	K	K	C	R	C	Y	Q	-COOH		

Fig. 3 Secuencias de tres toxinas de canales de potasio: Alineamiento de tres toxinas por su extremo amino terminal. Las cajas indican aminoácidos homólogos en la secuencia de las toxinas. Los espacios introducidos en la CTX y la IBX se indican con una línea (-). Dichos espacios permiten alinear las tres cisteínas en el extremo carboxilo terminal en las tres toxinas.

6. Especificidad de toxinas contra canales K_{Ca}

Apamina, un péptido obtenido del veneno de abeja, bloquea exclusivamente canales K_{Ca} de baja conductancia [3,24]. Originalmente se pensaba que CTX bloqueaba únicamente a canales de gran conductancia [12]. Experimentos recientes indican que CTX bloquea también a algunos canales K_{Ca} de mediana conductancia, lo cual ha hecho difícil el uso de CTX como una herramienta para determinar el papel funcional de canales de gran conductancia en varios tejidos.

Finalmente, NTX bloquea canales de mediana y gran conductancia, pero además bloquea canales no dependientes de calcio [6,31,40,42].

Si bien ésta relativamente baja selectividad de las toxinas por varios canales a desanimado a algunos investigadores, para otros brinda la oportunidad de explorar más de cerca aspectos estructurales en dichos canales, es decir, los receptores a dichas toxinas deben de compartir cierta similitud en su secuencia de aminoácidos [24]. Si estas toxinas bloquean a canales de potasio de diferentes conductancias y dependencias a voltaje, esto sugiere la presencia de motivos estructurales repetidos en dichos canales. De esta forma, utilizando estas toxinas o modificaciones de ellas nos puede permitir explorar similitudes estructurales en canales que de otra forma serían muy difíciles de evaluar. Esto permitirá eventualmente, la identificación de la secuencia de aminoácidos que forma al receptor para cada toxina en los diferentes canales de potasio. Estudios de este tipo permitirán definir si estas toxinas se unen a un sitio receptor común en los diferentes canales de potasio.

7. Estudios sobre la estructura y función de canales iónicos.

Lamentablemente conocemos muy poco acerca de la estructura tridimensional de canales iónicos. Los intentos por cristalizar canales iónicos con el fin de determinar su estructura por medio de cristalografía de rayos X han sido infructuosos. Al utilizar toxinas como sensores estructurales de canales iónicos podemos obtener información importante acerca de como funcionan dichos canales. Además se puede obtener información de la estructura que adoptan los canales al insertarse en la membrana plasmática [17]. Esta idea ha sido utilizada por algunos investigadores [12,28,41,43]. Conociendo la estructura primaria del canal y de la toxina se pueden hacer modificaciones en las secuencias de aminoácidos de ambos para determinar qué aminoácidos son importantes en el pegado al canal y qué aminoácidos forman parte del receptor a la toxina. Estudios de este tipo han permitido determinar qué secuencias del canal **Shaker** se proyectan extracelularmente y qué secuencias se localizan en el interior de la célula [43]. Combinando estudios hidropáticos con la información de sitios receptores a bloqueadores internos y externos en el canal ha sido posible delinear estructuras internas y externas en el canal. La figura 4 muestra los aminoácidos importantes en el receptor interno y externo a TEA, así como los aminoácidos relevantes en el receptor a CTX para **Shaker**. Estudios de este tipo han permitido delimitar las secuencias que se encuentran formando parte del poro en este canal [43]. Si bien estos resultados no han podido confirmarse por medios cristalográficos, esta información concuerda perfectamente con otros experimentos de mutaciones puntuales en el canal en los cuales ha podido cambiarse la selectividad del mismo al modificar uno o dos aminoácidos en esta región [43].

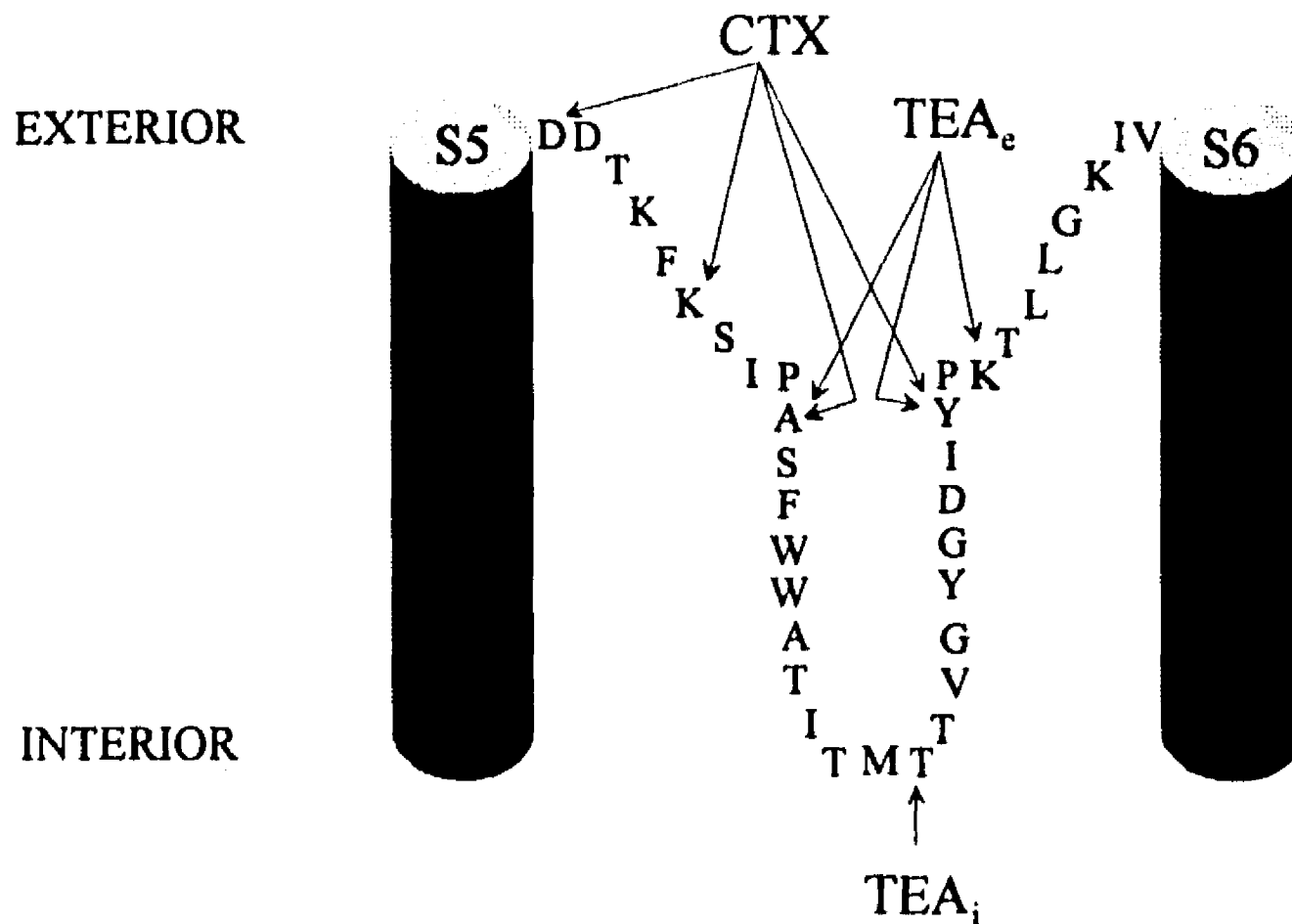


Fig. 4. El poro del canal de potasio: Este diagrama representa la región de aminoácidos la cual se cree, forma el poro de conducción de iones en el canal de potasio Shaker. Nótese los aminoácidos involucrados en el pegado a TEA intracelular (TEA_i) y extracelular (TEA_e), así como la región involucrada en el pegado de CTX. S5 y S6 representan los segmentos transmembranales 5 y 6 de acuerdo a la figura 1.

Por otro lado, conociendo que aminoácidos forman parte del receptor a la toxina, permitirá en el futuro determinar que cambios estructurales sufre el canal al entrar en contacto con la toxina resultando en el bloqueo del mismo.

Con esta información a la mano, es posible diseñar modelos que nos permitan entender que cambios estructurales surgen en el canal para moverlo del estado abierto al estado bloqueado. Otro objetivo importante es determinar, por ejemplo, si las diferentes toxinas que bloquean canales de potasio lo hacen por medio de mecanismos similares, o si cada toxina bloquea al canal usando un mecanismo diferente. Esto resulta interesante si consideramos que el estado conformacional del canal el cual denominamos "bloqueado" quizá represente en realidad varios estados diferentes (inducidos por cada una de las toxinas). Si este es el caso, hay varias especulaciones que resultan interesantes e informativas. Por ejemplo, sabemos que los tiempos de disociación de la NTX y la CTX son diferentes, es decir, la CTX pasa más tiempo asociada al receptor en el canal. Este resultado tiene (cuando menos) dos posibles interpretaciones, una es que el pegado de la CTX al receptor es más estable. La otra interpretación es que la CTX induce un cambio conformacional en el canal el cual estabiliza la unión toxina-canal. La primera interpretación implica que el reconocimiento de los aminoácidos del receptor y la toxina forman un enlace de alta afinidad, mientras que la segunda interpretación asume que la toxina puede inducir cambios conformacionales en el canal resultando en un pegado más fuerte entre ambas proteínas (toxina-canal). Si asumimos que la primera interpretación es la correcta, es decir, que la toxina y el canal forman un enlace de alta afinidad ($IC_{50} = 5 \text{ nM}$), resulta difícil entender porque cuando la toxina se disocia (CTX) tarda tanto tiempo en reasociarse al canal. Por otro lado, el bloqueo inducido por NTX es de baja afinidad ($IC_{50} = 300 \text{ nM}$), sin embargo cuando la NTX se

disocia del canal tiende a reasociarse rápidamente. Estos resultados sugieren que la relación toxina-canal es mucho mas compleja que el simple pegado a un receptor de alta o baja afinidad.

8. Por que las toxinas bloquean canales iónicos ?.

Los investigadores en el área de canales iónicos han ocupado buena parte de su tiempo en estudiar el efecto de varias toxinas bloqueadoras de canales [3,4,22,23,24]. La idea es obtener información de los cambios en el canal inducidos por la toxina. Existen varios modelos que pretenden explicar los resultados experimentales y predecir cambios estructurales en el canal inducidos por las toxinas [4,23,28,40]. Dichos modelos, aunque preliminares, sugieren que la interacción entre canal-toxina es una interacción compleja y no en todos los casos del mismo tipo. Por ejemplo, CTX e IBX, las cuales comparten alrededor de 70 % de similitud en su secuencia de aminoácidos, producen un tipo de bloqueo similar en el canal K_{Ca} de gran conductancia [4,12]. Ambas toxinas producen segmentos de bloqueo en el canal con varios minutos de duración. Sin embargo la NTX, la cual comparte alrededor de 50 % de similitud con las dos toxinas mencionadas anteriormente, induce un tipo de bloqueo diferente en el mismo canal. La NTX produce estados de bloqueo de unos milisegundos en duración [40,42]. El mismo resultado se observa en el canal K_{Ca} de mediana conductancia [40]. Como se muestra en la figura a continuación la NTX y la CTX, a pesar de compartir 50 % de similitud en su secuencia de aminoácidos (ver Fig. 3), producen un tipo de bloqueo diferente en el canal de mediana conductancia de células endoteliales (Fig. 5).

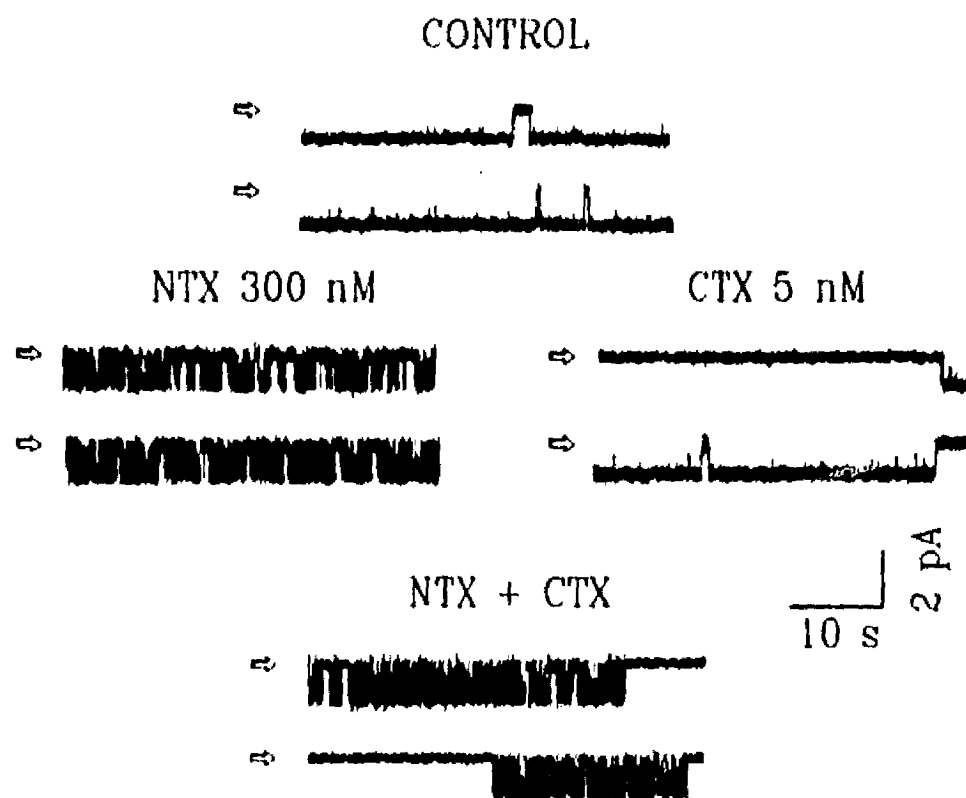


Fig. 5 Bloqueo producido por CTX y NTX. Ejemplos del bloqueo producido por NTX y CTX en el canal de mediana conductancia de endotelio. La solución utilizada es 150 mM de aspartato de potasio simétrico. El potencial de membrana fue fijado a -60 mV. Los experimentos representan membranas en la configuración de afuera hacia afuera. Las toxinas se agregaron a la solución extracelular en las concentraciones indicadas en la figura. Las concentraciones utilizadas representan la concentración de inhibición media (IC_{50}). Las flechas horizontales indican el nivel de cero corriente (línea de base).

Como se observa en la figura anterior, el tipo de bloqueo producido por la NTX y CTX en el canal de mediana conductancia de endotelio se asemeja al reportado para el canal de gran

conductancia de músculo [42]. Lo anterior sugiere que si bien ambos canales tienen propiedades distintas en cuanto a conductancia, sensibilidad a calcio intracelular y dependencia a voltaje, ambos canales deben de poseer estructuras similares las cuales son reconocidas por estas toxinas (receptores). Lo anterior también sugiere que el sitio de dependencia a voltaje y el sitio receptor a calcio se encuentran separados al sitio receptor para las toxinas (NTX y CTX), ya que dicho sitio debe presentar secuencias similares entre ambos canales.

Las concentraciones utilizadas en los experimentos ilustrados en la figura anterior corresponden a la concentración de bloqueo medio (IC_{50}) para la NTX (300 nM) y la CTX (5 nM). Como se aprecia en estos experimentos, la CTX tiene una afinidad 60 veces mayor por este canal que la NTX. Esta diferencia en afinidad también se observa en el canal de gran conductancia [42].

¿Cómo exactamente es que las toxinas inducen el estado de bloqueo en el canal? Al inspeccionar la figura 5 nos percatamos que la NTX debe de estar pegándose y despegándose de su sitio receptor a una velocidad altísima (milisegundos). Como resultado de esto el canal se encuentra cambiando rápidamente del estado bloqueado al estado abierto. El caso de la CTX es muy distinto, esta toxina se pega a su sitio receptor y se mantiene en él por varios segundos, llegando en algunos casos a 1 minuto. El caso de la IBX es aún más acentuado, dicha toxina produce estados de bloqueo de hasta 15 minutos en duración [4]. Los resultados anteriores indican que el tiempo de residencia (pegado) de las toxinas a sus respectivos receptores es diferente para cada una. La NTX pasa poco tiempo asociada a su receptor, sin embargo, una vez disociada tiende a reasociarse más rápidamente que las otras dos toxinas. De esta forma, el tiempo de asociación y disociación de la NTX a su receptor es más rápido que el de las otras dos toxinas (CTX e IBX). Esto se manifiesta como una fibrilación rápida entre el estado abierto y el estado bloqueado del canal (Fig. 5). Por otro lado, el tiempo de pegado de la CTX e IBX a su receptor es más largo (de segundos y minutos en duración), sin embargo, una vez que estas toxinas se disocian de sus receptores, el tiempo de reasociación es también mucho más largo que el de la NTX. Lo anterior se manifiesta como períodos de actividad en el canal en los cuales pareciera que no hay toxina presente en la solución, es decir, el canal se abre y cierra en forma similar al control (sin toxina presente) [4,12,22]. Como se explicó en las secciones anteriores, el mecanismo de bloqueo del canal por estas toxinas parece ser mucho más complejo que en el caso de pegado a receptores de alta y baja afinidad.

Estudios recientes con CTX e IBX indican que efectos electrostáticos entre el complejo toxina-canal juegan un papel importante en el bloqueo al canal K_{Ca} de gran conductancia [4]. Las cargas negativas localizadas en la parte exterior del canal cerca del poro tienden a aumentar la concentración local de toxina [4]. Esto es más evidente en el caso de la CTX ya que esta toxina posee una carga positiva mayor que la IBX. Por esta razón la afinidad de estas toxinas es dependiente de la fuerza iónica [2]. La constante de asociación para CTX disminuye mil veces cuando la fuerza iónica cambia de 20 mM a 800 mM [22].

El hecho de que TEA alivia el bloqueo por IBX y CTX sugiere que estos fármacos compiten por un mismo receptor o que los receptores se localizan en proximidad uno de otro [4,22].

Finalmente se ha demostrado que aumentando la concentración intracelular de potasio se reduce la afinidad de las toxinas por el canal [4,22]. Lo anterior sugiere que el mecanismo de bloqueo por CTX e IBX es similar, primero las toxinas se unen a su receptor en una reacción de

tipo bimolecular, en seguida las toxinas bloquean el paso de iones a través del poro del canal. Este tipo de bloqueo se denomina taponamiento.

9. Noxiustoxina.

La Noxiustoxina es un péptido de 39 aminoácidos obtenido del veneno del alacrán mexicano *Centruroides Noxius Hoffmann* [31]. Este péptido fué la primer toxina descrita como un bloqueador específico de canales de potasio [6]. El hecho de que la NTX posee tres puentes disulfuro sugiere una estructura compacta..

La Noxiustoxina se purifica del veneno total de alacrán por medio de varios pasos cromatográficos los cuales incluyen una filtración en sephadex G-50 seguida por intercambio iónico en una columna de carboximetilcelulosa con 20 mM de acetato de amonio pH 4.7 y posteriormente recromatografía en la misma columna con 50 mM de amortiguador de fosfatos pH 6.0 [31]. El paso final consiste en cromatografía líquida de alta presión con lo cual se obtiene un componente único. Posteriormente la NTX es identificada por medio del análisis de aminoácidos y secuenciación.

10. La Noxiustoxina bloquea varios canales de potasio.

Estudios electrofisiológicos han demostrado que la NTX puede bloquear varios canales de potasio con distintas afinidades. Originalmente se había demostrado que la NTX bloqueaba reversiblemente al canal de potasio de rectificación tardía con una afinidad de 290 nM [6]. Posteriormente se demostró que la NTX bloquea canales K_{Ca} con una afinidad de 450 nM [42]. Finalmente la NTX puede bloquear canales dependientes de voltaje en limfocitos con una afinidad de 0.2 nM [35]. En el caso del canal K_{Ca} de endotelio, nosotros encontramos que la NTX lo bloquea con una afinidad de 300 nM [40].

11. El sitio tóxico de la NTX se encuentra en la región amino terminal.

Estudios previos realizados con péptidos sintéticos de la NTX indicaban que el péptido 1-9 inducía liberación de neurotransmisores mediado por bloqueo de canales de potasio en sinaptosomas de ratón. Dichos estudios demostraban además que el péptido 1-9 era tóxico en bioensayos con roedores, sin embargo, péptidos de la región carboxilo terminal de la NTX no producían ninguna sintomatología en los bioensayos ni liberaban neurotransmisores [13]. Lo anterior sugería que en la región amino terminal se encuentra parte de la secuencia que se pega y bloquea canales de potasio. Sin embargo, mediciones directas por medios electrofisiológicos del efecto de dichos péptidos sintéticos sobre canales de potasio no han sido explorados hasta la fecha. En el presente trabajo se muestran por primera vez los efectos de varios péptidos sintéticos correspondientes a varios segmentos de la secuencia primaria de la NTX sobre el canal K_{Ca} de endotelio. Los resultados presentados a continuación concuerdan perfectamente con los experimentos de liberación de neurotransmisores y de toxicidad en bioensayos mencionados con anterioridad. Todos estos resultados sugieren fuertemente que en la región amino terminal de la NTX se encuentra la secuencia que se pega al receptor de esta toxina en el canal K_{Ca} .

Trabajo como primer autor.

**Vaca, L; Gurrola GB; Possani, LD & Kunze DL (1993). Blockade of a K_{Ca} channel with synthetic peptides from Noxiustoxin: A K⁺ channel blocker
J. Memb. Biol. **134**:123-129.**

Blockade of a K_{Ca} Channel with Synthetic Peptides from Noxiustoxin: A K^+ Channel Blocker

L. Vaca¹, G.B. Gurrola², L.D. Possani², D.L. Kunze¹

¹Department of Molecular Physiology and Biophysics, Baylor College of Medicine, 1 Baylor Plaza, Houston, Texas 77030

²Departamento de Bioquímica, Instituto de Biotecnología, Universidad Nacional Autónoma de México, Apartado Postal 510-3, Cuernavaca, Morelos 62271, México

Received: 4 September 1992/Revised: 6 January 1993

Abstract. Using the outside-out configuration of the patch-clamp method, we studied the effect of several synthetic peptides corresponding to various segments from the N-terminal region of noxiustoxin (NTX) on single Ca^{2+} -activated K^+ (K_{Ca}) channels of small conductance obtained from cultured bovine aortic endothelial cells. These peptides induced diverse degrees of fast blockade in the endothelial K_{Ca} channel. The most effective blockers were the peptides NTX₁₋₃₉ ($IC_{50} = 0.5 \mu M$) and NTX₁₋₂₀ comprising the first 20 amino acids from the native toxin ($IC_{50} \approx 5 \mu M$), while less effective was the hexapeptide NTX₁₋₆, from the first six amino acid residues of NTX ($IC_{50} = 500 \mu M$). This was the minimum sequence required to block the channel.

By testing overlapping sequences from the entire molecule, specially those corresponding to the N-terminal region of NTX, we have been able to determine their different apparent affinities for the K_{Ca} channel. Synthetic peptides from the C-terminal region produced no effect on the K_{Ca} channel at the concentrations tested (up to 1 mM). These results confirm that in the N-terminal region of the NTX is located part of the sequence that may recognize K^+ channels, as we have suggested previously from in vivo experiments. The blockade induced by native NTX was poorly affected by changes in membrane potential; however, the blockage induced by synthetic peptides lacking the C-terminal region was partially released by depolarization.

Key words: Noxiustoxin — Synthetic peptides — Patch clamp — K^+ channels

Introduction

Noxiustoxin (NTX) is a 39 amino acid peptide purified from the venom of the Mexican scorpion *Centruroides noxius* Hoffmann [14]. This was the first animal toxin described as a specific K^+ channel blocker [3]. NTX can reversibly block several types of K^+ channels, including the delayed rectifier [3], voltage-gated K^+ channels from human T lymphocytes [15], Ca^{2+} -activated K^+ (K_{Ca}) channels from skeletal muscle [18] and whole-cell K_{Ca} currents from bovine aortic endothelial cells [4]. However, NTX has no effect on the inward rectifier K^+ channel [4].

In previous studies we showed that the synthetic peptides corresponding to the amino acid sequence 1–9 (NTX₁₋₉) 1–20 (NTX₁₋₂₀) and 1–39 (NTX₁₋₃₉) of NTX are toxic to mice, inducing symptomatology similar to that produced by native NTX [9]. We have shown also that these synthetic peptides can induce neurotransmitter release mediated through K^+ channels, suggesting that the peptides are capable of blocking K^+ channels [9]. However, a direct measurement of the effect of these synthetic peptides on a K^+ channel has not been provided, thus far.

We show that several synthetic peptides corresponding to the N-terminal region of NTX can induce diverse degrees of blockade on a K_{Ca} channel from bovine aortic endothelial cells (BAECs), confirming an earlier suggestion [9] that part of the sequence that may recognize K^+ channels is located in this region.

Materials and Methods

REAGENTS

All salts, solvents and chemicals used were analytical grade, obtained as previously described [9]. Reagents used for peptide synthesis were HPLC grade. Protected amino acids (α -BOC-amino acids) and resins containing the first amino acid bound were purchased from Peninsula Laboratories. Solvents used for peptide synthesis were obtained from Aldrich and Pierce Chemical.

NOXIUSTOXIN

Purification of NTX from whole *C. noxius* venom was achieved as previously described [14], using a Sephadex G-50 gel filtration, followed by ion exchange chromatography in carboxymethyl-cellulose resins with 20 mM ammonium acetate pH 4.7, and re-chromatography with the same resin in 50 mM phosphate buffer, pH 6.0.

PEPTIDE SYNTHESIS AND CHARACTERIZATION

All synthetic peptides were synthesized using the solid phase method [11] as previously described [9]. The yield of each newly incorporated amino acid in the growing polypeptidic chain was ascertained by the ninhydrin reaction [16]. At the end of the synthesis, the peptides were liberated from the resin by cleavage with fluorhydric acid [11]. All peptides were purified by high performance liquid chromatography (HPLC) using a C18 reverse phase column eluted with a linear gradient of acetonitrile from 0 to 60% in presence of 0.1% trifluoroacetic acid. The resulting peptides were hydrolyzed by HCl 6 N, 110°C, and their compositions were determined by amino acid analysis [9]. When needed, an additional separation using an isocratic gradient was applied to the peptides. Some peptides were confirmed by direct amino acid sequence using an automatic Beckman 890M microsequencer. Only highly purified peptides were used for the experiments described here.

SOLUTIONS

The HiK solution contained in mM: 150 K aspartate, 10 HEPES, 2 $CaCl_2$, 2.2 EGTA. pH adjusted to 7.2 with H_2SO_4 . The free Ca^{2+} concentration was 1 μM [7]. All peptides were applied to the membrane patch with a perfusion system modified from Carbone and Lux [1] driven by gravity.

CELL CULTURE

BAECs were obtained as previously described [6]. Cells were kept in culture and used from passages 10 to 20 [4]. Confluent monolayers were mechanically dispersed with a plastic pipette and replated on a petri dish allowing cell reattachment for 10–20 min. With this procedure single cells were obtained and used for patch-clamp experiments.

SINGLE CHANNEL RECORDING

All experiments were performed at room temperature. The outside-out configuration of the patch clamp [10] was used to study single channels obtained from excised patches from single endothelial cells. Pipettes were fabricated from thick-walled glass (8161, Garner) using a two-stage pipette puller (Narishige), and fire-polished with a microforge (Narishige). Pipette resistances ranged from 5–12 $M\Omega$ when filled with the HiK solution. The reference electrode used was a Ag-AgCl plug connected to the bath solution via a 150 mM KCl agar bridge. The extracellular face of the patch was used to report voltages. The amplifier was the Axopatch 1C from Axon Instruments. Single channel fluctuations were initially stored on FM tape (Racal) and digitized later for computer analysis using an analog-to-digital interface (Axon Instruments) connected to an IBM 386 clone. The signal was filtered with a low-pass 8-pole Bessel filter (Frequency Devices) at 5 KHz and digitized at 10 KHz (100 μsec /sample). All the records with single channel activity were filtered at 1 kHz for illustrative purposes.

SINGLE CHANNEL ANALYSIS

Fetchan and Pstat (Axon Instruments) were used for data analysis. The half-amplitude criterion was used to distinguish between the open and the closed states of the channel [5]. P_o was calculated from 30–60 sec records using the equation $P_o = (\text{open time}/\text{total time})$. Time distributions have been binned logarithmically to improve the resolution of multiple exponential components [17]. The routine used to fit the data consisted of a generalized nonlinear least-squares procedure based on the Levenberg-Marquadt algorithm, which fit up to four exponentials to raw data. For previously binned data (distributions), the method used for fitting was the maximum likelihood. Fitting iterations proceeded until convergence was reached, as defined when successive improvements in parameters produce a change in the chi-square value less than 2.5×10^{-7} .

Results

SYNTHESIS OF PEPTIDES

Figure 1 shows the amino acid sequence of noxiustoxin with the peptides synthesized for this work underlined. Eight overlapping hexapeptides, corresponding to the full amino acid sequence of NTX were synthesized. A nonapeptide and an eicosapeptide from the N-terminal region and a pentapeptide and decapeptide from the C-terminal were also synthesized. Figure 2 represents an example of HPLC separation of a synthetic peptide. The main peak from the chromatogram was identified as the hexapeptide NTX_{1-6} by amino acid sequence. A similar procedure was followed to identify all the synthetic peptides used in this work.

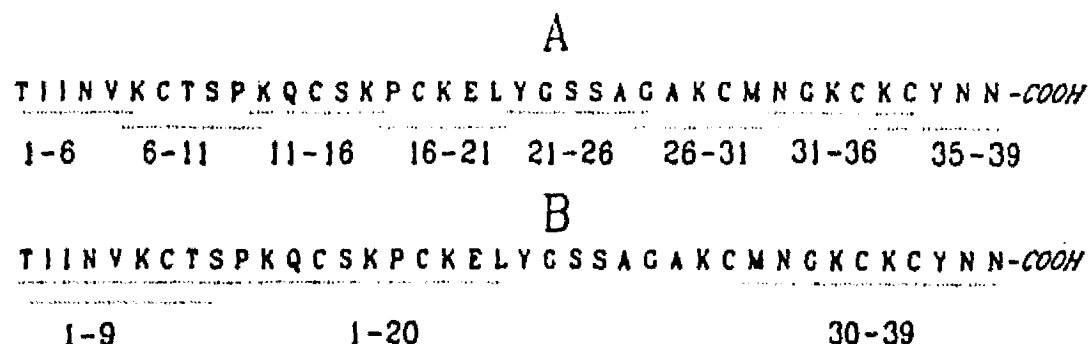


Fig. 1. Peptides synthesized for this work. Panel A: Small peptides (hexapeptides). Panel B: larger peptides. All peptides are aligned by their N-terminal region with NTX sequence.

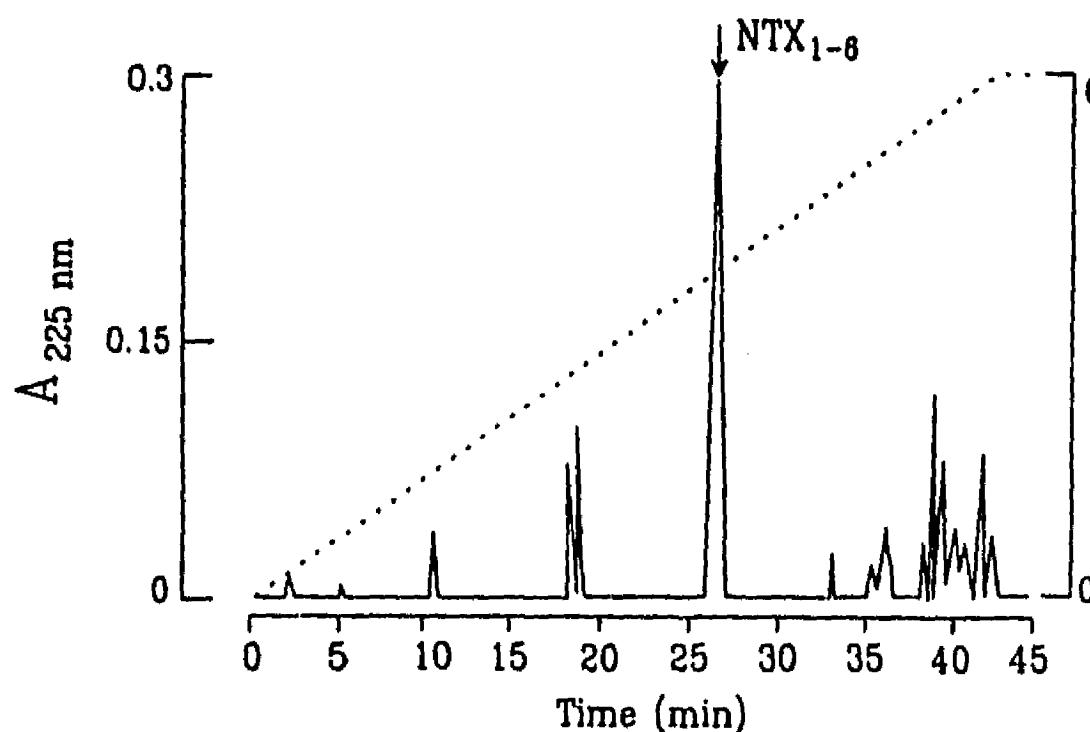


Fig. 2. HPLC separation of synthetic peptide NTX₁₋₆. The peptide (228 µg) was injected at time zero in a Beckman chromatographic system. An Altex C₁₈ reverse phase column was used to separate the peptides. An isocratic gradient from solvent A (0.12% trifluoroacetic acid in distilled water) to solvent B (0.1% trifluoroacetic acid in acetonitrile) was used to separate the components. Absorbance was measured at 225 nm. The largest peak in the chromatogram (indicated by the arrow) corresponds to NTX₁₋₆ according to amino acid analysis and sequence. Chromatographic separations like this one were used to purify the synthetic peptides in this study.

NTX BLOCKS SINGLE K_{Ca} CHANNELS

The effect of various concentrations of NTX on K_{Ca} channel activity is shown in Fig. 3. NTX induced a concentration-dependent reduction of channel open probability (P_o) with an apparent IC_{50} of ≈310 nM ($n = 4$). NTX blocked this channel only when used in the extracellular solution. When 1 µM NTX was applied to the intracellular face of the channel, no effect on channel P_o was observed ($n = 3$, *data not shown*).

BLOCKAGE INDUCED BY SYNTHETIC PEPTIDES

Synthetic peptides corresponding to overlapping regions from the primary structure of NTX (Fig. 1) were used at different concentrations to identify the region in the NTX sequence responsible for binding and blocking this K_{Ca} channel. Only sequences corresponding to the N-terminal region of NTX were capable of inducing a concentration-dependent reduction of channel P_o . Figure 4 shows the concentration-response curve for those peptides that affected

channel P_o . In general, we found that larger peptides were more effective in reducing channel P_o . The most effective channel blockers were the peptides NTX₁₋₃₉ ($IC_{50} \approx 0.5$ µM) and NTX₁₋₂₀ ($IC_{50} \approx 5$ µM) which comprise the first 20 amino acids from NTX. Less effective were the nonapeptide NTX₁₋₉ ($IC_{50} \approx 40$ µM) and the hexapeptide NTX₁₋₆ ($IC_{50} \approx 500$ µM). The pentapeptide NTX₃₅₋₃₉ and the decapeptide NTX₃₀₋₃₉ corresponding to the C-terminal region of NTX had no effect on channel P_o at the concentrations tested (up to 1 mM, $n = 3$, *data not shown*). The hexapeptides NTX₆₋₁₁ and NTX₁₁₋₁₆, which are contained in the peptide NTX₁₋₂₀, produced no effect on channel P_o at the concentrations tested (up to 1 mM, $n = 4$, *data not shown*). The hexapeptides NTX₁₆₋₂₁ and NTX₂₁₋₂₆ were also unable to modify channel P_o (1 mM, $n = 3$, *data not shown*), just like the other peptides from the C-terminal region of NTX. These results indicate that the first 1–20 amino acids of NTX are essential for recognizing this K_{Ca} channel but only the peptides containing the region 1–6 can block the channel. This was the minimum region required to block the channel.

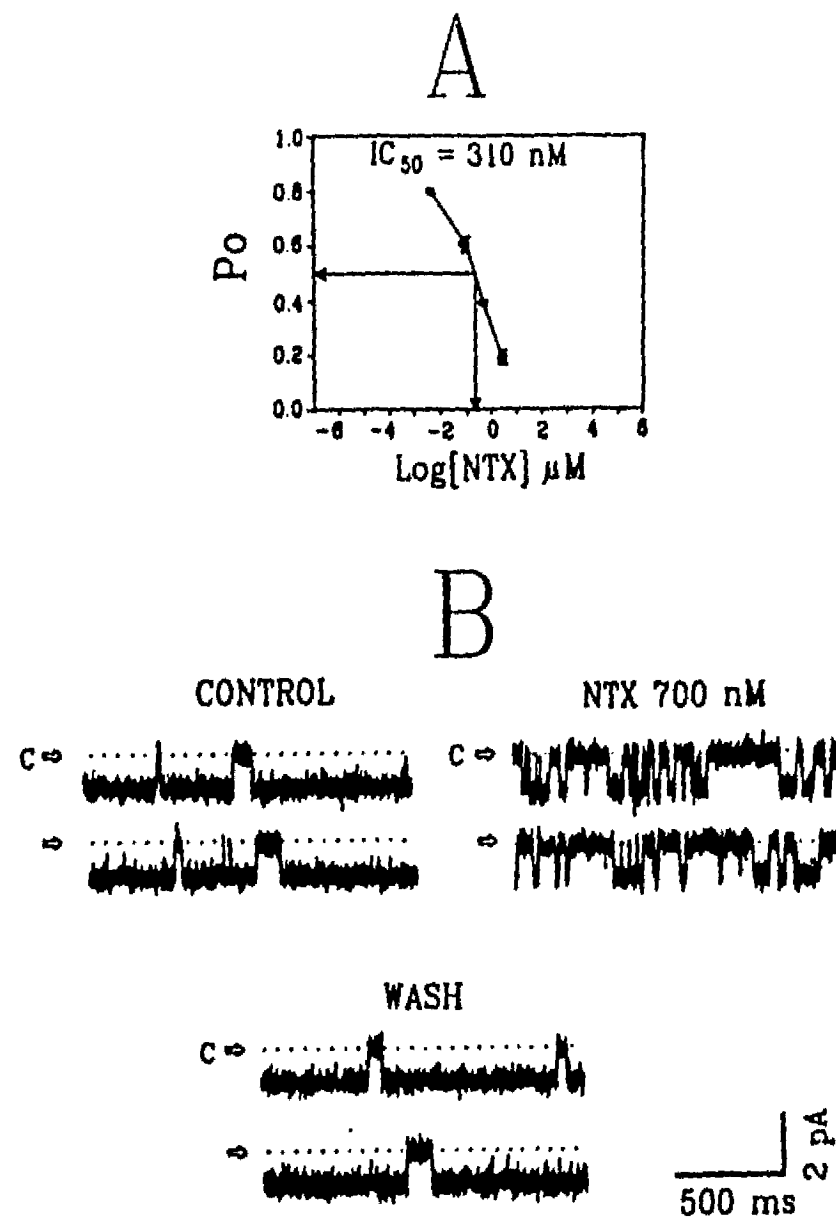


Fig. 3. Noxiustoxin blocks single K_{C_6} channels in BAECs. (A) Concentration-response curve for NTX obtained at -40 mV. Unbroken line was used to connect data points. The half inhibitory concentration (IC_{50}) = 310 nM ($n = 4$). (B) Examples with channel activity at -40 mV from an outside-out patch containing one K_{C_6} channel. Solutions used symmetrical HiK. The dotted line indicates the zero current level (baseline). Arrows point to the closed level (C). Channel activity was monitored under control conditions and after addition of several concentrations of NTX (only 700 nM shown). Full recovery was achieved after replacing the bath solution with toxin-free buffer.

MODULATION OF OPEN AND CLOSED TIMES

Figure 5 illustrates the effect of NTX on channel open and closed time distributions. Under control conditions the channel displayed two mean open and two mean closed times when measured at -40 mV. The time constants for the open time distributions were ≈ 150 and ≈ 6 msec. The time constants for the closed state were ≈ 0.6 and ≈ 8 msec. At the IC_{50} of the NTX the long-lived open time was reduced from 147 ± 6 msec (control) to 5.1 ± 2 msec (300 nM NTX). The short-lived open time was also affected by NTX. At the IC_{50} this time constant was reduced from 6.15 msec (control) to 0.38 msec (300 nM NTX).

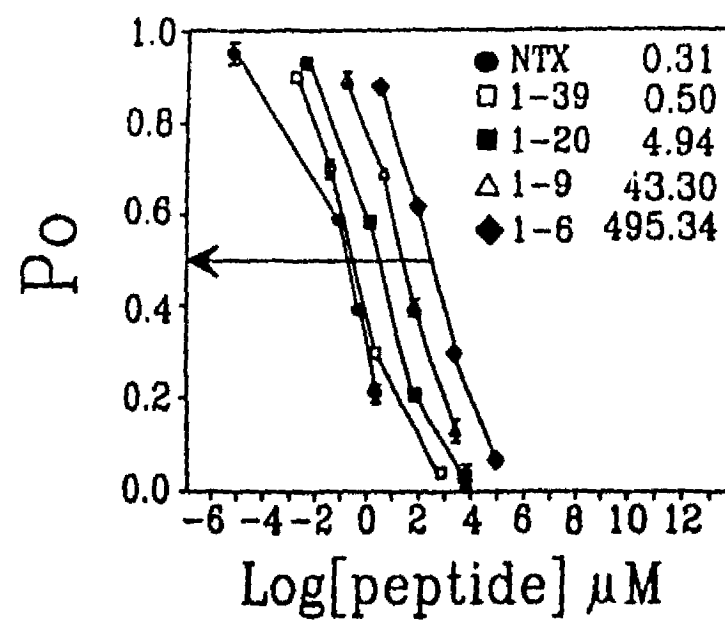


Fig. 4. Concentration-response curves for synthetic peptides. Concentration-response curve for the peptides that affected channel P_o . Half inhibitory concentrations for native NTX (●, $n = 4$), NTX₁₋₃₉ (□, $n = 3$), NTX₁₋₂₀ (■, $n = 5$), NTX₁₋₉ (△, $n = 4$) and NTX₁₋₆ (◆, $n = 6$). Unbroken lines were used to connect data points. The holding potential is -40 mV. Solutions used symmetrical HiK.

Figure 6 shows the effect of the N-terminal synthetic peptides on the time distributions. NTX and the synthetic peptides affected in a similar way the time distributions of the channel. All the effective peptides reduced the long-lived open time of the channel ≈ 25 – 30 times and the short open time ≈ 7 – 13 times with little effect on the closed time distributions.

EFFECT OF VOLTAGE ON K_{C_6} CHANNEL BLOCK

Previous studies reporting the effect of NTX on voltage-gated K^+ currents from squid axon indicated that at low concentrations the blockade induced by NTX was voltage insensitive but at larger concentrations (≥ 1.5 μM) the blockade was voltage sensitive [2]. Contrary to this report, we found that in this K_{C_6} channel the blockade induced by NTX was poorly affected by changes in the membrane potential; however, voltages outside the range ± 60 mV were not explored. Figure 7 illustrates the effect of two different voltages ($+60$ and -60 mV) on the IC_{50} for NTX and the synthetic peptides. Positive voltages released more effectively the blockade produced by the peptides NTX₁₋₆ and NTX₁₋₉, with little or no effect on the blockade produced by NTX, NTX₁₋₃₉ or NTX₁₋₂₀. This result indicates that the blockage by small peptides lacking the region NTX₁₀₋₂₀ can be slightly attenuated by membrane depolarization.

Discussion

BLOCKADE BY NTX AND SYNTHETIC PEPTIDES

The parallel shift in the concentration-response curves of NTX and the synthetic peptides suggests that the difference between the native toxin and the peptide fragments resides in their apparent affinities for the channel. We found that larger peptides were more effective channel blockers. However, large peptides lacking the sequence NTX₁₋₆ produced no effect on channel P_o (e.g., peptide NTX₃₀₋₃₉). The minimum sequence capable of blocking the channel was the hexapeptide NTX₁₋₆; however, the most effective channel blockers were the peptides NTX₁₋₃₉, NTX₁₋₂₀ and NTX₁₋₉ (in that order). When measuring in previous studies the ability of these peptides to induce neurotransmitter release in mouse synaptosomes mediated through voltage-gated K^+ channels, we found the same potency sequence [9]. This result suggests that the binding site recognized by NTX and the synthetic peptides is conserved among various types of K^+ channels. However, the affinity of NTX for different types of K^+ channels is variable. In this study we found an apparent affinity of ≈ 300 nM for native NTX. Valdivia et al. [18] reported that NTX blocks K_{C_6} channels of large conductance with an apparent affinity of 450 nM. Carbone et al. [2] reported an apparent affinity of 290 nM for the delayed rectifier while Sands et al. [15] found that NTX blocks voltage-gated K^+ channels from T lymphocytes with an apparent affinity of 0.20 nM. The apparent affinity reported here is within the range of previously published values obtained in whole-cell experiments with BAECs [4].

MODULATION OF OPEN TIME BY THE TOXINS

The major effect of NTX and synthetic peptides was the reduction of the open time constants with little or no effect on the closed time distributions. The affinity of the toxins (NTX and synthetic peptides) for the channel is proportional to the ability of the toxins to reduce the association constant. At the IC₅₀ of the toxins the long mean open time was reduced ≈ 30 times while the short-lived open time was reduced $\approx 7-13$ from the control values. Interestingly, a third nonconducting state (presumably the blocked state) could not be identified. This suggests that the mean lifetime of the blocked state is similar to that of the nonconducting (closed) states. The relative occurrence of the blocked state is difficult to calculate since the blocked and the closed states are nonconducting (they have the same ampli-

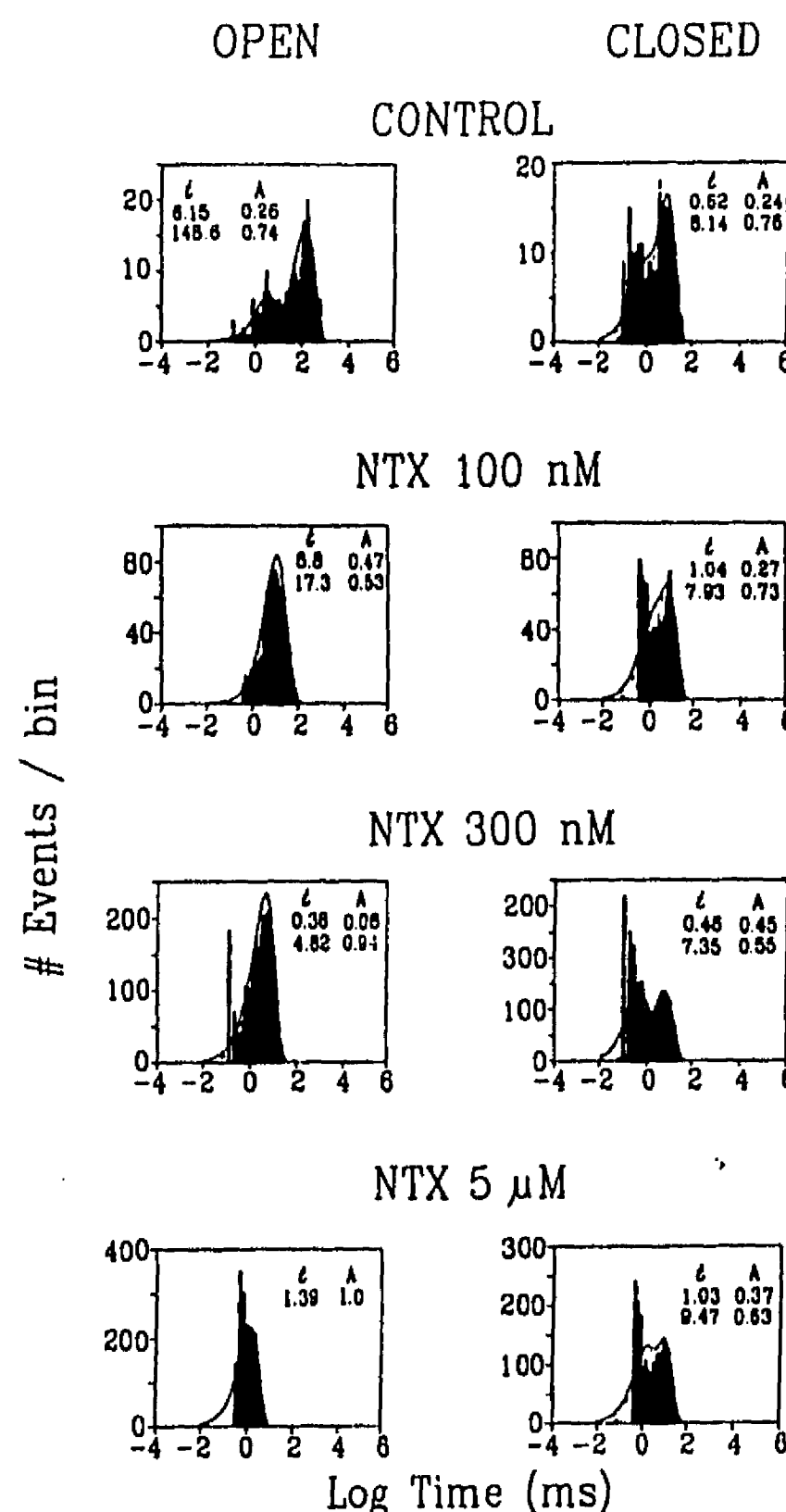


Fig. 5. Effect of NTX on channel open and closed time distributions. Dwell-time distributions obtained from one outside-out patch under control conditions and after addition of 100 nM, 300 nM and 5 μ M NTX to the bath (extracellular) solution. Open and closed time distributions were binned logarithmically from records containing 50–60 sec of continuous channel activity for each experimental condition. The binwidth used was 0.1 msec. Time constant (t) in milliseconds and amplitude (A) for each exponential component are shown in the inset. The P_o obtained for each experimental condition was 0.95 (control), 0.68 (100 nM), 0.52 (300 nM) and 0.14 (5 μ M). The dotted line indicates the individual exponential and the unbroken line represents the fit to a double exponential function. Holding potential for all measurements was -40 mV. Symmetrical HiK solution.

tudes) and no significant difference was observed on either closed time constants at any of the toxin concentrations tested.

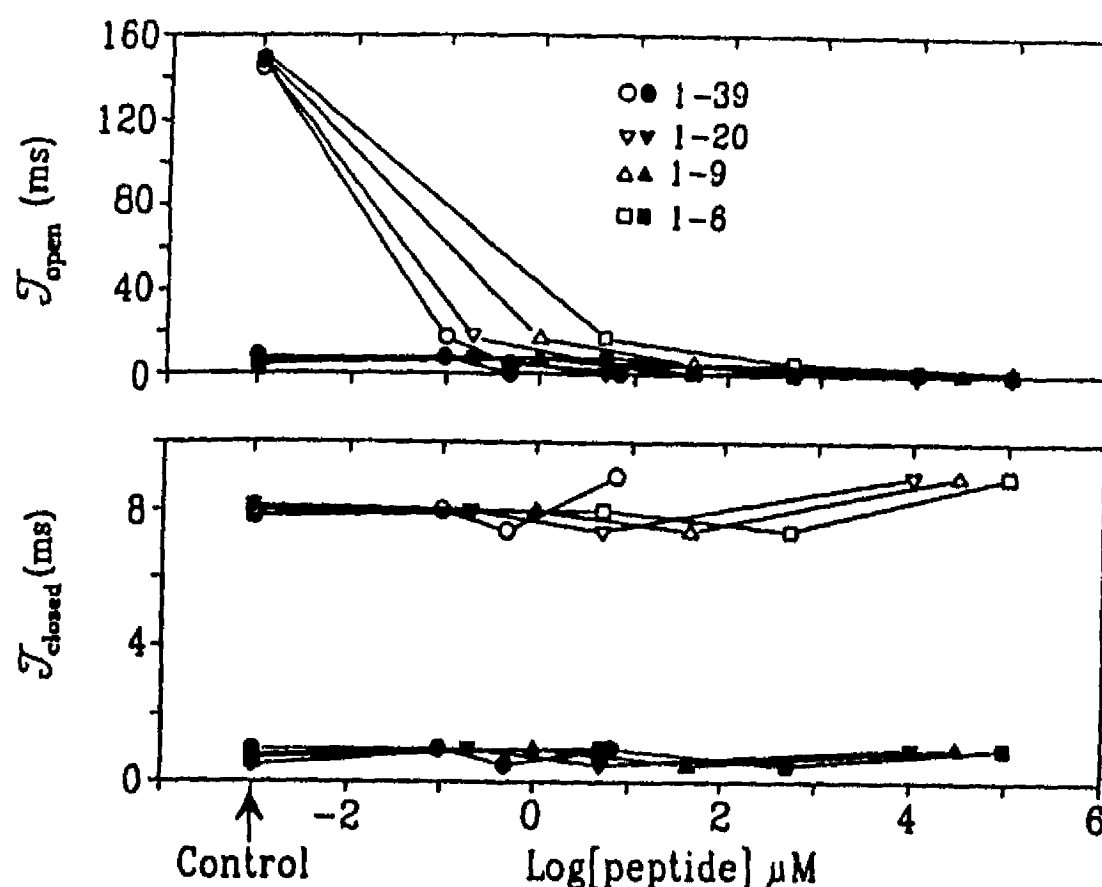


Fig. 6. Effect of synthetic peptides on channel open and closed time distributions. Mean open and closed times obtained at different concentrations of the synthetic peptides. These mean times were obtained after fitting with a double exponential function experiments like the one described in Fig. 5. Open symbols represent long-lived events while close symbols indicate short-lived events for NTX_{1-39} (\bullet , $n = 3$), NTX_{1-20} (∇ , $n = 4$), NTX_{1-9} (Δ , $n = 3$) and NTX_{1-6} (\square , $n = 2$). The unbroken lines through the data represent a linear least-squares fit. Holding potential for all measurements was -40 mV. Channel activity was obtained from at least one minute of continuous recording in symmetrical HIK solution.

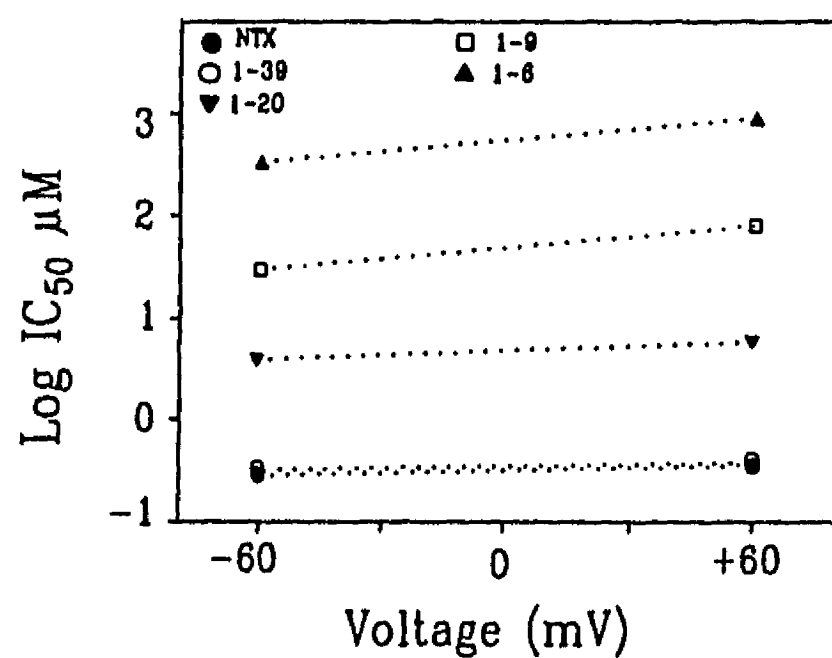
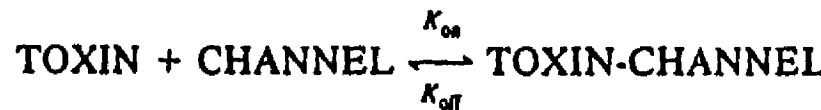


Fig. 7. Effect of voltage on channel blockade. The effect of two different voltages (-60 and $+60$ mV) on the IC_{50} of NTX (\bullet , $n = 3$) and the synthetic peptides NTX_{1-39} (\circ , $n = 3$), NTX_{1-20} (∇ , $n = 4$), NTX_{1-9} (\square , $n = 4$) and NTX_{1-6} (Δ , $n = 3$) explored in outside-out patches. The IC_{50} used here were obtained from concentration-response curves as those illustrated in Fig. 4. Solutions used symmetrical HIK.

If we assume a simple bimolecular binding model to approach the mechanism of block by the toxins, we can express it as follows:



Where K_{on} = association constant and K_{off} = dissociation constant. The equilibrium dissociation con-

stant should be $K_d = K_{\text{off}}/K_{\text{on}}$. For this model to be valid the following criteria need to be met. (i) The time constants of the blocked state ($1/K_{\text{off}}$) should be independent of the toxin concentration, (ii) the time constant of the unblocked state ($1/K_{\text{on}}$) should decrease proportionally with increasing toxin concentrations. Our results are consistent with this model.

EFFECT OF VOLTAGE ON CHANNEL BLOCKADE

The blockade induced by native NTX is insensitive to changes in membrane potential in the range ± 60 mV with symmetrical K^+ . However, the blockade produced by synthetic peptides lacking the C-terminal region of NTX can be partially released by depolarization. This result suggests that in the region 10–20 of the primary structure of NTX there is a specific sequence which prevents the release of blockade by depolarization. This sequence may stabilize the binding of the toxin to its receptor in the channel or prevent the toxin from sensing the transmembrane potential (or both).

STRUCTURE-FUNCTION RELATIONSHIPS

NTX belongs to a family of small peptides targeting K^+ channels. This family of toxins is composed of NTX, charybdotoxin (CTX) a toxin isolated from a European scorpion [12] and the recently isolated iberiotoxin (IBX) [8]. CTX and IBX share 68% sequence homology between them and about 50% ho-

mology with NTX. CTX and IBX block K_{Ca} channels in a similar way—both toxins induce long-lasting nonconducting periods of minutes in duration. The effect of NTX on the K_{Ca} channel is clearly different. NTX induces a fast flickering block in K_{Ca} channels ([17] and this study). We have shown here that the amino acid sequence that recognizes K_{Ca} channels is located in the N-terminal region of NTX. A recent report indicates that the C-terminal region of CTX appears to be involved in recognizing the K_{Ca} channel [13]. Point mutations of CTX at Arg25, Lys27 and Arg34 decreased the toxin affinity for the channel. In that study the affinity change was produced by an increased dissociation rate. In our study, changes in the toxin affinity for the K_{Ca} channel were related to a decrease in the association rate. Interestingly, the higher homology among these toxins (CTX, IBX and NTX) occurs at the C-terminal region. Amino acids 25, 27 and 34 are identical between CTX and IBX; however, in NTX the only amino acid conserved is Lys27, the other two amino acids are replaced by an Ala at position 25 and a Lys at position 34.

This study was supported by grant HL-45880 from the National Institutes of Health, and by grant 900946 from the American Heart Association to D.L.K. and Howard Hughes Medical Institute No. 75191-527104, CONACyT-Mexico No. 0018-N9105, and DGAPA-UNAM No. IN 202689 to L.D.P. This work was partially supported by a Grant-in-aid No. 92014250 from the American Heart Association to L.V.

References

- Carbone, E., Lux, H.D. 1987. Kinetics and selectivity of a low voltage activated calcium current in chick and rat sensory neurones. *J. Physiol.* 386:547–570
- Carbone, E., Prestipino, G., Spadavecchia, F., Francolini, F., Possani, L.D. 1987. Blocking of the squid axon K^+ channel by noxiustoxin: a toxin from the venom of the scorpion *Centruroides noxius*. *Pfluegers Arch.* 408:423–431
- Carbone, E., Wanke, E., Prestipino, G., Possani, L.D., MacLennan, A. 1982. Selective blockage of voltage-dependent K^+ channels by a novel scorpion toxin. *Nature* 296:90–91
- Colden-Stanfield, M., Schilling, W.P., Possani, L.D., Kunze, D.L. 1990. Bradykinin-induced K^+ current in cultured bovine aortic endothelial cells. *J. Membrane Biol.* 116:227–238
- Colquhoun, D., Sigworth, F.J. 1983. Fitting and statistical analysis of single-channel records. In: *Single-Channel Recording*. Chapter 11. B. Sakmann and E. Neher, editors. Plenum, NY
- Eskin, S.C., Sybers, H.D., Trevino, L., Lie, T., Chimoskey, J.E. 1978. Comparison of tissue-cultured bovine endothelial cells from aorta and saphenous vein. *In: Vitro Cell Dev. Biology* 14:903–910
- Fabiato, A. 1988. Computer programs for calculating total from specified free or free from specified total ionic concentrations in aqueous solutions containing multiple metals and ligands. *Methods Enzymol.* 157:378–417
- Galvez, A., Gimenez-Gallego, G., Reuben, J.P., Roy-Constantin, L., Feigenbaum, P., Kaczorowski, G.J., Garcia, M.L. 1990. Purification of a unique, potent, peptidyl probe for the high conductance calcium-activated potassium channel from venom of the scorpion *Buthus tamulus*. *J. Biol. Chem.* 265:11083–11090
- Gurrola, G.B., Molinar-Rode, R., Stiges, M., Bayon, A., Possani, L.D. 1989. Synthetic peptides corresponding to the sequence of noxiustoxin indicate that the active site of this K^+ channel blocker is located on its amino-terminal portion. *J. Neural Transm.* 77:11–20
- Hamill, O.D.P., Marty, A., Neher, E., Sakmann, B., Sigworth, F.J. 1981. Improved patch-clamp techniques for high-resolution current recording from cells and cell-free membrane patches. *Pfluegers Arch.* 391:85–100
- Merrifield, B.R. 1963. Solid phase peptide synthesis I: The synthesis of a tetrapeptide. *J. Am. Chem. Soc.* 85:2144–2154
- Miller, C., Moczydowski, E., Latorre, R., Phillips, M. 1985. Charybdotoxin, a protein inhibitor of single Ca^{2+} -activated K^+ channels from mammalian skeletal muscle. *Nature* 313:316–318
- Park, C.S., Miller, C. 1992. Mapping function to structure in a channel-blocking peptide: electrostatic mutants of charybdotoxin. *Biochemistry* 31:7749–7755
- Possani, L.D., Martin, B.M., Svenden, I. 1982. The primary structure of noxiustoxin: a K^+ channel blocker peptide purified from the venom of the scorpion *Centruroides noxius* Hoffmann. *Carlsberg Res. Commun.* 47:285–289
- Sands, S.B., Lewis, R.S., Cahalan, M.D. 1989. Charybdotoxin blocks voltage-gated K^+ channels in human and murine T lymphocytes. *J. Gen. Physiol.* 93:1061–1074
- Sarin, V.K., Kent, S.B.H., Tam, J.P., Merrifield, B.R. 1981. Quantitative monitoring of solid-phase peptide synthesis by ninhydrin reaction. *Anal. Biochem.* 117:739–750
- Sigworth, F.J., Sine, S.M. 1987. Data transformation for improved display and fitting of single-channel dwell time histograms. *Biophys. J.* 52:1047–1054
- Valdivia, H.H., Smith, J.S., Martin, B.M., Coronado, R., Possani, L.D. 1988. Charybdotoxin and noxiustoxin, two homologous peptide inhibitors of the K_{Ca} channel. *FEBS Lett.* 2:280–284

Trabajo como co-autor.

Possani, LD; Gurrola, GB; Portugal, GO; Zamudio, FZ; Vaca, L; Calderon, ESA & Kirsch, GE. (1991) Scorpion toxins: A model for peptide synthesis of new drugs. [IN] Proceedings of the first Brazilian congress on proteins. Editores Benedito Oliveira y Valdemiro Sgarbieri. Editorial Unicamp

Editors
Benedito Olivetra
Valdemiro Sgarbieri

**PROCEEDINGS OF THE
FIRST BRAZILIAN CONGRESS
ON PROTEINS**

~E

**FICHA CATALOGRÁFICA ELABORADA PELA
BIBLIOTECA CENTRAL - UNICAMP**

B739p	Brasília Congress on Proteins (1.; 1990 : UNICAMP <i>Proceedings of the / first Brazilian Congress on Proteins; editors Benedito de Oliveira Filho, Valdemiro C. Sgarbieri -- Campinas, SP: Editora da UNICAMP, 1991.</i> 1. Proteínas. 2. Bioquímica. I. Oliveira Filho, Benedito de. II. Sgarbieri, Valdemiro C. III. Título. ISBN 85-268-0201-1 20. CDD - 574.192 45 - 574.192
-------	--------------------------------------------------------------------------------------------------------------------------------------------------------------------------------------------------------------------------------------------------------------------------------------------------------------------------------------------------------------------------------------------------------------------

Índices para catálogo sistemático:

- | | |
|---------------|------------|
| 1. Proteínas | 574.192 45 |
| 2. Bioquímica | 574.192 |

Copyright © 1991 by Benedito de Oliveira Filho
Valdemiro C. Sgarbieri

Coordenação Editorial
Carmen Sívia Palma

Revisão
Lúcia Maria de Castro Gobos
Maria Victoria P. L. Castro

Composição
Microaser Editoração Eletrônica
Sociedade Comercial Ltda.

Arte-final
Edilson Trindade

Capa
Antonio Marchini

1991
Editora da Unicamp
Rua Cecílio Feltrin, 253
Cidade Universitária - Barão Geraldo
CEP 13083 - Campinas - SP - Brasil
Tel.: (0192) 39-3720
Fax: (0192) 39-3157

SCORPION TOXINS: A MODEL FOR PEPTIDE SYNTHESIS OF NEW DRUGS

L.D. POSSANI; G.B. GURROLA; T.O. PORTUGAL; E.Z. ZAMUDIO;
L.D. VACA; E.S.A. CALDERON and G.E. KIRSCH*

Department of Biochemistry, Centro de Investigación sobre Ingeniería Genética y Biotecnología,
Universidad Nacional Autónoma de México, Apartado Postal 510-3, Cuernavaca, 62270 México.
Department of Physiology and Molecular Biophysics, Baylor College of Medicine, Houston, Texas
77030, USA.

Scorpion toxins are basic polypeptides of relatively low molecular weight (1), that recognize Na^+ and K^+ ion channels of excitable membranes (2). Two families of scorpion toxins have been described (review 3): long-chain peptides with 60 to 66 amino acid residues tightly bound by four disulfide bridges (4,5), which are specific blockers of Na^+ channels (6, reviews 7 and 8) and short-chain peptides with 38-39 amino acid residues bound by three disulfide bridges (9,10), that block K^+ channels (11, 12, reviews 13 and 14) of several excitable tissues. The most thoroughly studied are the Na^+ channel blockers, for which two sub-types of toxins have been named: α toxins, initially found in the Old World (Asia and Africa) scorpions, which affect the inactivation mechanism of the Na^+ channels and β toxins, found originally in the New World (America) scorpions, which modify the activation mechanism of the Na^+ channels. The complete amino acid sequence for at least 20 such toxins have been reported. The tridimensional structure, by X-Ray diffraction, is presently known for two distinct Na^+ channel toxins (5). Studies on the structure-function relationship of these toxins started with chemical modifications of specific residues in the native peptides (15). Recently, entirely synthetic peptides corresponding to the amino acid sequences of native toxins have been prepared (16, 17). A final objective is to obtain information on structural features of the toxins, that cause a specific function on excitable tissues. An alternative goal is to modify the toxicity of these peptides without affecting too much their antigenic determinants, for possible applications of such compounds in serotherapy or in direct immunization schemes, as synthetic vaccines. The purpose of this manuscript is to address various aspects of these experimental strategies. First, we describe the synthesis of several fragments from toxic peptides extracted, purified and characterized from the Mexican scorpion *Centruroides noxius*. Second, we analyze the direct effect of the chemically obtained peptides on different biological preparations, and we verify their immunological properties in murine immune system. Finally, based on theoretical considerations of the structural similarities of Na^+ channel blocking toxins obtained through the metric analysis method (18), we report the design and synthesis of a chimeric toxin, and we study its biological properties, showing that scorpion toxins are good models for testing possible new pharmaceutical drugs.

MATERIAL AND METHODS**Purification and Characterization of Toxins.**

Venom from *Centruroides noxius* scorpions collected in Nayarit State (Mexico) was obtained by electrical stimulation of the glands (telsons), dissolved in water, centrifuged and the supernatant was freeze-dried and stored at -20°C, until used. Usually 10,000 scorpions are required to obtain 1 gram of venom.

Purification of toxins was carried out by the procedure previously described (3, 19). Briefly, soluble venom is separated by gel filtration in Sephadex G-50 column (0.9 x 200 cm), in 20 mM ammonium acetate buffer, pH 4.7. Toxic fractions are further separated by ion exchange chromatography in two steps: first, a carboxymethyl-cellulose column (0.9 x 30 cm) equilibrated with 20 mM ammonium acetate buffer, pH 4.7 and eluted with a sodium chloride gradient from 0.0 to 0.5 M; and second, a similar chromatographic column, but at 50 mM sodium phosphate buffer pH 6.0, eluted with NaCl gradient from 0.0 to 0.38M (3). Toxic components are monitored by intraperitoneal injection into albino mice (strain CD1), of 100 to 200 µl of fractions containing from 5 to 50 µg protein each. Lethality symptoms are salivation, lacrimation, dyspnea, sporadic convulsions, paralysis of rear limbs, diarrhea, respiratory or cardiac arrest (20). Homogeneity of peptides are followed by gel electrophoresis using the beta-alanine-urea system, described by Reisfeld *et al.* (21). Eventually, a fourth purification step is required for certain toxic fractions, consisting of high performance liquid chromatography (HPLC), through a reverse phase column with an octadecylsilane resin (18). Further chemical characterization of purified components are conducted by amino acid analysis of hydrolysates prepared by the method of Moore and Stein (22) in a Durrum D-500 amino acid analyzer (20). The primary structure determination follows the procedures earlier described (18), by means of automatic Edman degradation (23), using a Beckman 890M microsequencer, or an Applied Biosystem Sequencer (18).

Chemical Synthesis of Peptides

Peptides corresponding to the amino acid sequence of several toxins, purified and sequenced from the venom of the scorpion *C. noxius* (3, 18, 19, 23), was performed by the solid phase method of Merrifield (24). A detailed description of the technique used is found in our previous publications (17, 23). Briefly, this method consist of sequential condensation of protected amino acids, from which the first, at the C-terminal region, is covalently attached to a solid support (24), and subsequent enlargement of the polypeptide chain is obtained by polymerization with carbodiimide in presence of methylene chloride, used as solvent. Side-products are washed in each step of the cycle: deprotection, neutralization, condensation of each new amino acid added to the growing polymer. At the end of the synthesis, the resulting peptide is liberated from the solid support by fluorhydric acid cleavage, which also deprotects the reactive side-chains of some amino acids (24), depending on the specific sequences. For small peptides, containing only two or three amino acids the liquid phase method was used (25). Most peptides were synthesized manually; however, for very large peptides, like the chimeric toxin containing 57 amino acid residues, an automatic Applied Biosystem machine was used, according to the procedure implemented by the company. At the end of the synthesis all peptides were purified, either by thin layer chromatography (dipeptides and tripeptides) or by HPLC.

354 Proceedings of the First Brazilian Congress on Proteins

(larger peptides), as described (17, 25). Verification of the synthesis after purification was carried out mainly by amino acid analysis or by amino acid sequence determination, as described before for the native toxins.

Immunological Studies

Several immunization schemes were followed to produce polyclonal or monoclonal antibodies in mice (strains Balb/c or CD1), (24, 26). Usually pre-immune serum was obtained from each animal before starting an immunization scheme. Several groups of animals, containing 6 to 10 mice, were used for each immunization scheme. Peptide alone (3 to 50 µg) or peptide covalently attached to a carrier molecule, such as mouse serum albumin (24), tyroglobuline (26), or nitrocellulose paper (E. Calderon, unpublished) was used to immunize mice. Immunization proceeded either in presence of Freund adjuvant (24), alumina (26) or alone.

A typical immunization procedure will consist of 6 independent applications of antigens, separated on time by 15 days each, in every single animal. After one week of each injection, the animal were bled for testing the anti-sera. Double immuno-difusion was conducted in agar gels as described (24). Monoclonal antibodies were obtained, selected and cloned, after fusion of spleen cells of immunized mice with a myeloma cell line (SP2/0Ag-14), as described by E. Zamudio (23), and P. Herion, G. Gurrola, R. Saavedra, E. Zamudio, R. Sanchez, and L.D. Possani (in preparation). Radio-immune assay (RIA) or enzymatic-immuno assay (ELISA) were carried out, as described (23-26).

Bioassay and Physiological Characterization of Peptides

Values for medium lethal dose (LD₅₀) of native toxins were obtained as described (20), using six or ten mice for each dose and injecting groups of six or ten mice for every LD₅₀ determination (both for CD1 and Balb c strains of mice). Lethality tests were performed in albino mice (strain CD1) using the three routes of administration. A stock solution of synthetic peptides, corresponding to the amino acid sequence of Noxiustoxin from positions 1 to 9 (NTX1-9) and 30 to 39 (NTX30-39), 10 mg/ml in water, was used. Synthetic peptide NTX1-20 was also tested, but the solubility in water was poor; stock solutions were prepared in presence of organic solvents, such as dimethyl-formamide, and subsequently diluted in appropriated buffers. Anisol, organic solvents and dithiotreitol in water at the same equimolar concentrations as the peptides were also injected in control animals to rule out the possibility of artefactual effects of these possible contaminants. Three animals were injected intraperitoneally, subcutaneously and intraventricularly. The cerebro-ventricular localization of the intra-cranial injection was controlled using Evans-Blue as a marker. Synthetic long-chain chimeric toxin was assayed by intraperitoneal injections in mice (strain CD1), 50 to 400 µg/20 g mouse weight.

The experiments with synaptic terminals (synaptosomes) were performed with brains removed from adult albino mice (strain CD1). Brains without cerebellum of four mice were usually used to obtain purified synaptosomal fraction, following the method of Hajós (27), with slight modifications as described (28). Preloading of synaptosomes with [³H-3H-GABA], perfusion with the various experimental conditions and radioactivity measurements were performed as described (17).

Neutralization experiments with monoclonal or polyclonal antibodies were performed as indicated in the legends of the figures. For monoclonal antibody a 10 fold excess antibody over toxin was mix together and incubated for 1 hr, at room temperature, prior injection to the mice. The amount of toxin used was either the equivalent of one or ten LD₅₀ values. For polyclonal anti-peptide or anti-toxin serum an amount of one LD₅₀ value of toxin was preincubated 1 hr with 80 or 160 µl of serum prior injection to a group of 6 animals.

Cell culture (Neuroblastoma N18 cells) and electrophysiological recordings were performed as previously described (29, 31).

RESULTS AND DISCUSSION

Peptides corresponding to the amino acid sequence of toxins from the scorpion *C. hawaii*, that block both sodium and potassium channels of excitable membranes, were synthesized (Figure 1). From Naxiustoxin (9), the following peptides were prepared: hexapeptide (NTX1-6), nonapeptide (NTX1-9) and eicosapeptide (NTX1-20) from the N-terminal region; pentapeptide (NTX35-39), decapeptide (NTX30-39), nonidecapeptide (NTX21-39) from the C-terminal part of the molecule; the full lenght peptide (NTX1-39) and a discontinuous hexapeptide containing the amino acid sequence of the tripeptide from the C-terminal part, covalently linked to the tripeptide from the N-terminal (NTX-110) region of the toxin. From the Na⁺ channel blocker toxin II-9.22 (19,23), two peptides were synthesized: tetradecapeptide from positions 1 to 14 and a pentapeptide from positions 61 to 65. Finally, a decapeptide from the N-terminal region of toxin II-10 (19, and unpublished) was also synthesized. All peptides were purified by high performance liquid chromatography, their amino acid compositions were determined, and when necessary the amino acid sequence was confirmed by direct Edman degradation in a microsequencer Beckman 890M (17, 23, 26). The long-chain peptide (chimeric-toxin) of 57 amino acid residues was also synthesized and used for toxicity, immunological and electrophysiological experiments (Figure 2.) This chimeric toxin was design following general features of a comparative study, by the metric analysis method (18), of the primary structures of known sodium channel blocking toxins isolated from the venom of scorpion from all over the world. Figure 2 shows some of these characteristics. On the upper part, the α helix (a) and the β sheet (b) forming regions of variant 3 toxin, from *C. sculpturatus*, are shown, based on the X-ray data of this model toxin (5). On the bottom part, all common amino acids, highly conserved, are also indicated. Thirteen primary structures of scorpions toxins are compared. In order to enhance similarities among these sequences, gaps have to be introduced on the primary structures of the toxins from both North African and Asian scorpions, at the N-terminal part of the molecule, approximately at positions 17 to 20, which corresponds to the loop J of the tridimensional structure of the toxin. These peptides belong to the group of the α -scorpion toxins (32), while the toxins from American scorpions, represented by model toxin II of *C. suffusus suffusus*, belong to the β -scorpion toxins (32). The last family of toxins have gaps in the region of the loop B, corresponding to amino acids at positions 43 to 50. α -toxins affect the inactivation mechanism of Na⁺ channel, and β -toxins affect the activation mechanism (32). In designing chimeric toxin β , shown at the lower bottom part of Figure 2, similar amino acids to the American scorpion toxins were chosen, specially at the α helix and β sheet forming amino acids segments of the peptide. All cysteines were conserved and gaps were introduced in the loop J region.

356 Proceedings of the First Brazilian Congress on Proteins

The idea was to preserve general features, typical of the β -scorpion toxins. Two additional amino acids at positions corresponding to the J loop were introduced with the hope to modify affinity for the channel. We expect to obtain a novel synthetic β -scorpion toxin. The results presented here were obtained with the β -chimeric peptide, as produced by the automatic synthesizer, without further purification.

Figure 1. Amino Acid Sequence of Synthetic Peptides.

Peptides	Amino Acid Sequences		
NTX1-39	1	5	10
	Thr-Ile-Ile-Asn-Val-Lys-Cys-Thr-Ser-Pro-		
	11	15	20
	Lys-Gln-Cys-Ser-Lys-Pro-Cys-Lys-Glu-Leu-		
	21	25	30
	Tyr-Gly-Ser-Ser-Ala-Gly-Ala-Lys-Cys-Met-		
	31	35	39
	Asn-Gly-Lys-Cys-Lys-Cys-Tyr-Asn-Asn.		
NTX1-6	Thr-Ile-Ile-Asn-Val-Lys.		
NTX1-9	Thr-Ile-Ile-Asn-Val-Lys-Cys-Thr-Ser.		
NTX1-30	Thr-Ile-Ile-Asn-Val-Lys-Cys-Thr-Ser-Pro-		
	Lys-Gln-Cys-Ser-Lys-Pro-Cys-Lys-Glu-Leu.		
NTX35-39	Lys-Cys-Tyr-Asn-Asn.		
NTX30-39	Met-Asn-Gly-Lys-Cys-Lys-Tyr-Asn-Asn.		
NTX21-39	Tyr-Gly-Ser-Ser-Ala-Gly-Ala-Lys-Cys-Met-		
	Asn-Gly-Lys-Cys-Lys-Cys-Tyr-Asn-Asn.		
NTX110	Tyr-Asn-Asn-Thr-Ile-Ile.		
II-9.2.2(1-14)	1	5	
	Lys-Glu-Gly-Tyr-Leu-Val-Asp-Lys-Asn-		
	10	14	
	Thr-Gly-Cys-Lys-Tyr.		
II-9.2.2(61-65)	61	65	
	Pro-Asn-Lys-Arg-Ser.		
II-10(1-10)	1	5	10
	Lys-Glu-Gly-Tyr-Leu-Val-Asn-Ser-Tyr-Thr.		

X-ray		bbbbb	aaaaaaa	bbbbb	bbbbb
AaH	II	1 VEDGTIVDDVN CTYPC	10 GRAYTCHEEC TELK GESCTCQNASPTGMACTCTKLPDVWTRG PCK CR	10	50 60 70
Lqq	V	1 LDGTIVDDKM CTYPC	GRAYTCHEEC KK KCGESCTCQNASPTGMACTCTKLPDVWTRG PCK CR	CR	CR
Bc	II-10	1 DGTIADDKD CAYPC	GRAYTCHEEC KK GAESCTCQNASPTGMACTCTKLPDVWTRG PCK CR	CR	CR
Lqq	IV	1 GVDAYLADDKQ CVYTC	GSNSYCATEC TK DGAESCTCQMLGKTYGMAWCIRLPDVWPIR PCK CR		
AaH	I	1 KDGTVVYDQN CYTNC	VP F CGGLC KDGGSQSCF LVPAGLACWCIRLPDVWPIR PCK CR		
Ts	gamma	KECTYLMDK ECGRLSCPFR PSCYCCRECCIK K GSSTCAM P	ACYCYGLPMWVKYMDRATNKG		
Ts	III-8	KECTYAMDK ECGRLSCPFR PAGFCDCYCTKMK ASSCTCAM P	ACYCYGVPMK...		
Ts	IV-5	KDGTVVYDQN CAYICWY DMAYCOKLCIK K ADGTCCTW K	ILCYCYGLPXX...		
Css	II	KECTLVSESTGCKYECLELGCDNDYCLAECKQQYCKSSCGYCTA F	ACWCTKLYEQAVVVPLPNETCS		
CsE	V3	KECTLVSESTGCKYECLELGCDNDYCLAECKQQYCKSSCGYCTA F	ACWCEGLPESTPTVPLPNETCS		
CsE	I	KDGTVVYDQN CCGKTCYECLELGCDNDYCLAECKQQYCKSSCGYCTA F	GCTCEGLPDSQTQVPLPNETCS		
Cn	II-14	KDGTVVYDQN ECGKTCYECLELGCDNDYCLAECKQQYCKSSCGYCTA F	CCTCEGLSDSTPTWPLTNETCS		
Clt	I	KECTLVSESTGCKYECPLGCDNDYCLAECKQQYCKSSCGYCTA F	CCWCTKLYEQAVVVPLPNETCS		
Common		Y C C — C C C — C C C			
		loop J loop B			
β -Chimeric		KECTYLMDKSDGC C GAGEG	MDYCLAECKQQYCKSSCGYCTA AG F ACCYC ELCGQ VAG TK C		

Figure 2. Comparison of Primary Structure of Several Toxins by the Method of Metric Analysis. The following sequences were compared (see review 3): AaH II is toxin II from Androctonus australis; Lqq, from scorpion *Leiurus q. quinquestriatus*; Bc, from *Buthus eupeus*; Ts, from *Tityus serrulatus*; Css, from *Centruroides c. suffusus*; CsE, from *C. sculpturatus* Ewing; Cn, from *C. noxius* and Clt from *C. limpidus tecomanus*. The chimeric toxin, type β , was design after this analysis (last sequence). The upper part shows the X-ray diffraction results, where the α and β sheet forming amino acid sequence are labeled (5). In the bottom part of the sequences are also indicated the common amino acids and the loop J and B region of the molecule.

All the above mentioned synthetic peptides were tested for toxicity in mice. Table 1 shows that the most relevant information obtained is the presence of toxicity in peptides corresponding to the N-terminal amino acid sequence of Noxiustoxin (17), and toxin II-10 of *C. noxius*. The β -chimeric peptide was toxic at high concentration. However, peptides corresponding to the C-terminal part of Noxiustoxin were not toxic at very high dose (400 μ g/20 g mouse weight). Lethality tests have shown that the effects were dose dependent, but were independent of the route of administration of the peptides (intraperitoneally, subcutaneously or intra-cranially). Synthetic peptides corresponding to the C-terminal region of NTX were not toxic. The "in vivo" tests were confirmed by "in vitro" experiments using two systems, the neurotransmitter release assay with radiolabeled GABA preloaded to mouse brain synaptosomes (28), and an electrophysiological preparations by means of voltage-clamped measurements on excitable membranes (29). Figure 3 shows the results of some synthetic peptides on 3H-GABA release from synaptic terminals. It is clear from these experiments that the N-terminal fragments: NTX1-9 and NTX1-20 are active on neurotransmitter release, similarly to the effect of native Noxiustoxin, while the C-terminal peptide NTX30-39 is not (17), given additional support to the lethality tests verified in mice. Further evidence showing that the N-terminal nonapeptide and eicosapeptide of Noxiustoxin affect K^+ ion channels was obtained by experiments done with voltage-clamped dorsal root ganglion neurons (33). NTX1-19 blocks the K^+ currents, in a similar manner, as the native toxin; the effect is reversible by washing the preparation with buffer (E. Carbone and L.D. Possani, unpublished).

358 Proceedings of the First Brazilian Congress on Proteins

Table 1. Lethality Tests of Synthetic Peptides.

Peptide (dose μg)	Administration route		
	Intrapерitoneally	Subcutaneously	Intraventricularly
NTX1-9 (200)	Intoxication symptoms within 20 min. Death after 4 hr	Intoxication symptoms within 20 min. hyperexcitability lacrimation, survived	Intoxication convulsions within 12 min. Death before 20 min.
NTX1-9 (100)	Doubtful symptoms	No symptoms	Toxic, death within 20 hr
NTX1-9 (20)	No symptoms	No symptoms	Symptoms slightly different from NTX
NTX1-20 (200)	Deadly	Not tested	Not tested
NTX30-39 (400)	No symptoms	No symptoms	No symptoms
Native NTX (40)	Deadly	Deadly	Deadly
II-10(1-10)-MSA	Deadly	Not tested	Not tested
β -chimeric-57 (400)	Deadly	Not tested	Not tested

Note: MSA is mouse serum albumin to which peptide II-10(1-10) from *C. nasicus* was coupled.

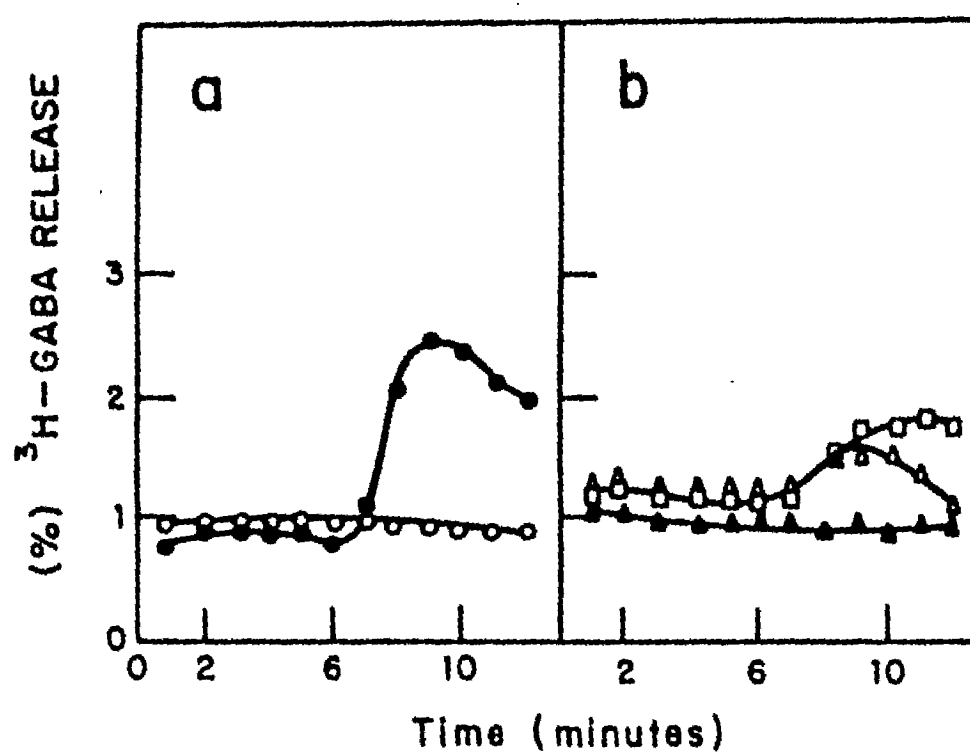


Figure 3. Effect of Native NTX and Synthetic Peptides on Transmitter Release. Synaptosomes obtained from mice were loaded with labeled GABA and perfused with standard Ringer's perfusion medium. Left (a) represents the effect of 0.2 μM native NTX (closed circles) and control (open circles). Right (B) the effect of 100 μM NTX1-9 (open triangles), 100 μM NTX30-39 (closed triangles), and 100 μM NTX1-20 (open squares).

Figure 4 shows the effect of β -chimeric peptide on a N18 neuroblastoma cell line, maintained in voltage-clamped experiments (29). Panels A and B show superimposed Na^+ current records obtained before and eight minutes after adding $9.2 \mu\text{M}$ β -chimeric peptide to the bathing solution. In the presence of toxin, currents were larger at more negative test potentials (A) but smaller at more positive potentials (B). The waveform of the currents in panel B was not altered by synthetic peptide; in particular, the fact that the inactivation phase was unchanged indicates that the chimeric toxin does not behave like an α toxin. Panel C shows the complete current-voltage (I-V) relationships before (open circles) and after (filled circles) chimeric toxin application. Toxin treatment resulted in both a shift of the I-V curve to more negative potentials and a 20% block of maximum conductance. The block could be relieved by washing with toxin-free solution (not shown) but the shift could not. A similar degree of shift was detected in voltage dependence of steady-state inactivation (D). The chimeric toxin therefore shows the characteristic features of β -scorpion toxins, as predicted by the metric analysis studies and by the designin features discussed above (Figure 2). However, the potency seems reduced compared with native toxin, as also expected, although other reason could explain the low toxicity levels of the β -chimeric peptide. For example, the possibility of the presence of undesirables synthetic peptides (crude preparation of synthetic β -chimeric toxin) and/or the presence of wrong formation of the appropriate disulfide bridges. We should recall that this peptide has eight cysteines, with the possibility of forming 4 different disulfide bridges.

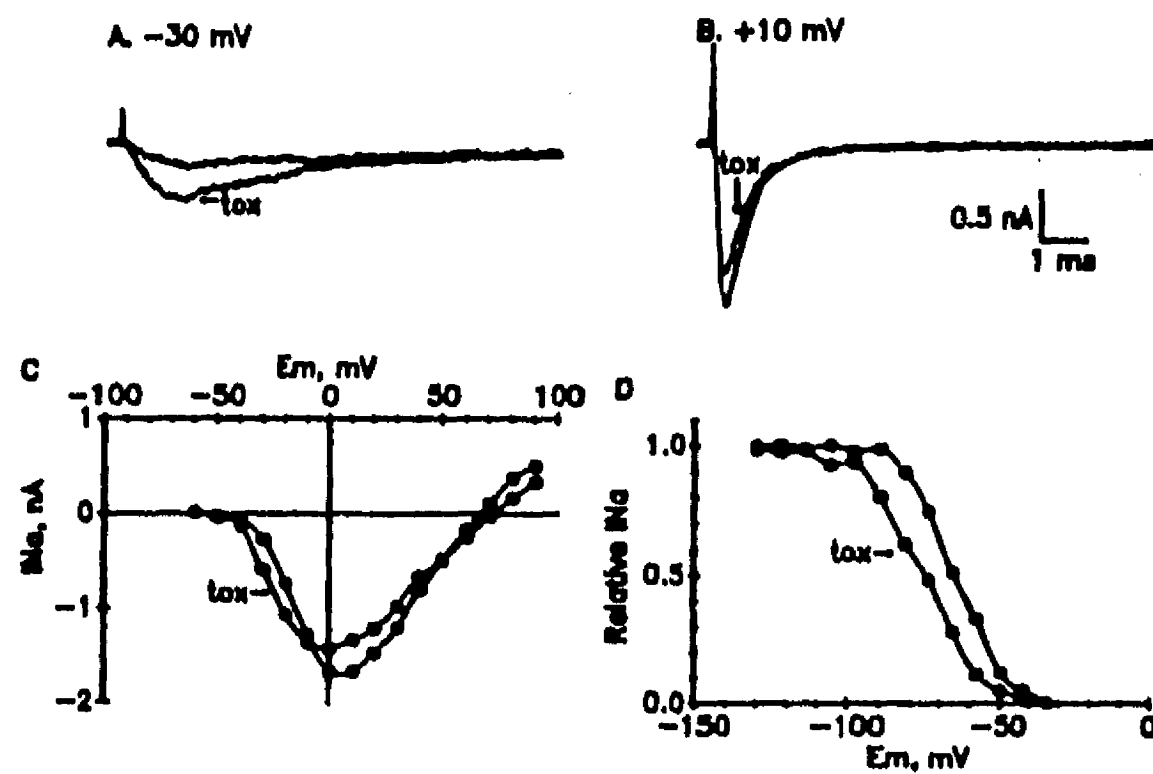


Figure 4. Effects of Chimeric Peptide1-57 on Na^+ currents of N18 Neuroblastoma Cell. Holding potential was -90 mV . The records were filtered at 5 kHz (-3 dB). Panels A-B show superimposed Na^+ current records obtained before and eight minutes after adding $9.2 \mu\text{M}$ toxin to bathing solution. Panel C shows the complete current-voltage (I-V) relationship before (open circles) and after (filled circles) toxin application. A similar degree of shift was detected in the voltage dependence of steady-state inactivation (D). The experiments were performed at room temperature (25°C). Similar results were obtained in 4 additional experiments.

360 Proceedings of the First Brazilian Congress on Proteins

In conclusion, these data shows that it is possible to obtain synthetic peptides, with amino acid sequence corresponding to native toxins, which mimic the function of naturally occurring peptides; hence, opening the possibility of designing new pharmacological drugs to study or to interfere with the normal function of excitable tissues.

The second important set of experiments conducted with the synthetic peptides of Figure 1 and 2 concern the immunological properties of these peptides. As shown in figures 5 to 7, all peptides are capable of eliciting an immunological response in mice. Figure 5 shows the results of immunodiffusion in agarose gels.

Figure 5. Immunodiffusion with Sera Anti-synthetic Peptides. The central well contains synthetic NTX1-39 coupled to mouse serum albumin. Peripheral wells contain anti-sera obtained against synthetic peptides NTX1-39 (lower well), NTX21-39 (right well), NTX30-39 (upper well), and control with buffer-saline (left well).

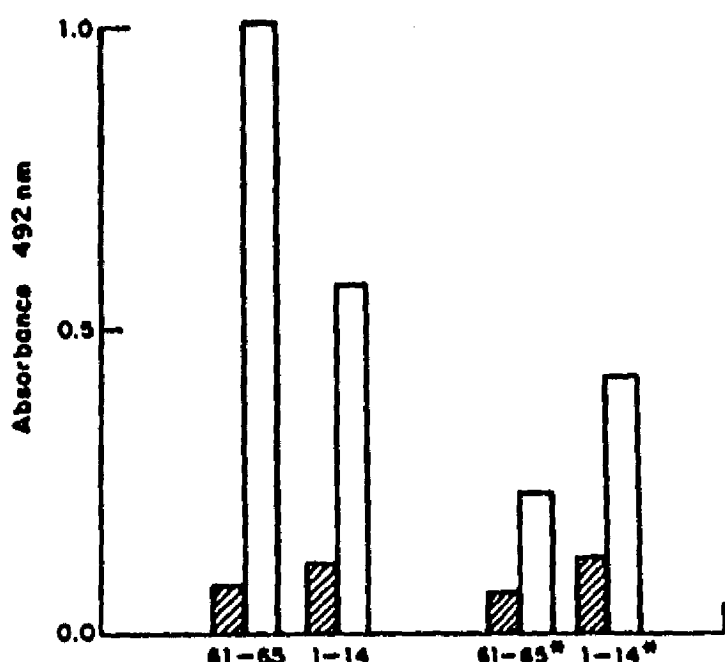
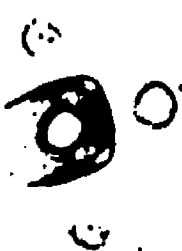


Figure 6. ELISA Assays with Serum from Mice Immunized with Synthetic Peptides. ELISA plates were coated with, either synthetic peptides covalently linked to albumin (left set of bars), or peptides alone* (right set of bars). Anti-sera were obtained with synthetic peptides II-9.2.2(1-14) and II-9.2.2.(61-65). Bars (white) represent immune sera, while shadowed bars are from pre-immune mice.

The central contains well contains full lenght synthetic Noxiustoxin (NTX1-39) coupled to mouse serum albumin, and in the peripheral wells several anti-sera obtained against synthetic peptides NTX1-39 (lower well), NTX21-39 (wright well), NTX30-39 (upper well) and control with buffer-saline (left well). All anti-sera recognize the full lenght synthetic peptide NTX1-39. Care must be taken, because mouse serum albumin treated with carbodiimide alone is also a good antibody forming agent (data not shown). Pre-adsorption of antibodies to albumin must be performed, before assaying the hyper-immune serum, in order to avoid artefactual positive results. Furthermore, mice immunized with synthetic peptide (NTX1-39) are protected when challenged with a lethal dose of native NTX (24). Figure 6 shows the profile of ELISA assays conducted with serum obtained from mice immunized against synthetic tetradecapeptide toxin II-9.2.2 (at positions 1-14), and pentapeptide (positions 61 to 65), corresponding to the C-terminal amino acid sequence of the same toxin from *C. nasicus*. The readings at 492 nm in the ELISA plates were higher for the sera of immunized mice (right bars), compared to pre-immune sera (left bars). Adsorption of peptides linked to a carrier molecule (left set of bars), gives better results than peptide alone (right set of bars). Note that the carrier molecule used for the ELISA assay was albumin, while the carrier used for immunization was tyroglobulin.

This strategies diminishes the probability of false positive results. Another hand the apparent lower levels of antibodies obtained with peptide alone could be due to a lesser extent of binding of the synthetic peptides to the ELISA plates. Regardless of the actual level of antibodies, it seems clear from these experiments, that both peptides (1-14 and 61-65) are immunogenic in mice. The next set of experiments (Figure 7) shows that mice (strain Balb C) immunized with native toxin II-9.2.2 or with β -chimeric peptide1-57 (Figure 2) produces antibodies capable of recognizing the native toxin. In Figure 7 A we show the results of a LD75, that is, the native toxin concentration capable of killing 75% of a mouse population (control mice). Figure 7 B shows the results of direct challenging immunized mice with a LD75 of native toxin. The mice assayed in B were previously immunized with native toxin (six injections of a sub-lethal dose); 100% survival was obtained. Therefore, native toxin II-9.2.2 immunizes mice by producing protecting antibodies. Figure 7 C shows the results of a group of mice used for the determination of the LD50 value of native toxin II-9.2.2; and D shows the challenge of mice (six) with a LD50 concentration (always corrected to 20 g of mouse body weight) of native toxin to mice previously immunized with β -chimeric peptide. No apparent protection was found in this experiment. However, in Figure 7, E and F a definitive result was obtained, showing that animals immunized with the synthetic β -chimeric peptide1-57 produce serum capable of protecting third animals in "in vivo" challenge, after pre-mixing anti-sera against chimeric toxin with native toxin II-9.2.2, in amounts of an equivalent LD50 value. In Figure 7 E, 160 ml of serum from mice immunized with β -chimeric toxin were mixed with buffer containing native toxin II-9.2.2. (one LD50 value), incubated for 1 hr at room temperature and challenged a third group of mice (non immunized); 100% survival was observed. In Figure 7 F, the same experiment was conducted, but decreasing the amount of anti-serum to 80 μ l; a partial protection was obtained, 25% of mice died. The last two experiments show that the serum produced by mice immunized against the synthetic β -chimeric toxin, when mixed with native toxin (one LD50 value) and injected in control mice protect them in a dose dependent manner. An amount equivalent to 160 ml of anti-serum is required to neutralize one LD50 value of native toxin. Taking together the experimental results of Figure 7 C to F we conclude that β -chimeric toxin is potentially promising to serve as a

362 Proceedings of the First Brazilian Congress on Proteins

model for production of a synthetic vaccine against scorpion toxins. The inconclusive results of Figure 7 D can be explained, among other things, by the appearance of immunological sensitization, due to the use of impure antigens (synthetic β -chimeric toxin), which is not an unusual phenomenon.

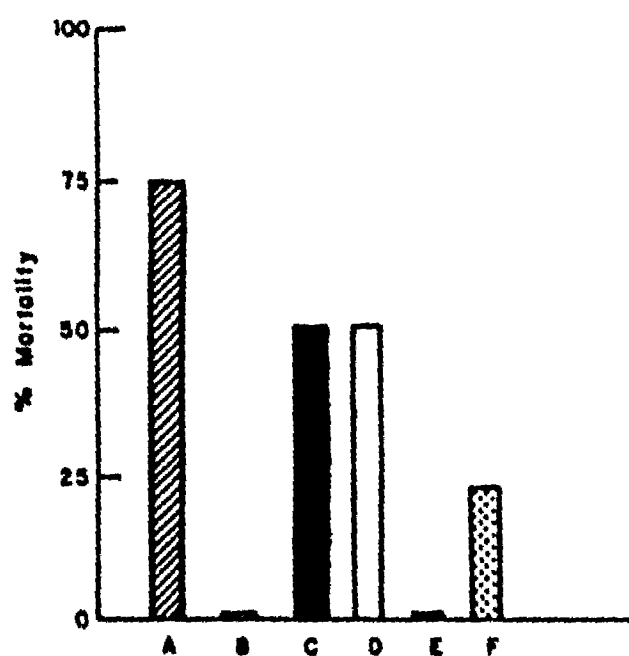


Figure 7. "In vivo" Challenge of Control and Immunized Mice with Native Toxin. Letters A and C represent respectively, the LD₇₅ and LD₅₀ of native toxin II-9.2.2 injected in control animals. B is 100% survival of mice pre-immunized with native II-9.2.2, and challenged with one LD₇₅ of the same toxin. D represents mice pre-immunized with β -chimeric peptide and challenged with one LD₅₀ value of toxin II-9.2.2. E and F are experiments using control animals injected with a mixture of native toxin (one LD₅₀ value) and two different volumes (E is 160 μ l, and F is 80 μ l) of sera obtained from mice preimmunized with β -chimeric peptide 1-57.

Finally, another approach has been followed to study relevant antigenic determinants in the structure of scorpion toxins, by means of the use of monoclonal antibodies.

Figure 8 shows displacement curves of a monoclonal antibody (BNTX-16, produced by P. Hérion, G. Gurrola, R. Saavedra, R. Sánchez, F. Zamudio and L. Possani, unpublished) performed through ELISA assays, using native Noxiustoxin and several synthetic peptides containing amino acid sequences of NTX. The pentapeptide (NTX35-39) is not capable of displacing the binding of native NTX, while synthetic hexapeptide NTX1-6 and the discontinuous peptide NTX10 are capable of displacing almost entirely the binding of native toxin to the monoclonal antibody. The discontinuous peptide is more efficient than the linearly continuous peptides. This type of experiments is useful for determination of possible epitopes in the antigenic molecules, specially if complemented with neutralization experiments, as shown in Table 2. This table reports the results of mixing toxin II-9.2.2 with various distinct monoclonal antibodies (23) and injecting into mice. Toxin alone injected to 5 mice at a dose of 10 LD₅₀ kills all mice within 20 min. The same happens when 10 LD₅₀ doses of toxin are premixed with a non related monoclonal

antibody (BTX-16). However, one of the monoclonal antibodies against toxin II-9.2.2 (BCF2) was capable of prolonging the life of 3 animals for approximately three days (60hr) and actually 2 out of 5 animals survived several weeks (they did not die by scorpion toxin action). If an LD50 dose is used, the 5 animals survive the injection. Other monoclonal antibodies (BCF1, BCF3, BCF7 to 9) prolonged the survival from 15 to 20 hr (data not shown), but all mice eventually died, when injected with an excess of 10 LD50 values of toxin preincubated with purified antibodies (10 fold excess antibody over the molar ratio of toxin). These data were interpreted as follows: only one of the six distinct monoclonal antibodies obtained (23) was able to produce neutralizing antibodies against toxin II-9.2.2.

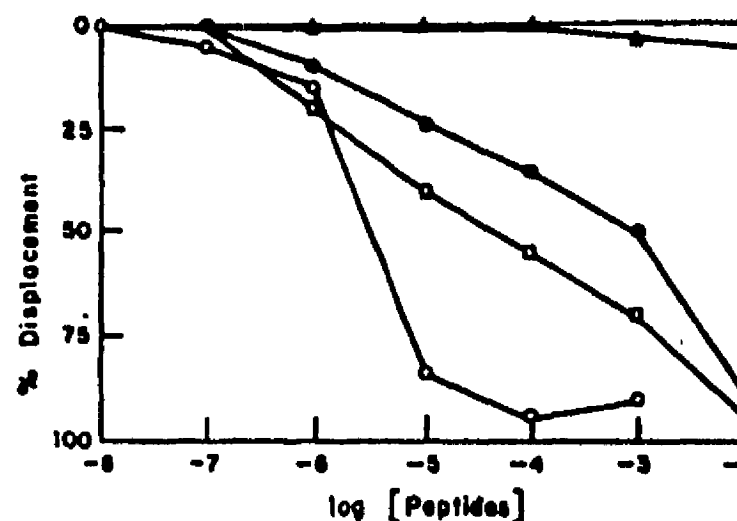


Figure 2. Displacement Curves of Monoclonal Antibody BNTX 16 with Synthetic Peptides. Native Notoxins attached to the ELISA plate is capable of binding monoclonal antibody BTX16. The binding of BNTX16 is displaced by addition of excess free NTX, as indicated by open circles, but is not displaced by synthetic NTX35-39 (open triangles). Two synthetic peptides: NTX1-6 (closed circles) and a discontinuous peptide H10 (open squares) are capable of competing with native toxin for the binding to the monoclonal antibody. Rabbit anti-mouse immunoglobulines attached with peroxidase were used to develop the ELISA color on the plates.

Table 2. "In vivo" Neutralization Assay with Monoclonal Antibodies Anti-toxin C. noxius II-9.2.2.

Mixture injected (toxin + antibody)	Mice Survival (alive/total)	Time of Survival (mean value hours)
Toxin alone	0/5	1/3
Toxin + BNTX16	0/5	1/3
Toxin + BCF1,8,9	0/5	60
Toxin + BCF5	0/5	15
Toxin + BCF2	2/5 [*]	60
Toxin + BCF2	5/5 ^{**}	Indefinite

Quantities of toxin equivalent to ten LD50 values were mixed with antibodies at molar ratio 1:10 (toxin:anti-body), incubated at room temperature for 1 hr, before intraperitoneal injection in 5 mice each experiment; Two mice survived more than 3 weeks, in good health; In this experiment toxin equivalent to one LD50 value was mixed with the monoclonal BCF2.

364 Proceedings of the First Brazilian Congress on Proteins

This antibody (BCF8) is now been examined against a variety of synthetic peptides to determine a plausible epitope, capable of displacing the binding of the monoclonal antibody to the parent toxin. It is expected that a similar result as the one obtained in Figure 8 might be found. In this event, a new synthetic peptide will be designed with the expectancy of obtaining a possible antigen to be used as a vaccine against toxin II-9.2.2 from *C. noxius*. This leads to another problem, since scorpion venoms are composed by families of related toxic peptides and it is important to synthesize a peptide that could protect against all the toxins. Figure 9 shows displacement experiments were a monoclonal antibody (BCF8) was similarly displaced by a variety of different toxins from *C. noxius* venom and by a toxin from another scorpion species *C. limpidus lecomanus*. Analysis of the primary structure of these toxins has provided evidence for conservative regions of the primary structure of the toxins assayed (23). Thus, using this approach relevant information can be obtained, that may turn out to be important in designing new drugs (synthetic vaccines).

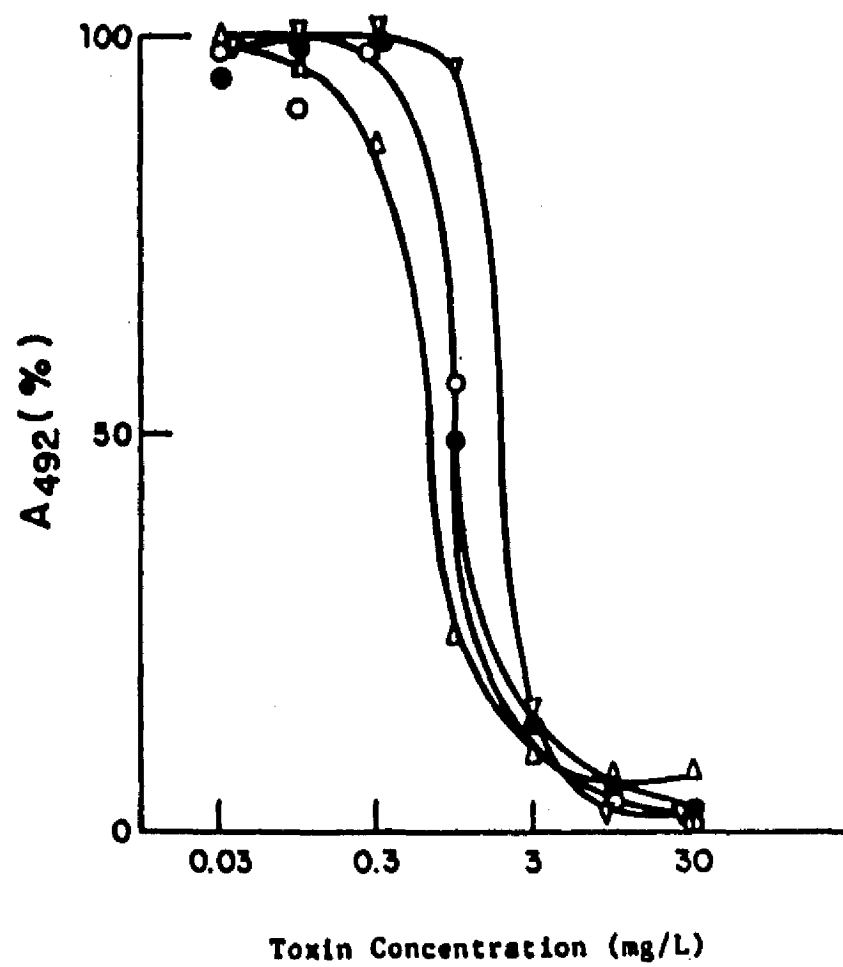


Figure 9. Displacement Experiments with Monoclonal Antibody BCF8. Toxin II-9.2.2 attached to ELISA plates are recognized by the monoclonal antibody BCF8. The binding of this monoclonal is displaced by addition of free native toxin (open circles) at the concentrations indicated. Toxin II-14 (triangles pointing upward) from the same scorpion *C. noxius* is as potent as toxin II-9.2.2 in displacing the binding of monoclonal BCF8 to the plates. Similarly two other toxins: II-10 from *C. noxius* (closed circles) and toxin I from *C. limpidus lecomanus* (triangles pointing downward) are very effective competitors. Rabbit anti-mouse immunoglobulines labeled with peroxidase were used as second antibodies.

SUMMARY

This communication reports experiments utilizing a series of synthetic peptides, which corresponds to the amino acid sequences of fragments of the primary structure of sodium and potassium channel blocking peptides, purified from scorpion venoms. Among these synthetically obtained fragments, some are toxic "per se" and eventually could be used as new drugs for studying ion channel of excitable membranes, such as the nonapeptide NTX1-9. Others are not toxic, but are immunogenic. Larger synthetic peptides, like NTX1-39 and beta-chimeric peptide I-57 are probably better candidates to be used in immunization protocols. In summary, our work documents a number of potentially valuable experimental approaches for the development of new pharmaceutical drugs, namely: the use of monoclonal antibodies obtained against native toxins, displacement experiments with synthetic peptides containing amino acid sequences identical or similar to that of natural toxins, neutralization experiments followed by "in vivo" challenges, and finally, direct lethality tests in conjunction with electrophysiological recordings.

ACKNOWLEDGEMENTS

The technical assistance of Mr. Fredy I. Coronas Valderrama and Humberto Moncada is greatly appreciated. The authors also thank Prof. Dr. Emilio Carbone from the University of Torino (Italy) and Prof. Dr. Arthur Brown from the Baylor College of Medicine (USA) for support and discussions. Dr. Alejandro Bayon and Dr. Maria Sitges from the National University of Mexico (Mexico), are also acknowledged for Figure 3.

This work was partially supported by a grant from Rockefeller Foundation (RF870349, #26), and by grants PVI/QI/NAI/84/2182, PVI/AI/NAI/85/3029 from the Mexican Council of Science and Technology (CONACYT).

REFERENCES

1. MIRANDA, E.; ROCHAT, H.; and LISSITZKY, S. *J. Chromatography*, **7**:142-154, (1962).
2. KOPPENHÖFER, E.; and SCHIMIDT, H. *Pflügers Arch. ges. Physiol.*, **303**:133-149, (1968).
3. POSSANI, L.D. Structure of scorpion toxins, in *Handbook of Natural Toxins* (Ed. A.T.Ib), vol. 2, pp. 513-550, Marcel Dekker Inc., New York, (1984).
4. ROCHAT, H.; BERNARD, P. and COURAUD, E. Scorpion toxins: chemistry and mode of action, in *Advances of Cytopharmacology* (Eds. Ceccarelli, B. and E. Clementi), vol. 3, pp 325-334, Raven Press, New York, (1979).
5. FONTECILLA-CAMPS, J.C.; ALMASSY, R.J.; SUDIDATI, E.L.; WAIT, D.D. and BUGG, C. *Proc. Natl. Acad. Sci. (USA)*, **77**:6496-6500 (1980), and Fontecilla-Camps, J.C., Habersetzer-Rochat, C. and Rochat, H. *Proc. Natl. Acad. Sci. (USA)*, **85**:7443-7447, (1988).
6. CATTERALL, W. *J. Biol. Chem.*, **251**:5528-5536, (1976).
7. MEIVES, H.; SIMARD, J.M. and WAIT, D.D. *Ann. New York Acad. Sci.*, **479**:113-132, (1986).

366 Proceedings of the First Brazilian Congress on Proteins

8. LAZDUNSKI, M.; FRELIN, C.; BARTANIN, J.; LOMBET, A.; MEIRI, H.; PAURON, D.; ROMEY, G.; SCHMID, A.; SCHWEITZ, H.; VIGNI, P. and VIJVERBERG, H.P.M.: *Ann. New York Acad. Sci.*, 479:204-220, (1986).
9. POSSANI, L.D.; MARTIN, B.M. and SVENDSEN, I. *Carlsberg Res. Commun.*, 47:285-289, (1982).
10. GIMÉNEZ-GALLEGO, G.; NAVIA, M.A.; REUBEN, J.P.; KATZ, G.M.; KAC-ZIROWSKI, G.J. and GARCIA, M.L. *Proc. Natl. Acad. Sci. (USA)*, 85:3329-3333, (1988).
11. CARBONE, E.; WANKE, E.; PRESTIPINO, G.; POSSANI, L.D. and MAHLICKE, A. *Nature*, 296:90-91, (1982).
12. MILLER, C.; MOCZYDŁOWSKI, E.; LATORRE, R. and PHILLIPS, M. *Nature*, 313:316-318, (1985).
13. CASTLE, N.A.; HAYLETT, D.G. and JENKINSON, D.H. *Trends Neurosci.*, 12:59-65, (1989).
14. MOCZYDŁOWSKI, E.; LUCCHESI, K. and RAVINDRAN, A. *J. Membrane Biol.*, 105:95-111, (1988).
15. HABERSITZER-ROCHAT, C. and SAMPIERI, F. *Biochemistry*, 15:2254-2261, (1976).
16. GRANIER, C.; BAURAQUI, E.; VAN RIETSCHOTER, ROCHAT, H. and ELAYEB, M. *Int. J. Peptide Protein Res.*, 23:187-197, (1984).
17. GURROLA, G.B.; MOLINAR-RODE, R.; SITGES, M.; BAYON, A. and POSSANI, L.D. *J. Neural Transm.*, 77:11-20, (1989).
18. POSSANI, L.D.; MARTIN, B.M.; SVENDSEN, I.; RODE, G.S. and ERICKSON, B.W. *Biochem. J.*, 229:739-750, (1985).
19. POSSANI, L.D.; DENT, M.A.R.; MARTIN, B.M.; MAHLICKE, A. and SVENDSEN, I. *Carlsberg Res. Commun.*, 46:207-214, (1981).
20. POSSANI, L.D.; ALAGON, A.C.; FLETCHER, Jr. P.L. and ERICKSON, B.W. *Arch. Biochem. Biophys.*, 180:394-403, (1977).
21. REISFIELD, R.A.; LEWIS, U.J. and WILLIAMS, D.E. *Nature*, 195:281-283, (1962).
22. MOORE, S. and STEIN, W.H. Chromatographic determination of amino acids by the use of automatic recording equipment. In: *Methods of Enzymology* (Eds. Colowick, S.P. and Kaplan, N.O.) vol. 6, pp 816-831, Academic Press, New York, (1963).
23. ZAMUDIO, E.Z. Obtención, caracterización y uso de anticuerpos monoclonales para el estudio de estructura y función de toxinas de alacranes. Master of Sciences Thesis presented at the School of Chemistry, Universidad Nacional Autónoma de México, (1989).
24. GURROLA, G.B. Síntesis química de péptidos correspondientes a secuencias de aminoácidos de toxinas de alacranes y sus propiedades. Master of Sciences Thesis presented at the School of Chemistry, Universidad Nacional Autónoma de México (1986).
25. VACA, L.A.D. Síntesis de péptidos correspondientes a la secuencia de la Noxius-toxina: Determinantes antigenicos y efectos sobre canales iónicos. Master of

Sciences Thesis presented to Colegio de Ciencias y Humanidades, Universidad Nacional Autonoma de Mexico, (1989).

26. OLAMENDI, T.C.P.; GURROTA, G.B. and POSSANI, L.D. Respuesta immune de ratones a peptidos sinteticos correspondientes a la secuencia de aminoacidos de la toxina II-9.2.2. del alacran *C. novirus*. Abstract 0142, Proceedings VIII National Congress of the Mexican Immunology Society, S. Luis Potosi, Mexico, (1989).
27. HAJÓS, E. Brain Res., **93**:485-489.
28. SITGES, M.; POSSANI, L.D. and BAYON, A. J. Neuroscience, **6**:1570-1574, (1986).
29. KIRSCH, G.E.; SKATTEBOE, A.; POSSANI, L.D. and BROWN, A.M. J. Gen. Physiol., **93**:67-83, (1989).
30. HAMILI, O.P.; MARTY, A.; SAKMANN, B.; and SIGWORTII, F.J. Muellers Archive, **391**:85-100, (1981).
31. LUX, H.D. and BROWN, A.M. J. Gen. Physiol., **117**:500-544, (1984).
32. JOVER, E.; COURAUD, E. and ROCHAT, H. Biochem. Biophys. Res. Commun., **95**:1607-1614, (1980).
33. CARBONI, E. and LUX, H.D. J. Physiol., **386**:547-570, (1987).

DISCUSION Y CONCLUSIONES

Síntesis de Peptidos. Mediante la técnica de síntesis de péptidos se han obtenido una serie de péptidos sintéticos de diversos tamaños los cuales bloquean al canal de potasio activado por calcio con distintas afinidades. La estructura mínima capaz de bloquear al canal es un hexapeptido constituido por los primeros seis aminoácidos de la región amino terminal de la NTX. Peptidos de mayor tamaño mostraron una afinidad mayor por el canal, sin embargo, péptidos de mediana longitud correspondientes a la región carboxilo terminal no produjeron ningún efecto en el canal. Lo anterior sugiere fuertemente que en esta región (amino terminal) se localiza el receptor a la NTX. Este resultado concuerda con estudios previos de toxicidad y de liberación de neurotransmisores en sinaptosomas realizados con los mismos peptidos [13]. Este es el primer reporte en la literatura demostrando que peptidos pequeños correspondientes a la secuencia de una toxina son capaces de inducir bloqueo en el canal en forma similar a la toxina nativa [40].

Tipo de bloqueo inducido por la NTX y péptidos sintéticos. La forma en la que estos péptidos afectan al canal es la misma, tanto la toxina nativa como los péptidos sintéticos reducen el tiempo de apertura (T_o) de larga duración sin afectar el tiempo de apertura de corta duración o los tiempos de cerrado (T_c) del canal.

Los resultados presentados aquí sugieren que la interacción entre los péptidos sintéticos (o la toxina nativa) y el canal es de tipo bimolecular. Dicha interacción queda expresada en la siguiente ecuación:



En esta ecuación K_{on} = constante de asociación; K_{off} = constante de disociación. La constante de afinidad se define como ($K_d = K_{\text{off}} / K_{\text{on}}$). Para que este modelo sea válido dos premisas deben de cumplirse : 1) el tiempo de bloqueo ($1 / K_{\text{off}}$) debe de ser independiente de la concentración de toxina y 2) el tiempo de apertura ($1 / K_{\text{on}}$) debe decrecer proporcionalmente con concentraciones crecientes de toxina. Ambas premisas se cumplen en los resultados presentados aquí.

Estudios realizados en el canal K_{Ca} de gran conductancia de músculo sugieren que tanto la CTX como la IBX bloquean al canal en forma similar, ambas toxinas se unen a su receptor en forma bimolecular y posteriormente "taponan" al canal impidiendo el paso de iones de potasio [4,22]. Este tipo de bloqueo por "taponamiento" parece ser similar al bloqueo inducido por la NTX en el canal K_{Ca} de mediana conductancia [40].

Efecto de voltaje en el bloqueo. El bloqueo inducido por péptidos en los que la secuencia NTX10-20 es omitida es parcialmente liberado por medio de la aplicación de voltaje. Esto sugiere que dicha secuencia (aminoácidos 10-20) estabiliza el pegado de la toxina a su receptor, de tal forma que no puede ser liberado por la aplicación de voltajes depolarizantes. Una explicación alternativa es que péptidos de pequeño tamaño entran más profundamente en el poro del canal que péptidos de mayor longitud. De esta forma, cambios en el voltaje de la membrana no son sentidos por los péptidos cuando entran en la profundidad del poro. La conclusión anterior es compatible con el hecho de que únicamente el tiempo de apertura largo del canal es reducido por

la toxina y los péptidos sintéticos. Esto indica que la toxina necesita que el canal este abierto cuando menos 100 ms para ser bloqueado. Este tiempo crítico sugiere que tanto la toxina nativa como los péptidos sintéticos requieren que el canal este abierto por ese lapso de tiempo para que dichos péptidos puedan penetrar en el poro abierto y bloquear al canal. Cuando el canal se abre por menos de 100 ms las toxinas (péptidos sintéticos y toxina nativa) no pueden bloquearlo. Lo anterior explica el porque el tiempo de apertura corto del canal no es afectado por las toxinas [40]. La duración media de dicho tiempo es de tan solo unos cuantos milisegundos, lo cual no es suficiente para que los péptidos se adentren en el poro del canal..

Los tiempos de cerrado del canal tampoco son afectados por las toxinas. De esta forma, los resultados obtenidos indican que las toxinas solo pueden bloquear al canal cuando este se encuentra abierto. Cuando el canal se cierra es inaccesible a las toxinas tal y como se muestra en la figura 6 del trabajo original [40].

Dinamica molecular de la relación toxina-canal. El tipo de bloqueo producido por CTX es claramente diferente al producido por NTX (o los péptidos sintéticos de la NTX). Dicha toxina (CTX) si afecta el tiempo de cerrado del canal (figura 5, antecedentes). El tiempo de apertura del canal no es afectado por la CTX. Cuando el canal se abre su comportamiento es como el del control (sin anadir CTX) tal y como se aprecia en la figura 5. Este efecto habia sido previamente reportado para el canal de alta conductancia de músculo liso [42]. La IBX afecta de forma similar al canal K_{Ca} de gran conductancia.

Los resultados anteriores demuestran que si bien NTX, CTX e IBX comparten regiones similares en su secuencia de aminoacidos, dichas toxinas interactuan con el canal de forma diferente. Como se mencionó con anterioridad (antecedentes), la NTX se asocia y disocia de su receptor mas rápidamente que las otras dos toxinas (CTX e IBX). Esto produce cambios rápidos en el canal el cual fibrila entre el estado abierto y el bloqueado en milisegundos. La CTX, a su vez, se asocia y disocia de su receptor mas lentamente que la NTX. De esta forma, cuando la CTX se asocia a su receptor el canal permanece bloqueado por varios segundos. Igualmente, cuando la CTX se disocia de su receptor, el canal se cierra y abre como si no hubiera toxina presente. El caso de la IBX es aun mas acentuado. Los tiempos de asociación y disociación de dicha toxina son de varios minutos de duracion [4]. Lo anterior sugiere que los cambios conformacionales que el canal debe de sufrir para que la IBX se una a su receptor son, termodinamicamente hablando, poco favorables (muy lentos) en comparación con la NTX y la CTX. Esto resulta interesante ya que como se reportó recientemente el sitio tóxico de la CTX parece localizarse hacia su región carboxilo terminal [28]. Lo anterior contrasta con los resultados presentados aquí para la NTX, ya que como se demostró en la presente tesis, en la NTX el sitio de pegado se localiza en su región amino terminal [40].

Otro resultado importante es que los tiempos de asociación y disociación de la NTX y los péptidos sintéticos pequeños no son muy diferentes. Esto indica que el tamaño de la toxina no es lo que determina el tiempo de pegado al canal, sino la presencia de ciertos aminoacidos que interactuan con el receptor.

PLANES FUTUROS

Los planes futuros incluyen 3 objetivos principales, tal y como se describe a continuación:

- 1) Determinar si IBX bloquea al canal K_{Ca} de endotelio.
- 2) Sintetizar péptidos de regiones homologas a la NTX en las otras dos toxinas bloqueadoras de canales de potasio (CTX y IBX).

La finalidad de este objetivo es la de determinar que región de la CTX e IBX es responsable por el bloqueo al canal.

- 3) Comparar los efectos de dichos péptidos sintéticos sobre los tiempos de apertura y cierre del canal con los efectos producidos por péptidos sintéticos de la NTX. Esto permitirá determinar si las constantes de asociación y disociación entre CTX, IBX y NTX son diferentes.

ANEXOS

1. Trabajo de primer autor describiendo la caracterización y regulación del canal K_{Ca} en endotelio.

Vaca L, Schilling WP and Kunze DL (1992) G-protein-mediated regulation of a Ca^{2+} -dependent K^+ channel in cultured vascular endothelial cells. *Pflügers Archiv.* 422:66-74.

G-Protein-mediated regulation of a Ca^{2+} -dependent K^+ channel in cultured vascular endothelial cells

Luis Vaca, William P. Schilling, and Diana L. Kunze

Department of Molecular Physiology and Biophysics, Baylor College of Medicine, Houston, TX 77030, USA

Received February 4, 1992/Received after revision June 25, 1992/Accepted July 7, 1992

Abstract. The purpose of the present study was to determine the mechanism by which bradykinin activates the small conductance, inwardly rectifying, Ca^{2+} -activated K^+ channel (K_{Ca}) found in cultured bovine aortic endothelial cells. Channel activity was studied using the patch-clamp technique in whole-cell, cell-attached, inside-out and outside-out configurations. Channel conductance at potentials positive to 0 mV was $10 \pm 2 \text{ pS}$ and at potentials negative to 0 mV $30 \pm 3 \text{ pS}$ ($n = 7$) when examined in symmetrical K^+ (150 nmol/l) solutions. The channel open probability (P_o) was only weakly voltage dependent changing approximately 0.2 units over 160 mV. In contrast, raising the intracellular Ca^{2+} concentration from 100 nmol/l to 10 $\mu\text{mol/l}$ at -60 mV produced a graded increase in channel P_o from 0.15 to 0.96; the concentration required for half-maximum response (apparent $K_{0.5}$) was 719 nmol/l. At a constant Ca^{2+} concentration, application of guanosine triphosphate (GTP) to the cytoplasmic surface of the patch increased channel P_o . This effect was dependent upon the simultaneous presence of both GTP and Mg^{2+} , and was reversed by the subsequent application of the guanosine diphosphate (GDP) analogue, guanosine-5'-O-(2-thiodiphosphate) (GDP β S). The hydrolysis-resistant GTP analogue, guanosine-5'-O-(3-thiotriphosphate) (GTP γ S), induced a long-lasting increase in channel P_o . In the presence of Mg^{2+} -GTP, the apparent $K_{0.5}$ for Ca^{2+} decreased from a control value of 722 nmol/l to 231 nmol/l. Addition of bradykinin to outside-out patches previously exposed to intracellular Mg^{2+} -GTP further enhanced K_{Ca} activity, shifting the apparent $K_{0.5}$ for Ca^{2+} from 228 nmol/l to 107 nmol/l. This activation by bradykinin was not observed in patches following prior exposure to GDP β S. These results suggest that bradykinin can activate the K_{Ca} channel of vascular endothelial cells via a G-protein-mediated change in the sensitivity of the channel for Ca^{2+} . We postulate that vasoactive agonists may use this mechanism to maintain an elevated K^+ permeability as the

intracellular Ca^{2+} concentration returns towards normal resting levels.

Key words: Ca^{2+} -activated K^+ channel – G-proteins – Guanosine-triphosphate – Endothelial cells – Bradykinin

Introduction

The endothelium is a specialized monolayer that lines the lumen of all vessels of the cardiovascular system. The role of the endothelium in regulating vascular smooth muscle tone has been well recognized [15]. Endothelial cells secrete a variety of vasoactive substances in response to specific agonists including bradykinin (BK), adenosine triphosphate (ATP), histamine, and acetylcholine (ACh). The receptors for some of these agonists are coupled to a family of membrane bound proteins capable of binding guanine nucleotides (G-proteins) with subsequent activation or inhibition of effector enzymes or ion channels [2].

One of the earliest steps in the endothelial cell response to agonist stimulation is a rise in intracellular free Ca^{2+} concentration [$\text{Ca}^{2+}]_i$] [9]. The rise in [$\text{Ca}^{2+}]_i$ reflects stimulation of phosphoinositide turnover via G-protein-mediated activation of phospholipase C [29] with subsequent release of Ca^{2+} from internal stores and influx of Ca^{2+} from the extracellular space. Concomitant with this event is the development of a K^+ current, produced by Ca^{2+} -activated K^+ channels (K_{Ca}) [4, 9, 10, 25]. Recent experimental findings indicate that although K_{Ca} channel activity in cell-attached patches is observed following agonist stimulation, simultaneous measurements of whole-cell recordings and intracellular Ca^{2+} with the fluorescent indicator [1-(2-[5-Carboxyoxazol-2-yl]-6-aminobenzofuran-5-oxy)-2-(2'-amino-5'-methyl-phenoxy)-ethane-N-N-N'-tetraacetic acid] Fura-2, suggests that BK-stimulated K^+ currents remain after

Correspondence to: L. Vaca

$[Ca^{2+}]_i$ has returned to basal levels. These findings suggest that agonist stimulation may activate the K_{Ca} channel in endothelium via a mechanism that does not require the continued elevation of $[Ca^{2+}]_i$.

A recent study of the smooth muscle maxi- K_{Ca} channel in planar lipid bilayers suggests that channel activity may be regulated via a G-protein-mediated mechanism [28]. Thus, the purpose of the present study was to determine the role of G-proteins in BK-stimulated activation of the K_{Ca} channel in endothelial cells. The results suggest that BK, via a G-protein, activates the K_{Ca} by changing the sensitivity of the channel for Ca^{2+} .

Materials and methods

Culture and preparation of vascular endothelial cells. Bovine aortic endothelial cells (BAECs) were isolated and maintained in culture as previously described [13]. Cells (passages 5 to 20), were prepared for patch-clamp experiments in one of two ways. Either the nourishing media from confluent monolayers was replaced with bath solution (see below) and the cells used directly, or the monolayers were treated for 2 min with Hank's solution containing 0.02% trypsin, followed by washing (twice) with the bath solution. No differences in the results were observed between the two methods, however the percentage of successful giga-seal formations from trypsin-treated monolayers was 3-fold higher than with untreated monolayers. In the present study 65% of the patches were obtained from trypsin-treated cells.

Solutions and reagents. Experiments were performed using two solutions:

1. A high K^+ solution (HiK) containing in mmol/l: 150 K-Aspartate, 5 NaCl, 10 4-(2-hydroxyethyl)-1-piperazineethanesulphonic acid (HEPES), 1 $MgCl_2$ (where indicated) and various [ethylenebis(oxonitriolo)]tetraacetic acid (EGTA) and Ca^{2+} concentrations to obtain specific calculated free Ca^{2+} concentrations [14].

2. A low K^+ solution (LoK) containing in mmol/l: 145 NaCl, 5 KCl, 10 HEPES, 1 $MgCl_2$ (where indicated) and free Ca^{2+} concentrations as indicated in the text. The solutions were adjusted to pH 7.2 with N-methyl-D-glucamine (NMDG) hydroxide. All salts used were analytical grade (Sigma). Guanosinetriphosphate (GTP), guanosine-5'-O-(3-thiotriphosphate) (GTPyS), guanosine-5'-O-(2-thiodiphosphate) (GDP β S) and BK were obtained from Sigma. The high affinity BK antagonist [*N*-adamantane-acetyl-D-Arg⁰, Hyp³, Thi^{5,8}, D-Phe⁷]-bradykinin was obtained from Calbiochem. All reagents were applied to the membrane patches using a multibarrel perfusion system. Perfusion was driven by gravity.

Patch-clamp protocol. The patch-clamp technique was used in the whole-cell, cell-attached, inside-out and outside-out configurations to study patches obtained from confluent endothelial monolayers. For whole-cell experiments isolated cells were selected to avoid electrical coupling to the monolayer. All experiments were performed at room temperature. Pipettes were obtained from 8161 or 7052 glass (Garner Glass) with resistances of 5 to 12 M Ω when filled with HiK. Seal resistance ranged from 40–100 G Ω . The reference electrode used was an Ag-AgCl plug connected to the bath solution via a 150 mmol/l KCl agar bridge. All voltages are reported with the extracellular face of the patch as reference. For cell-attached patches membrane potentials refer to the inner surface (V_{inside} – $V_{outside}$), according to the convention for intact cells. For these calculations we have assumed a cell resting potential (V_{inside}) of –65 mV [10]. The amplifier employed was the Axopatch 1C (Axon Instruments). Single channel fluctuations were initially stored on FM tape (Racal) and subsequently digitized for computer analysis. The signal was filtered with a low-pass 8-pole Bessel filter (Frequency Devices) at 5 kHz and digitized at 10 kHz. Cumulative open

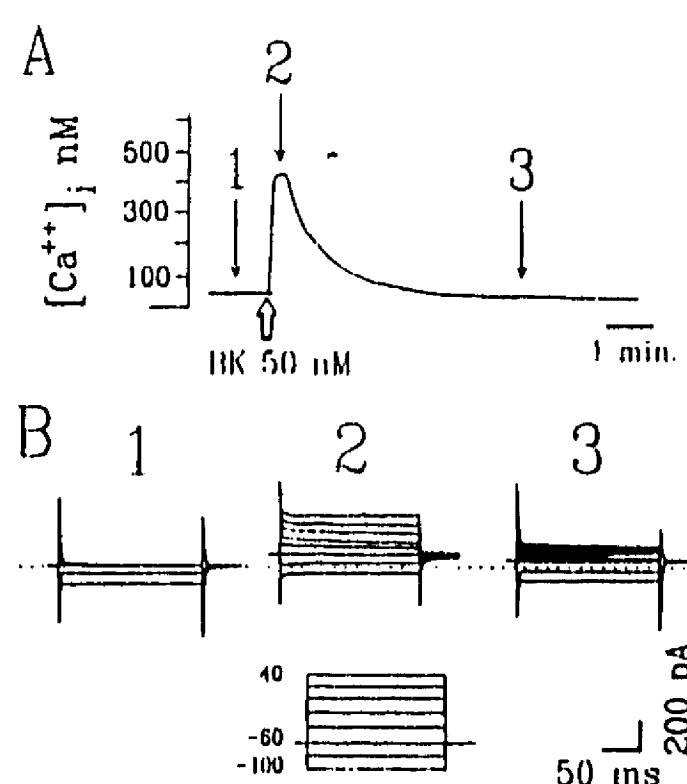


Fig. 1A, B. Simultaneous measurements of intracellular calcium concentration $[Ca^{2+}]_i$ and whole-cell currents. A $[Ca^{2+}]_i$ obtained from a single cell. The pipette solution contained HiK with 50 nmol/l Ca^{2+} buffered by addition of [ethylenebis(oxonitriolo)]tetraacetic acid (EGTA, see Methods) and 50 μ mol/l Fura-2 K^+ . The bath solution contained LoK with 2 mmol/l Ca^{2+} . At the time indicated by the broad arrow 50 nmol/l bradykinin (BK) was added. B Examples of the whole-cell currents obtained from the same cell at the times indicated by the corresponding numbers in A. Resting conditions (1), after addition of BK (2) and after $[Ca^{2+}]_i$ returns to the control value (3). The holding potential was –60 mV. The voltage protocol consisted of 20 mV steps with a duration of 400 ms with 1 s holding at –60 mV between pulses. The dotted line in panel B indicates the zero current level

probabilities were obtained after integrating open probabilities every 50 s, with the probability of being open defined by the equation, $P_o = \text{open time/total time}$. Selected examples with single channel events were obtained from the binary data file, filtered to 1 kHz and transformed to HPGL files (Hewlett Packard Graphics Language) for illustrative purposes. Histograms and cumulative plots were created with SigmaPlot 4.1 (Jandel).

Simultaneous measurements of $[Ca^{2+}]_i$ and whole-cell recordings. $[Ca^{2+}]_i$ was measured in single cells using the fluorescent Ca^{2+} indicator, Fura-2. Cells were gently removed from the dish with a pasteur pipette and placed on glass coverslips allowing 1 h for cell re-attachment. The pipette solution contained 50 μ mol/l of the impermeable analogue Fura-2 (K^+ salt). The pipette solution used was HiK with 50 nmol/l free Ca^{2+} buffered with EGTA and the bath solution was LoK with 2 mmol/l Ca^{2+} . The coverslip was mounted in a perfusion chamber and placed on the stage of an inverted microscope (Nikon) which was optically connected to a SLM-8000C spectrophotofluorometer (Urbana II.). $[Ca^{2+}]_i$ was determined as previously described [20].

Results

BK activates a K_{Ca} current in whole-cell recordings from BAECs

Simultaneous measurements of $[Ca^{2+}]_i$ using the fluorescent dye Fura-2 and whole-cell currents indicate that

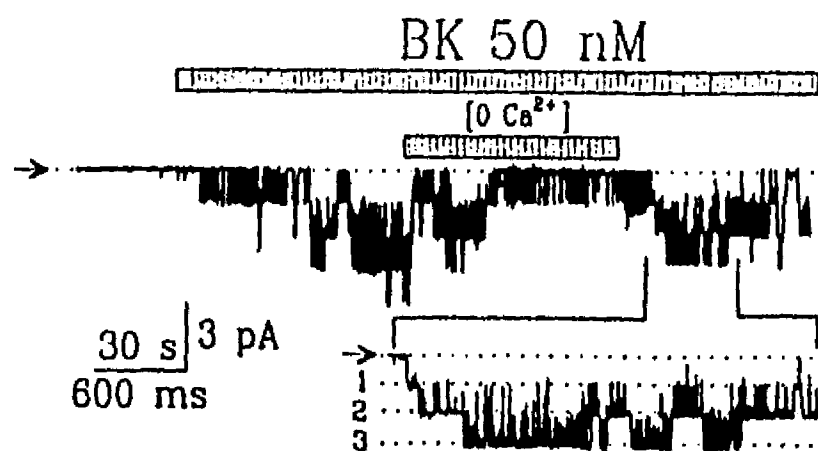


Fig. 2. BK activates K_{Ca} channels in cell-attached patches from BAECs. An example of a cell-attached patch maintained at the cell resting potential (0 mV applied) with HiK in the pipette and LoK in the bath solution (2 mmol/l Ca^{2+}). In control conditions no channel activity was observed (in this experiment there was no inward rectifier K^+ channel). After addition of 50 nmol/l bradykinin (BK) inward current was developed representing multiple channels ($n = 3$). Channel activity could be recorded throughout the experiment in the continuous presence of BK. Perfusion of the cell with LoK containing 10^{-9} mol/l Ca^{2+} buffered with EGTA reduced substantially channel activity (indicated as $[0 Ca^{2+}]$). After returning to the original bath solution (2 mmol/l Ca^{2+}) channel activity was restored showing multiple discrete current steps. The inset shows a fragment of the record with the time scale expanded. Notice the dotted lines indicating base line and three active channels of similar amplitude labeled as 1, 2 and 3. The amplitude scale indicates 3 pA and the time scales are, for the upper recording 30 s and for the inset 600 ms. The arrows indicate the zero current level (channel closed)

the BK-activated K_{Ca} current does not follow the time course of the $[Ca^{2+}]_i$. Large K^+ currents were recorded at the peak of $[Ca^{2+}]_i$ response (Fig. 1B, 2), however a substantial amount of the K^+ current remains for several minutes despite the return of $[Ca^{2+}]_i$ toward basal levels ($n = 4$). The remaining current has identical pharmacological characteristics to the K_{Ca} current that we previously described [10]. At low $[Ca^{2+}]_i$ prior to addition of BK only the inwardly rectifying K^+ current is present (Fig. 1B, 1). As previously reported addition of BK produces a net K^+ outward current at -80 mV and more positive potentials [9, 10].

BK activates single channels in cell-attached recordings

In the absence of added agonist only the inward rectifier K^+ channel is observed in cell-attached patches as we and others have previously reported [10, 25]. Within the first 10 s after addition of 50 nmol/l BK multiple discrete inward current steps were observed in each of the three cells explored in this configuration (Fig. 2). After about 1 min of perfusing the cell with a solution containing 10^{-9} mol/l free Ca^{2+} , channel activity was substantially reduced. Returning to the original bath solution containing 2 mmol/l Ca^{2+} increased channel activity to previous levels. Multiple channels were observed in the continuous presence of BK for the duration of the experiment (3–4 min). With HiK as the pipette solution all the BK-

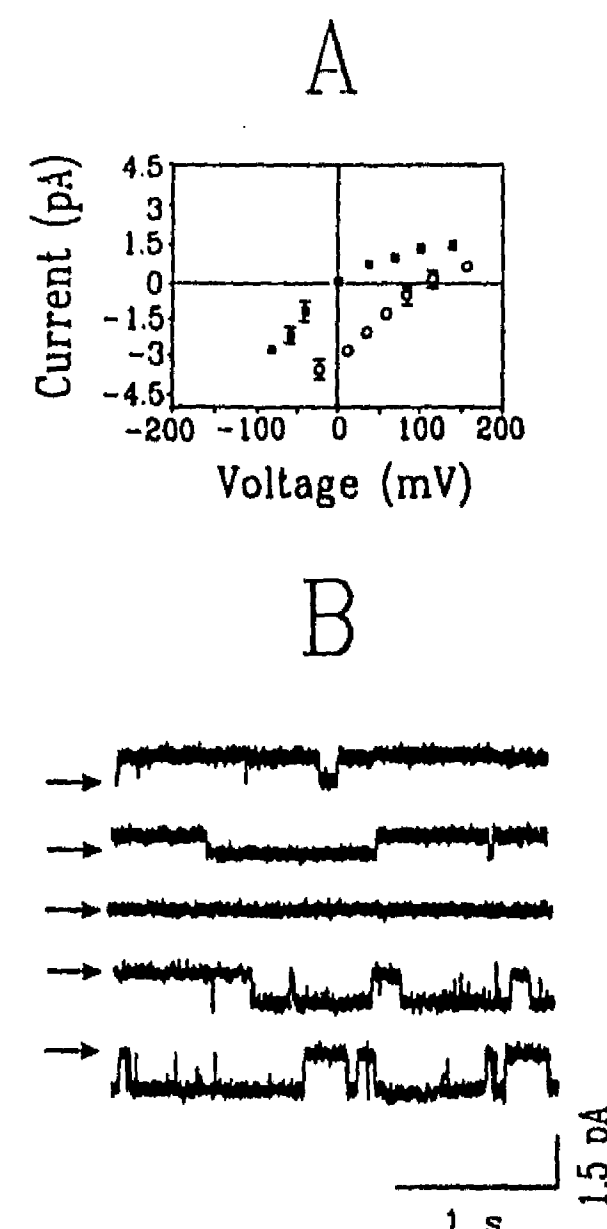


Fig. 3A, B. Current/voltage relationships for the K_{Ca} channel of BAECs. A The single channel amplitude (mean \pm SEM) at various membrane potentials was obtained from inside-out patch recordings in symmetrical HiK solutions (■, $n = 7$) and after replacing the bath solution (intracellular surface) for LoK buffer (○, $n = 5$). Where not shown, the SEM was smaller than the size of the symbol. B Examples of channel activity are shown with symmetrical HiK taken at the voltages indicated to the left of each trace. The intracellular Ca^{2+} concentration was 10 μ mol/l. The arrows indicate the closed channel current level

activated channels reversed current direction at -3 mV (data not shown).

Measurement of single K_{Ca} channels in excised patches

Channel activity was observed in approximately 30% of excised patches when the Ca^{2+} concentration at the cytoplasmic surface was equal to or greater than 100 nmol/l ($n = 36$). The remaining 70% of the patches did not show K^+ channel activity with any of the procedures to be described. The effect of changes in the K^+ gradient on single-channel conductance and reversal potential was obtained from inside-out patches (Fig. 3). Under symmetrical K^+ conditions, the reversal potential obtained was 0 ± 3 mV ($n = 7$). After replacing the bath solution for LoK the single channel currents reversed at 85 ± 3 mV. Under this condition, the calculated K^+ equilibrium potential was 85.6 mV indicating that the

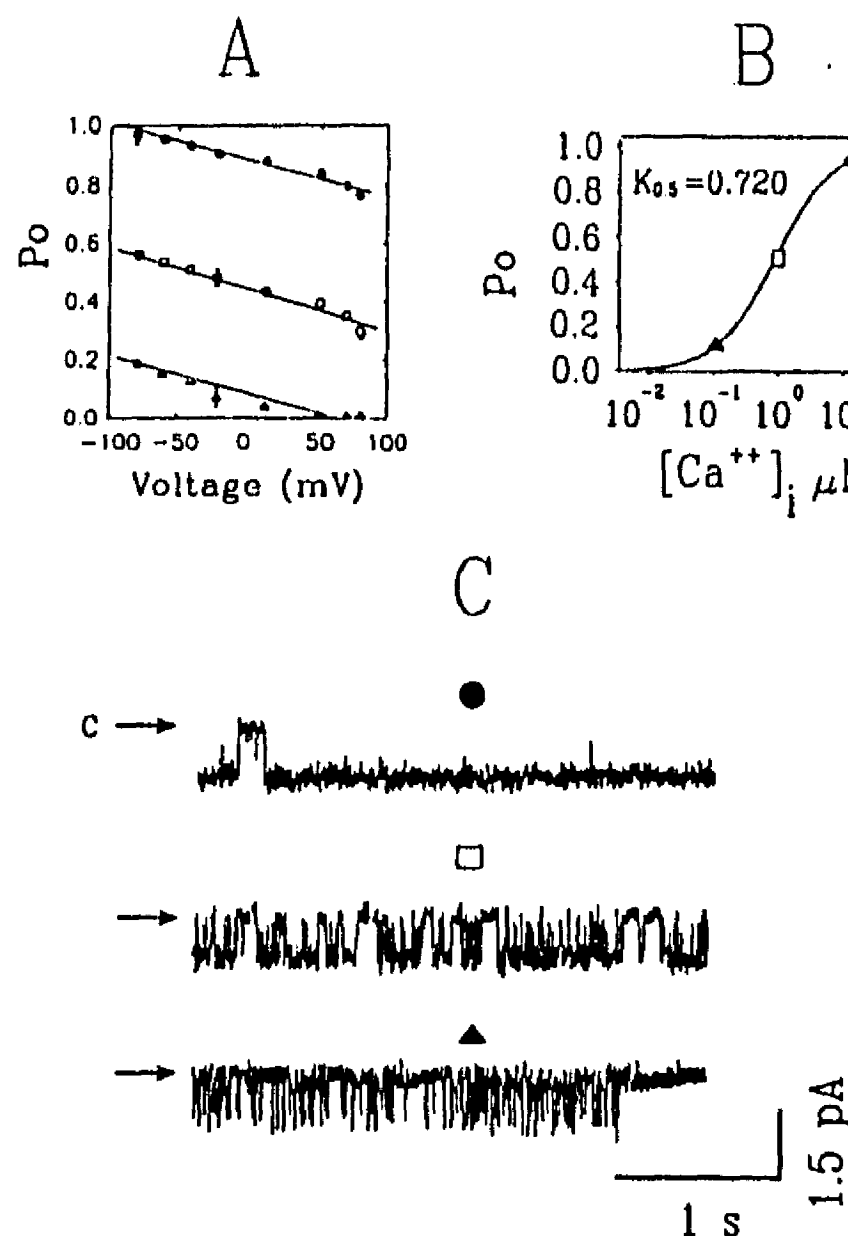


Fig. 4A–C. Effect of varying $[Ca^{2+}]_i$ on single K_{Ca} channel activity. A The effect of $[Ca^{2+}]_i$ on channel open probability (P_o) was measured in inside-out patch configuration. Channels were recorded in symmetrical HiK buffer. Following giga-seal formation, the patch was excised into a bath solution containing 100 nmol/l Ca^{2+} and the currents were recorded for at least 1 min at the indicated voltages (▲). $[Ca^{2+}]_i$ was subsequently increased to 1 (□) and 10 $\mu mol/l$ (●). Cumulative P_o was determined as described in Methods section. The values represent the mean \pm SEM from five patches. Where not shown, the SEM was smaller than the size of the symbol. B The average P_o at -40 mV from A is plotted as a function of $[Ca^{2+}]_i$. The solid line represents the best fit to a single binding site model with an apparent $K_{0.5}$ for Ca^{2+} of 720 nmol/l. C Examples of channel activity are shown at a holding potential of -40 mV and the $[Ca^{2+}]_i$ indicated in B. Arrows indicate the closed channel current level

primary current-carrying species was K^+ . The channel exhibited inward rectification in symmetrical K^+ solutions. The conductance at potentials positive to 0 mV was 10 ± 2 pS ($n = 7$) and at potentials negative to 0 mV 30 ± 3 pS ($n = 7$) as determined from the slope of the linear regression analysis for outward and inward currents respectively.

Voltage and Ca^{2+} sensitivity of the K_{Ca} channel

To determine the role of $[Ca^{2+}]_i$ in regulating the K^+ channel, single channel activity was monitored while the

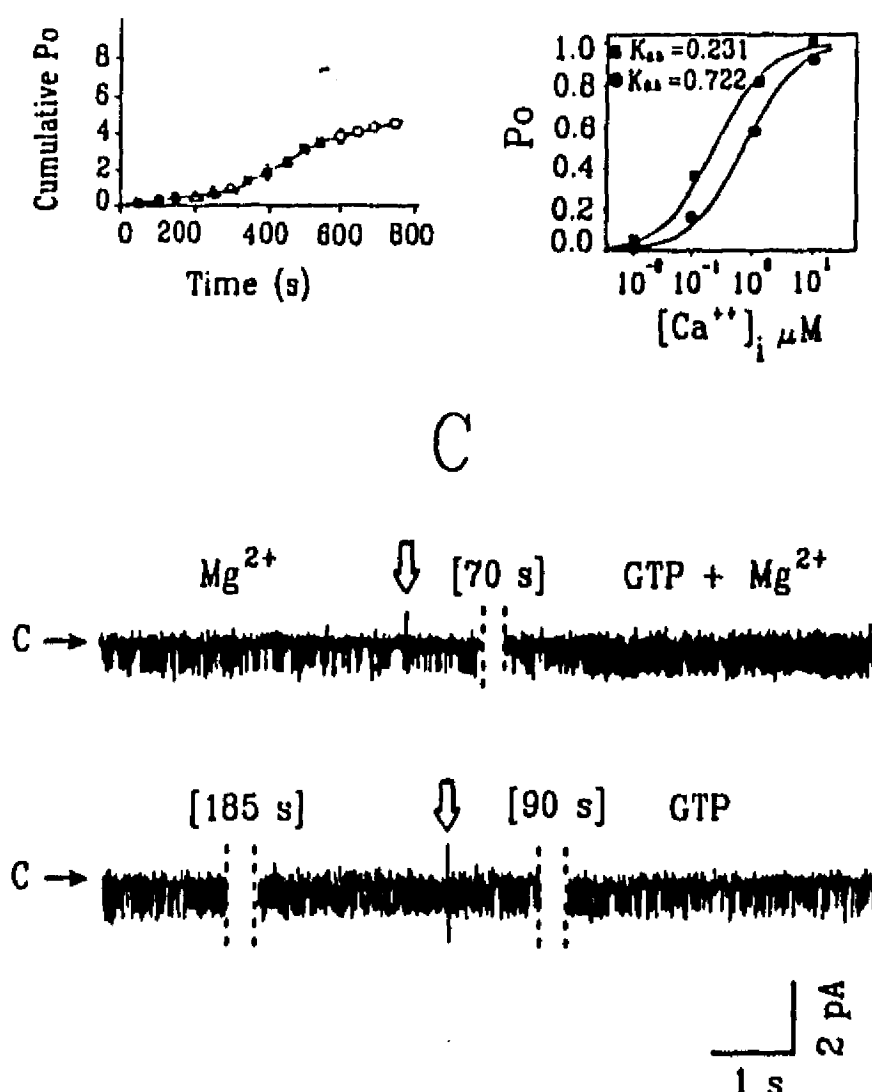


Fig. 5A–C. Effect of guanosine triphosphate (GTP) and Mg^{2+} on K_{Ca} channel activity. A The effect of GTP and Mg^{2+} on channel P_o was determined in inside-out patch configuration. Channels were recorded in symmetrical HiK buffer. Following giga-seal formation, the patch was excised into a bath solution containing 100 nmol/l Ca^{2+} and the currents were recorded at -40 mV for 150 s (control, ●). The bath solution was sequentially changed to HiK solution containing 1 mmol/l $MgCl_2$ (Δ), 100 $\mu mol/l$ GTP in the presence of Mg^{2+} (■) followed by removal of Mg^{2+} from the solution in the continuing presence of GTP (○). Values represent the mean \pm SEM cumulative P_o from five patches. Where not shown, the SEM was smaller than the size of the symbol. B The average channel P_o was measured at the indicated $[Ca^{2+}]_i$ under control conditions (●), and after addition of Mg^{2+} -GTP (■) as in A. The lines through the data represent the best fit to a single binding site model. C An entire experiment is illustrated beginning with the application of Mg^{2+} to the excised patch. Solution changes are indicated by the vertical arrows and time gaps are designated by the vertical dotted lines with the time indicated in brackets (in seconds). Horizontal arrows indicate the closed channel current level (C)

Ca^{2+} concentration of the bath (intracellular) solution was changed (Fig. 4). With low Ca^{2+} (100 nmol/l) at the cytoplasmic face of the patch, P_o varied from 0 at 80 mV to 0.2 at -80 mV. Increasing $[Ca^{2+}]_i$ increased P_o at all voltages explored (± 80 mV) without altering the voltage dependence of the channel (slope of the curves in Fig. 4A). The concentration/response curve (Fig. 4B) could be fitted to a single binding site model with a concentration for half-maximal response (apparent $K_{0.5}$) for Ca^{2+} of 720 nmol/l.

Modulation of the K_{Ca} channel by Mg^{2+} -GTP

To test for involvement of a G-protein in activation of the K_{Ca} channel, cumulative P_o was determined following the sequential perfusion of the cytoplasmic membrane surface of an inside-out patch with HiK solution containing 100 nmol/l Ca^{2+} and (1) Mg^{2+} alone, (2) Mg^{2+} plus GTP, or (3) GTP alone (Fig. 5). Application of Mg^{2+} alone had no effect on channel P_o . In contrast, addition of GTP in the presence of Mg^{2+} produced a dramatic increase in channel P_o as indicated by the change in slope of the relationship between cumulative P_o and time (Fig. 5A). Subsequent removal of Mg^{2+} in the continuous presence of GTP caused P_o to return to control levels. No further activation was seen when the GTP concentration was increased to 1 mmol/l (data not shown). Thus, GTP produced channel activation only in the presence of Mg^{2+} . To determine the mechanism by which Mg^{2+} -GTP increased channel P_o , this experiment was repeated at various Ca^{2+} concentrations. The presence of Mg^{2+} -GTP shifted the apparent $K_{o.s}$ for Ca^{2+} from 722 nmol/l (control) to 231 nmol/l (Fig. 5B).

If a G-protein is involved in the activation seen with Mg^{2+} -GTP, channel activity should be attenuated by addition of the GDP analogue, $GDP\beta S$, to the intracellular solution following activation of the channel with GTP. Furthermore, addition of the hydrolysis-resistant GTP analogue, $GTPyS$, should cause a long-lasting activation of the channel. As seen in Fig. 6, channel activity was increased by addition of Mg^{2+} -GTP and returned to control levels within 1–2 min of exposing the patch to $GDP\beta S$ in the continuous presence of Mg^{2+} -GTP. Application of $GTPyS$ also increased channel P_o (Fig. 7), however, the channel remained activated for the remainder of the recording period (3–4 min) following removal of $GTPyS$ from the perfusion buffer. These results clearly suggest that G-proteins can participate in regulation of K_{Ca} channel activity in BAECs. The $K_{o.s}$ for Ca^{2+} obtained after $GTPyS$ stimulation was 110 nmol/l (Fig. 7B).

Effect of BK on K_{Ca} channel activity in BAECs

To test the hypothesis that BK-induced activation of the K_{Ca} channel is, in part, mediated via G-protein(s), the effect of Mg^{2+} -GTP at the cytoplasmic membrane surface was examined using outside-out patch configuration in the presence and absence of BK in the extracellular buffer (Fig. 8). Mg^{2+} -GTP was added to the pipette solution and an outside-out patch was formed. As shown above (see Figs. 5, 6), channel activity was elevated over control levels with Mg^{2+} -GTP. Addition of 50 nmol/l BK to the bath produced a 2-fold increase in channel P_o (Fig. 8A). This result is achieved by shifting the apparent $K_{o.s}$ for Ca^{2+} from 228 nmol/l with Mg^{2+} -GTP alone to 107 nmol/l with BK receptor stimulation (Fig. 8B). Application of the antagonist following activation by BK produced a rightward shift in $K_{o.s}$ to 698 nmol/l (Fig. 8B), a value similar to control (i.e. in the absence of Mg^{2+} -GTP, see Figs. 4, 5). In addition to this we

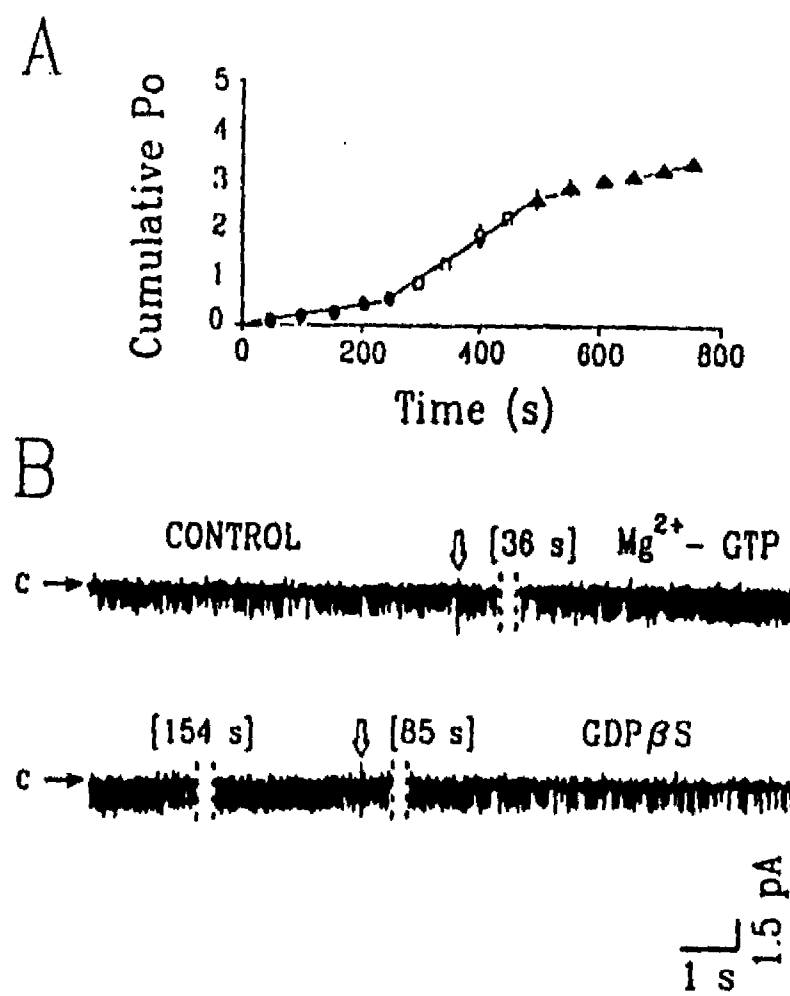


Fig. 6 A, B. Effect of guanosine-5'-O-(2-thiodiphosphate) ($GDP\beta S$) on K_{Ca} channel activity. A The effect of GTP and Mg^{2+} on channel P_o was determined in inside-out patch configuration. Channels were recorded in symmetrical HiK buffer. Following giga-seal formation, the patch was excised into a bath solution containing 100 nmol/l Ca^{2+} and the currents were recorded at -40 mV for 250 s (control, ●). The bath solution was sequentially changed to HiK solution containing 1 mmol/l $MgCl_2$ and 100 μ mol/l GTP (□), and 300 μ mol/l $GDP\beta S$ (▲) in the continuing presence of Mg^{2+} -GTP. Values represent the mean \pm SEM cumulative P_o from five patches. Where not shown, the SEM was smaller than the size of the symbol. B Time course of the experiment beginning with the control conditions. Solution changes are indicated by the vertical arrows and time gaps are designated by the vertical dotted lines with the time indicated in brackets (in seconds). Horizontal arrows indicate the closed channel current level (C)

found that 50 nmol/l BK had no effect on channel P_o in outside-out patches containing 300 μ mol/l $GDP\beta S$ in the pipette (intracellular) solution ($n = 4$, data not shown).

Discussion

The present studies describe several mechanisms of regulation of the Ca^{2+} -activated K^+ channel in BAECs.

Voltage sensitivity

The K_{Ca} channel in BAECs is weakly influenced by the membrane voltage. A change of P_o of only 0.2 is observed over a 160 mV range (± 80 mV) with P_o increasing with hyperpolarization. The voltage sensitivity is not affected by cytosolic Ca^{2+} as illustrated by the parallel upward shift in the P_o/V relationship as $[Ca^{2+}]_i$ is increased from 10^{-7} to 10^{-5} mol/l. The weak voltage sensitivity of this

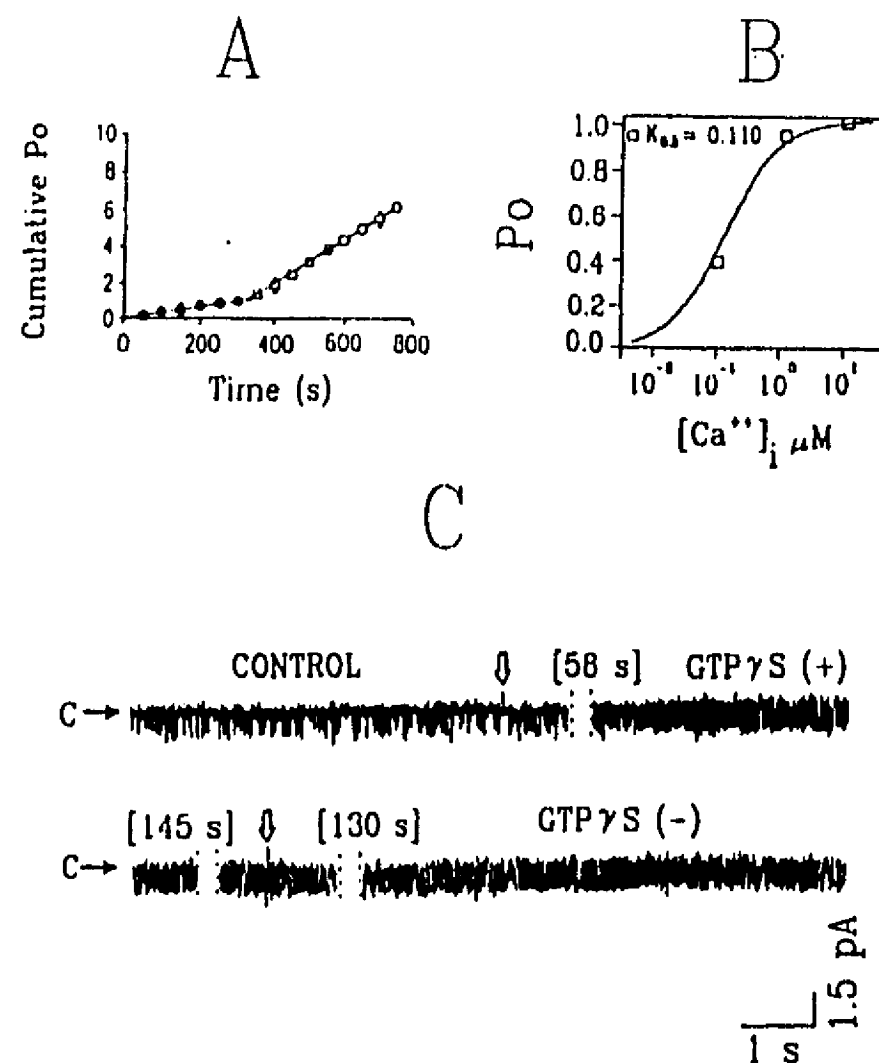


Fig. 7A–C. Effect of guanosine-5'-O-(3-thiophosphate) (GTP γ S) on K_{C_4} channel in BAECs. **A** The effect of GTP γ S and Mg^{2+} on channel P_o was determined in inside-out patch configuration. Channels were recorded in symmetrical HiK buffer. Following giga-seal formation, the patch was excised into a bath solution containing 100 nmol/l Ca^{2+} and the currents were recorded at -40 mV for 300 s (control, ●). The bath solution was changed to HiK solution containing 1 mmol/l $MgCl_2$ and 100 μ mol/l GTP γ S (□) and subsequently changed to HiK solution with Mg^{2+} but without GTP γ S (○). Values represent mean \pm SEM cumulative P_o from five patches. Where not shown, the SEM was smaller than the size of the symbol. **B** Channel P_o at three different $[Ca^{2+}]_i$, the solid line indicates the fit to a single binding site model with a $K_{0.5}$ of 110 nmol/l. **C** Channel activity illustrating the experimental conditions described above. Solution changes are indicated by the vertical arrows and time gaps are designated by the vertical dotted lines with the time indicated in brackets (in seconds). Horizontal arrows indicate the closed channel current level (C)

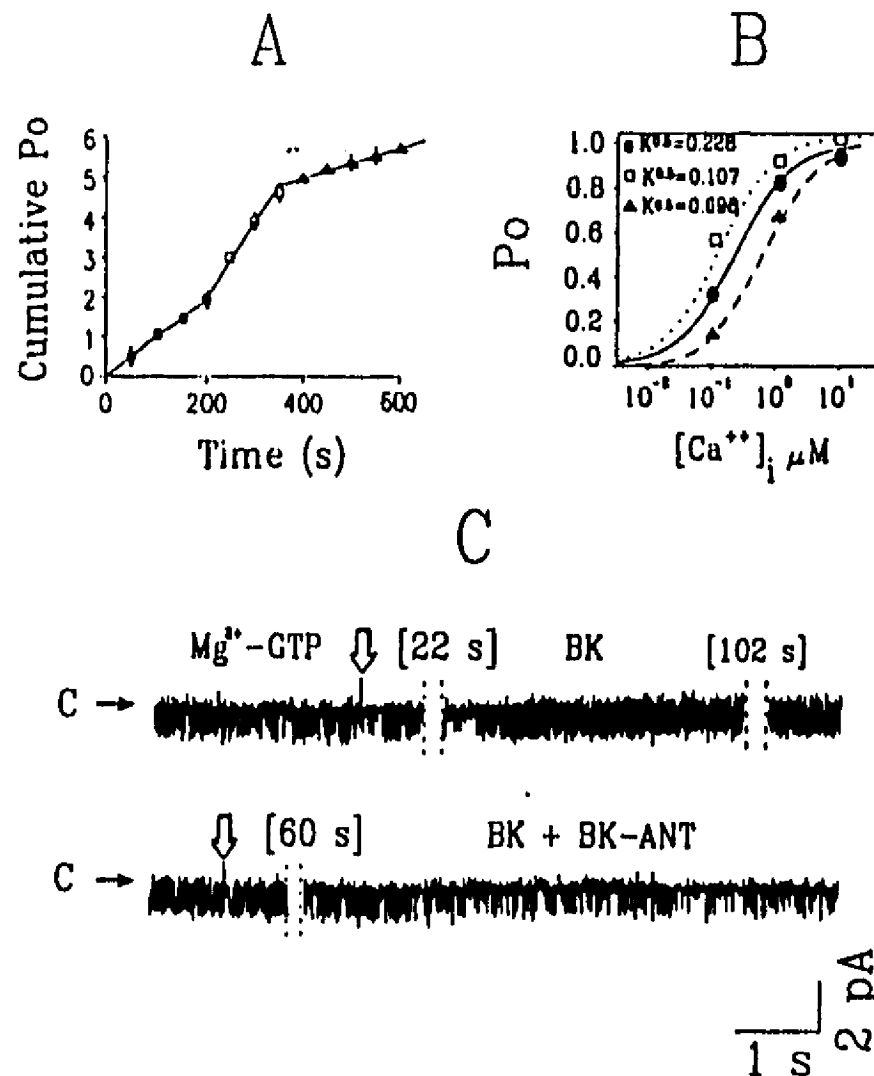


Fig. 8A–C. Effect of BK on K_{C_4} channel activity. **A** The effect of BK on single K_{C_4} channel activity was examined in outside-out patch configuration. Following patch excision, channels were recorded for 200 s at -40 mV in symmetrical HiK solution containing 100 nmol/l Ca^{2+} , 1 mmol/l $MgCl_2$, and 100 μ mol/l GTP in the pipette solution (●). BK (final concentration, 50 nmol/l) was added to the bath (extracellular) solution (□) followed by addition of the BK antagonist, (1 μ mol/l, ▲) in the continuing presence of BK. Values represent the mean \pm SEM cumulative P_o from seven patches. Where not shown, the SEM was smaller than the size of the symbol. **B** The average channel P_o was measured at the $[Ca^{2+}]_i$ under control conditions (●), and after addition of BK (□) and the BK antagonist (▲) as in A. The lines through the data represent the best fit to a single binding site model. **C** Channel activity illustrating the different experimental conditions described above. Solution changes are indicated by the vertical arrows and time gaps are designated by the vertical dotted lines with the time indicated in brackets (in seconds). Horizontal arrows indicate the closed channel current level (C)

channel in BAECs is in marked contrast to the strong voltage dependence generally observed in the large conductance maxi- K_{C_4} channel [19], but is consistent with several smaller conductance K_{C_4} channels for which little voltage sensitivity has been reported: HeLa cells [23], mammary cells [12], GH3 cells [8] and red blood cells [17]. In particular, the K_{C_4} channel in red blood cells shows a similar voltage sensitivity to that reported here. P_o changes only by 0.35 over 170 mV, also increasing as the membrane potential becomes more negative. An earlier investigation [24] also examined the voltage dependence of P_o of the K_{C_4} channel from BAECs. The authors concluded that P_o was insensitive to voltage over the range of 40 to -100 mV. At positive membrane potentials P_o rose, in contrast to our studies.

Calcium sensitivity

The P_o is dramatically affected by $[Ca^{2+}]_i$. The $P_o/[Ca^{2+}]_i$ relationship obtained at -40 mV was fitted by a single binding site model with an apparent $K_{0.5}$ of 720 nmol/l, suggesting that the binding of a single Ca^{2+} ion is sufficient for channel activation. In another study on the BAECs K_{C_4} channel a Ca^{2+} sensitivity less than we report was described [24]. Although a full concentration/response curve was not presented, these data predict a $K_{0.5}$ greater than 1 μ mol/l. The discrepancy between this data and the present findings may result from the fact that two different open periods with sufficiently long dwell times are reported so that the recording period of

30–60 s may not have been sufficient to capture the actual P_o . One state was characterized by frequent brief openings from the closed state while the other showed brief closures from the open state. As the authors point out, the recording period may bias the results by concentrating on one of the two opening modes. In our studies we did not observe switching between two long-lasting modes at constant $[Ca^{2+}]_i$. On the other hand, the channel activity found in cell-attached patches in that study is higher than should be expected from the Ca^{2+} sensitivity of the channel the authors found in excised patches. For instance, in order to obtain the channel activity presented in their Figs. 7 and 8 [24] the $[Ca^{2+}]_i$ would have to rise to 7–10 $\mu\text{mol/l}$ according to the results shown in excised patches in their Fig. 5A. In experiments in which $[Ca^{2+}]_i$ was monitored in BAECs using Fura-2, we have never found such high values for $[Ca^{2+}]_i$ [9, 26, 27]. The results presented in that study [24] suggest indirectly that the Ca^{2+} sensitivity of the K_{Ca} channel may be different in intact cells. More recently, a report by the same group [25] evaluated the effect of BK in cell-attached patches from BAECs. They suggest that K_{Ca} channel activity may reflect changes in $[Ca^{2+}]_i$, however simultaneous, direct measurements of K_{Ca} channel activity and $[Ca^{2+}]_i$ were not presented. As we have shown here (Fig. 1) the development of a BK-activated K^+ current coincides with the initial peak in $[Ca^{2+}]_i$, however a substantial amount of the BK-induced K^+ current remains after $[Ca^{2+}]_i$ returns to basal levels. We have also shown that in cell-attached patches K_{Ca} channel activity is observed in the continuous presence of BK, even after the extracellular Ca^{2+} concentration has been reduced to 10^{-9} mol/l (Fig. 2). As previously shown [27], reducing extracellular Ca^{2+} by addition of EGTA results in a reduction of $[Ca^{2+}]_i$ to below 50 nmol/l . At this low $[Ca^{2+}]_i$ K_{Ca} channel P_o would be expected to be very low (< 0.05), however we have observed a substantial channel P_o in whole-cell and cell-attached patch experiments (Figs. 1, 2). These results support our conclusion that the Ca^{2+} sensitivity of the K_{Ca} channel may be modulated in intact cells.

Calcium sensitivity is modulated by Mg^{2+} -GTP

Mg^{2+} -GTP increases the Ca^{2+} sensitivity of the endothelial channel as indicated by parallel shift in the $P_o/[Ca^{2+}]_i$ relationship, leading to a decrease in the apparent $K_{0.5}$ of the K_{Ca} channel for $[Ca^{2+}]_i$ from approximately 720 nmol/l to 228 nmol/l . Using analogues of the guanine nucleotides we demonstrated that this effect is mediated via a G-protein since, in the presence of Mg^{2+} -GTP, the channel activity can be returned to control values by the GDP analogue GDP β S, and is irreversibly enhanced by the hydrolysis-resistant GTP analogue, GTPyS. In a previous report [28] data is provided to suggest that G-proteins influence the gating of another K_{Ca} , the myometrial maxi- K_{Ca} channel, possibly by increasing the affinity of the channel for Ca^{2+} .

Mechanism of GTP activation

Most G-protein-mediated actions are thought to be ligand initiated [2]. The G-protein cycles between active and inactive forms. In this cycle $G_{\alpha\beta\gamma}$ -GDP is the inactive form of the heterotrimeric G-protein. Ligand catalyses activity by promoting the rate of GDP dissociation and subsequent GTP association. Following GTP binding the $\beta\gamma$ subunits of the G-protein dissociates allowing the G_α -GTP to couple to the effector (ion channel or enzyme). The G_α subunit hydrolyses the GTP ($2–10 \text{ min}^{-1}$) and the resulting G_α -GDP reassociates with the $\beta\gamma$ subunit [21]. In the absence of ligand the guanosine triphosphatase (GTPase) activity of G-protein is limited by the rate at which GDP dissociates from the protein, which normally is extremely slow ($0.01–0.1 \text{ min}^{-1}$, [2, 5]). Thus, in our studies performed in the absence of BK, we would expect initial activation by GTP to be slow in onset as it depends first on GDP dissociation. Subsequent activity would then be cyclic with periods of reduced activity representing the slow GDP dissociation. One explanation for the unexpected rapidity of the GTP effects in our studies is that in the absence of ligand the unoccupied receptor promotes the GTPase activity. Several recent reports provide support for G-protein-mediated ion channel activation in the absence of ligand. It has been reported that, in the absence of agonist, Mg^{2+} -GTP modifies the activity of a K_{Ca} channel from myometrial membranes incorporated into lipid bilayers [28]. Similar results have been obtained by others [22]. These authors examined the dependence of the rate of activation of the cardiac K_{ACh} channel on the concentration of Mg^{2+} -GTP in the presence and absence of the agonist (ACh). At 100 $\mu\text{mol/l}$ GTP the rates of activation were similar whether agonist was present or not. However, at concentrations of GTP of between 1 and 100 $\mu\text{mol/l}$ the activation was more rapid with ACh. Further support for the role of unoccupied receptors comes from the studies showing that the GTPase activity of G-proteins reconstituted with β -adrenergic [6] or α_2 -adrenergic receptors [7] is higher than if G-proteins alone are studied.

An alternative explanation for the effects of GTP in the absence of added ligand is that an endogenous agonist is present in the cultures of endothelial cells and maintains a low level of G-protein activation. We cannot rule out the presence of an unidentified substance released by the endothelial cells and coupling through its receptor via a G-protein to the K_{Ca} channel. Even if such a ligand were present it is unlikely that it would remain in sufficient concentration in the isolated patches to modulate activity for the duration of the experiment. Furthermore, it seems unlikely that the activity induced by such a ligand would be affected by a specific BK receptor antagonist as observed in our results.

Effects of bradykinin on K_{Ca} channel activity

BK in the presence of 100 $\mu\text{mol/l}$ Mg^{2+} -GTP enhances the activity of the K_{Ca} channel. This results in a shift of the $P_o/[Ca^{2+}]_i$ relationship from a $K_{0.5}$ of 228 nmol/l to

107 nmol/l and is consistent with evidence that an agonist-occupied receptor increases the GTPase cycle-promoting effector activity [2, 16]. That BK is acting on the K_{Ca} channel via a G-protein is supported by two results. First, in the experiments described in Fig. 7, the B_2 receptor antagonist, when added in the presence of Mg^{2+} -GTP, shifted the $K_{o,s}$ to the control value observed before the addition of Mg^{2+} -GTP (compare Fig. 5, control). Second, the $K_{o,s}$ obtained with GTPyS (110 nmol/l, Fig. 7) is essentially the same as that obtained with Mg^{2+} -GTP + BK (107 nmol/l, Fig. 8). This is further supported by the lack of effect of BK in patches preincubated with 300 μ mol/l GDP β S. We suggest that the antagonist binding to the receptor prevents the receptor-G-protein interaction necessary for modulation of the K_{Ca} channel. Consistent with this result is a study reporting that specific antagonists of a G-protein coupled opiate receptor in NG108-15 cells reduce the basal rate of GTP hydrolysis in the absence of agonist [11].

Functional implications of the Ca^{2+} and G-protein regulation

We have found resting values of $[Ca^{2+}]_i$ of 60–100 nmol/l in BAECs [9]. The $P_o/[Ca^{2+}]_i$ relationship obtained in the presence of 100 μ mol/l GTP would predict a P_o at resting Ca^{2+} of 0.2–0.3. However, recordings from cell-attached patches in the absence of agonist generally yield values of P_o that are less than 0.1 (Fig. 2 and [10]). Furthermore, there is a lack of effect of tetrabutylammonium or noxiustoxin, both inhibitors of K^+ movement through the BAEC K_{Ca} channel, on basal $^{86}Rb^+$ efflux [10]. This suggests that other factors within the cell, such as the cellular GTP/GDP ratio, the presence of free $\beta\gamma$ subunits, or the free Mg^{2+} concentration, may modulate the influence of the G-proteins on channel activity [18].

As we have previously shown, BK increases $[Ca^{2+}]_i$ in BAECs to values between 300–700 nmol/l [9, 27] which, based on the present results, would raise P_o to values greater than 0.5. The dual effect of BK, i.e., an increase in $[Ca^{2+}]_i$ accompanied by a G-protein-mediated shift in the sensitivity of the channel to Ca^{2+} , may explain our earlier results in which whole-cell K_{Ca} currents were elicited and maintained by BK although the Ca^{2+} in the pipette solution was buffered to 10^{-8} mol/l [9]. This result may reflect a BK-induced increase in the sensitivity of the channel for Ca^{2+} . This would also imply that sufficient GTP remains associated with the membrane in spite of the dilution of the cytoplasm with the pipette solution in the whole-cell experiment. Furthermore, in experiments which employed BK-stimulated ^{86}Rb efflux as an index for activation of the K_{Ca} channel, flux remained elevated for at least 5 min despite a drop in $[Ca^{2+}]_i$ over the same time to approximately 125 nmol/l [27]. Finally, we have shown in simultaneous measurements of K_{Ca} activity and $[Ca^{2+}]_i$ by means of whole-cell recordings and Fura-2 that, after BK stimulation, a substantial amount of the

BK-induced K^+ conductance remains for several minutes, after $[Ca^{2+}]_i$ returns to control values (Fig. 1).

Cell hyperpolarization is closely related to K_{Ca} channel activation in this endothelium [25]. Cell hyperpolarization may provide a favorable electrochemical gradient for Ca^{2+} influx from the extracellular solution [25, 26]. Thus the G-protein-mediated regulation of K_{Ca} channel activity may provide a mechanism to modulate membrane potential, and therefore Ca^{2+} influx, at a constant intracellular Ca^{2+} concentration.

We have previously postulated that the K_{Ca} channel in BAECs plays a role in maintaining membrane potential in the presence of the depolarizing influence of BK which opens a Ca^{2+} influx pathway [10]. We now propose that this effect may be enhanced by a BK-G-protein-induced shift of the sensitivity of the channel to Ca^{2+} . Variations in cytosolic GTP (or the ratios of the guanine nucleotides) may also play a role in modulating channel activity in the absence of BK.

Acknowledgements. This study was supported by grant HL44119 from the United States Public Health Service, National Institutes of Health, and by grant 900946 from the American Heart Association. This work was done during the tenure of an Established Investigatorship of the American Heart Association awarded to W. P. Schilling.

References

1. Birnbaumer L, Codina J, Yatani A, Maltsev R, Graf R, Olale J, Theminen APN, Liao CF, Sanford J, Okabe K, Imoto Y, Zhou Z, Abramowitz J, Suki WN, Hamm HE, Iyengar R, Birnbaumer M, Brown AM (1989) Molecular basis of regulation of ionic channels by G-proteins. *Recent Progr Horm Res* 45:121–208
2. Birnbaumer L, Abramowitz J, Brown AM (1990) Receptor-effector coupling by G-proteins. *Biochim Biophys Acta* 1031:163–224
3. Brown AM, Birnbaumer L (1988) Direct G-protein gating of ion channels. *Am J Physiol* 254:H401–H410
4. Busse R, Fitchner H, Luckhoff A, Kohlhardt M (1988) Hyperpolarization and increased free calcium in acetylcholine-stimulated endothelial cells. *Am J Physiol* 255:H965–H969
5. Casey PJ, Gilman AG (1988) G-protein involvement in receptor-effector coupling. *J Biol Chem* 263:2577–2580
6. Cerione RA, Staniszewski C, Benovic JL, Lefkowitz RJ, Caron MG (1985) Specificity of the functional interactions of the β -adrenergic receptor and rhodopsin with guanine nucleotide regulatory proteins reconstituted in phospholipid vesicles. *J Biol Chem* 260:1493–1500
7. Cerione RA, Regan JW, Nakata H, Codina J, Benovic JL, Gierschik P, Somers RL, Spiegel AM, Birnbaumer L, Lefkowitz RJ, Caron MG (1986) Functional reconstitution of the A_2 -adrenergic receptor with guanine nucleotide regulatory proteins in phospholipid vesicles. *J Biol Chem* 261:3901–3909
8. Codina JD, Hildebrandt D, Birnbaumer L, Brown AM (1987) Hormonal regulation of pituitary GH3 cell K channels by G_K is mediated by its A-subunit. *FEBS Lett* 216:104–106
9. Colden-Stansfield M, Schilling WP, Ritchie AK, Eskin SG, Navarro LT, Kunze DL (1987) Bradykinin-induced increases in cytosolic calcium and ionic currents in cultured bovine aortic endothelial cells. *Circ Res* 61:632–640
10. Colden-Stansfield M, Schilling WP, Possani LD, Kunze DL (1990) Bradykinin-induced K^+ current in cultured bovine aortic endothelial cells. *J Membr Biol* 116:227–238
11. Costu T, Lang J, Gless C, Herz A (1990) Spontaneous association between opioid receptors and GTP-binding regulatory

- proteins in native membranes: specific regulation by antagonists and sodium ions. *Mol Pharmacol* 37: 383–394
12. Enomoto KL, Furuya K, Maeno T, Edwards C, Oka T (1991) Oscillating activity of a calcium activated K^+ channel in normal and cancerous mammary cells in culture. *J Membr Biol* 119: 133–139
 13. Eskin SG, Sybers HD, Trevino L, Lie T, Chimoskey JE (1978) Comparison of tissue-cultured bovine endothelial cells from aorta and saphenous vein. *In Vitro Cell Dev Biol* 14: 903–910
 14. Fabiato A (1988) Computer programs for calculating total from specified free or free from specified total ionic concentrations in aqueous solutions containing multiple metals and ligands. *Methods Enzymol* 157: 378–417
 15. Furchtgott RF, Zawadski J (1980) The obligatory role of endothelial cells in the relaxation of arterial smooth muscle by acetylcholine. *Nature* 228: 373–376
 16. Gilman AG (1987) G-proteins: Transducers of receptor-generated signals. *Annu Rev Biochem* 56: 615–649
 17. Grygorczyk R, Schwartz W (1983) Properties of the Ca^{2+} -activated potassium conductance of human red cells as revealed by the patch clamp technique. *Cell Calcium* 4: 499–510
 18. Iyengar R, Birnbaumer L (1982) Hormone receptor modulates the regulatory component of adenylyl cyclase by reducing its requirement for Mg^{2+} and enhancing its extent of activation by guanine nucleotides. *Proc Natl Acad Sci USA* 79: 5179–5183
 19. Latorre R, Oberhauser A, Labarca P, Alvarez O (1989) Varieties of calcium-activated K^+ channels. *Annu Rev Physiol* 51: 385–399
 20. Makoto M, Eskin SG, Schilling WP (1991) Flow-induced changes in Ca^{2+} signalling of vascular endothelial cells: effect of shear stress and ATP. *Am J Physiol* 29: H1698–H1707

21. Neer EJ, Clapham DE (1988) Roles of G-protein subunits in transmembrane signalling. *Nature* 333: 129–134
22. Okabe K, Yatani A, Brown AM (1991) The nature and origin of spontaneous noise in G-protein-gated ion channels. *J Gen Physiol* 97: 1279–1293
23. Sauve R, Simoneau C, Monette R, Roy G (1986) Single channel analysis of K^+ permeability in HeLa cancer cells: Evidence for a calcium-activated K^+ channel of small unitary conductance. *J Membr Biol* 92: 269
24. Sauve R, Parent L, Simoneau C, Roy G (1988) External ATP triggers a biphasic activation process of a calcium-dependent K^+ channel in cultured bovine aortic endothelial cells. *Pflügers Arch* 412: 469–481
25. Sauve R, Chahine M, Tremblay J, Hamel P (1990) Single-channel analysis of the electrical response of bovine aortic endothelial cells to bradykinin stimulation: contribution of a Ca^{2+} -dependent K^+ channel. *J Hypertension* 8 (Suppl 7): S193–S201.
26. Schilling W (1989) Effect of membrane potential on cytosolic calcium of bovine aortic endothelial cells. *Am J Physiol* 257: H778–H784
27. Schilling WP, Ritchie AK, Navarro LT, Eskin SG (1988) Bradykinin-stimulated calcium influx in cultured bovine aortic endothelial cells. *Am J Physiol* 255: H219–H227
28. Toro L, Ramos-Franco J, Stefani E (1990) GTP-dependent regulation of myometrial K_{Ca} channels incorporated into lipid bilayers. *J Gen Physiol* 96: 373–394
29. Voyno-Yasenetskaya T, Panchenko MP, Nupenko EV, Rydin VD, Tkachuk VA (1989) Histamine and bradykinin stimulate phosphoinositide turnover in human umbilical vein endothelial cells via different G-proteins. *FEBS Lett* 259(1): 67–70

ESTA TESIS NO DEBE
SALIR DE LA BIBLIOTECA

REFERENCIAS

- (1) Atkinson, N.S.; Robertson, G.A. & Ganetzky, B. (1991) *Science*. **253**:551-554.
- (2) Aveyard, R. & Haydon, D.A. (1973). Introduction to the principles of surface chemistry. Cambridge University Press. Cambridge UK.
- (3) Blatz, AL & Magleby, KL (1986) *Nature* **323**:718-720.
- (4) Candia, S Garcia, ML & Latorre, R. (1992). *Biophys. J.* **63**:583-590.
- (5) Clapham, D.E. & DeFelice, L.J. (1984). *Biophys. J.* **45**:40-42.
- (6) Carbone, E; Wanke, F; Prestipino, G; Possani, L. D. & Maelicke, A. *Nature* (1982). **295**:90-91.
- (7) Castle, NA; Haylett, DG & Jenkinson DH. (1989). *TINS* **2**:59-65.
- (8) Conti, F. & Neher, E. (1980). *Nature*. **285**:140-143.
- (9) Cook, NG. (1988). *TIPS* **9**:21-28.
- (10) Fukushima, Y. (1982). *J. Physiol.* **331**:311-331.
- (11) Furchtgott, R.F. & Vanhoutte, P.M. (1989). *Faseb J.* **3**:2007-2018.
- (12) Galvez, A; Gimenez-Gallego, G; Reuben, JP; Roy-Constancin, L; Feigenbaum, F; Kaczorowski, F.G. & Garcia M.L. (1990) *J. Biol. Chem.* **265**:11083-11090.
- (13) Gurrola, GB; Molinar-Rode, R; Stiges, M; Bayon, A & Possani, LD. (1989) *J. Neural Transm.* **77**:11-20.
- (14) Hamill DP; Marty E; Neher, E; Sakmann, B & Sigworth, FJ. (1981). *Pflügers Archiv.* **391**:85-100.
- (15) Hagiwara, S.; Kusano, K. & Saito, N. (1961). *J. Physiol.* **155**:470-489.
- (16) Hassessian, H.; Vaca, L. & Kunze, D.L. (1994). *British J. Pharmacol.* (in press).
- (17) Hille, B. Ionic Channels of Excitable Membranes. Ed. Sinauer Associates Inc.
- (18) Hodgkin, A.L. & Huxley, A.F. (1952) *J. Physiol.* **117**:500-504.
- (19) Hunter, M; Lopes, AG; Boulaep, EL & Giebisch GH (1984). *PNAS* **81**:4237-39.
- (20) Jones, S.W. & Adams, P.R. (1987). En: Neuromodulation. The biochemical control of neuronal excitability. Kaczmarek, L.K. & Levitan, I.B. editors. 159-186. Oxford Press, New York.
- (21) Matsuda, H.; Saigusa, A. & Irisawa, H. (1987). *Nature*. **325**:156-159.
- (22) Miller, C. (1990). *Biochemistry*. **29**:5320-5325.
- (23) Miller, C; Moczydlowski, E; Latorre, R & Phyllips, M. (1985). *Nature* **313**:316-318.
- (24) Moczydlowski, E; Lucchesi K & Ravindran A. (1988) *J. memb. Biol.* **105**:95-111.
- (25) Moncada, S; Gryglewski, R; Bunting, S & Vane, J, R. *Nature* (1976) **263**:663-665.
- (26) Narahashi, T.; Shapiro, B.J.; DeGuchi, T.; Scuka, M. & Wang, C.M. (1972) *Am. J. Physiol.* **222**:850-857.
- (27) Ohmri, H.; Yoshida, S. & Hagiwara, S. (1981). *PNAS* **78**:4960-64.
- (28) Park, CS & Miller, C. (1992) *Biochemistry*. **31**:7749-7755.
- (29) Petersen, O.H. & Maruyama, Y. (1984). *Nature*. **307**:693-696.
- (30) Possani, LD. Structure of Scorpion Toxins. En Handbook of Natural Toxins. Vol 2. 513-550. Insect poisons, allergens and other invertebrate venoms. Editor Anthony T. Tu. Editorial Marcel Dekker Inc.
- (31) Possani, LD; Martin, BM & Svenden, I. (1982) *Carlsberg Res. Commun.* **47**:285-289.
- (32) Reuter, H. & Stevens, C.F. (1980). *J. Memb. Biol.* **57**:103-121.

- (33) Romey, G.; Hugues, M.; Schmid-Antomarchi, H. & Lazdunski, M. (1984). *J. Physiol.* **79**:259-264.
- (34) Sackmann, B. & Trube, G. (1984). *J. Physiol.* **347**:641-657.
- (35) Sands, SB; Lewis, RS & Cahalan, MD (1989) *J. Gen. Physiol.* **93**:1061-1074.
- (36) Schmid-Antomarchi, H. (1984). *Eur. J. Biochem.* **142**:1-6.
- (37) Schwartz, W. & Passow, H. (1983). *Ann. Rev. Physiol.* **45**:359-374.
- (38) Siegelbaum, S.A. (1987). En: Neuromodulation. The biochemical control of neuronal excitability. Kaczmarek, L.K. & Levitan, I.B. editors. 187-205. Oxford Press, New York.
- (39) Stiges, M; Possani, LD & Bayon, A. (1986). *Journal of Neuroscience*. **6**(6): 1570-1574.
- (40) Vaca, L; Gurrola GB; Possani, LD & Kunze, DL (1993). *J. Memb. Biol.* **134**:123-129.
- (41) Vaca L, Schilling WP and Kunze DL (1992). *Pflügers Archiv*. **422**:66-74.
- (42) Valdivia, H; Smith, J; Martin, BM; Coronado, R & Possani, LD. (1988) *Febs Letters*. **226**:280-284.
- (43) Yellen, G.; Jurman, M.E.; Abramson, T. & MacKinnon, R.(1991). *Science*. **251**(4996):939-42.